Fast Numerical Algorithms for Multi-component and Long Term Reactive Transport Simulation in Parallel Context

By
TUSHAR KANTI PAL
PHYS01201304045

Bhabha Atomic Research Centre, Mumbai

A thesis submitted to the
Board of Studies in Physical Sciences

In partial fulfillment of requirements
for the degree of

DOCTOR OF PHILOSOPHY
of
HOMI BHABHA NATIONAL INSTITUTE

April, 2019

Homi Bhabha National Institute

Recommendations of the Viva Voce Committee

As members of the Viva Voce Committee, we certify that we have read the dissertation prepared by **Tushar Kanti Pal** entitled **"Fast Numerical Algorithms for Multi-Component and Long Term Reactive Transport Simulation in Parallel Context"** and recommend that it may be accepted as fulfilling the thesis requirement for the award of Degree of Doctor of Philosophy.

Chairman – Prof. T. C. Kaushik **Date:** 29/03/2019

Guide / Convener – Prof. D. Datta DDatta **Date:** 29/3/2019

Examiner – Prof. Joytirmay Banerjee **Date:** 29th March 2019

Member 1- Prof. Anurag Gupta **Date:** 29/3/19

Member 2- Prof. Indranil Mukhopadhyay **Date:** 29/03/2019

Member 3- Prof. R. K. Bajpai **Date:** 29/3/19

Final approval and acceptance of this thesis is contingent upon the candidate's submission of the final copies of the thesis to HBNI.

I/We hereby certify that I/we have read this thesis prepared under my/our direction and recommend that it may be accepted as fulfilling the thesis requirement.

Date: 29/03/2019

Place: Mumbai

DDatta

<Signature>

Guide

STATEMENT BY AUTHOR

This dissertation has been submitted in partial fulfillment of requirements for an advanced degree at Homi Bhabha National Institute (HBNI) and is deposited in the Library to be made available to borrowers under rules of the HBNI.

Brief quotations from this dissertation are allowable without special permission, provided that accurate acknowledgement of source is made. Requests for permission for extended quotation from or reproduction of this manuscript in whole or in part may be granted by the Competent Authority of HBNI when in his or her judgment the proposed use of the material is in the interests of scholarship. In all other instances, however, permission must be obtained from the author.

(TUSHAR KANTI PAL)

DECLARATION

I, hereby declare that the investigation presented in the thesis has been carried out by me. The work is original and has not been submitted earlier as a whole or in part for a degree / diploma at this or any other Institution / University.

(TUSHAR KANTI PAL)

List of Publications arising from the thesis

Journal

1. ”Development of Possibilistic Statistics and Its Application to Quantify Uncertainty of Subsurface Solute Transport Model”, T.K. Pal, D. Datta, Sādhanā, **2019**, 44(2), Article ID 44.
2. ”Modeling Advection and Anisotropic Dispersion of Radionuclides through Geological Media Using Diffusion Velocity Lattice Boltzmann Scheme”, D. Datta, T.K. Pal, SciFed Journal of Nuclear Science, **2018**, 2(1), 1-9.
3. ”A Lattice Boltzmann Scheme for Diffusion Equation in Spherical Coordinate”, D. Datta, T.K. Pal, International Journal of Mathematics and Systems Science, **2018**, 1(4), 1-4
4. ”Parametric uncertainty analysis of solute transport process using fuzzy lattice Boltzmann scheme”, T. K. Pal, D. Datta, Life Cycle Reliability and Safety Engineering, **2017**, 6, 239-249.
5. ”Development of Fuzzy Differential Quadrature Numerical Method and its Application for Uncertainty Quantification of Solute Transport Model”, D. Datta, T. K. Pal, International Journal of Energy, Information and Communications, **2017**, 8, 1-12.
6. ”Development of Differential Quadrature based Computational Scheme in Cylindrical Geometry and Its application to Simulate Radionuclide Leaching from Radioactive Waste Form”, T. K. Pal, D. Datta, R. K. Bajpai, SRESA’s International Journal of Life Cycle Reliability and Safety Engineering, **2016**, 5, 1-7.
7. ”Address of Geo-hydrological Problem using Lattice Boltzmann and Differential Quadrature Methods”, D. Datta, T. K. Pal, SRESA’s International Journal of Life Cycle Reliability and Safety Engineering, **2016**, 5, 16-20
8. ”Numerical Simulation of Reaction-Diffusion Process in Geological Media using Lattice Boltzmann Based Diffusion Model Coupled with Geochemical Reaction Solver”, T.K. Pal, D. Datta, Global Journal of Pure and Applied Mathematics, **2016**, 12, 429-433.
9. ”Numerical Solution of Solute Transport Model Using Cellular Automata”, D. Datta, T. K. Pal, Global Journal of Pure and Applied Mathematics, **2016**, 12, 131-135.

Chapter in books and lectures notes

1. ”Lattice Boltzmann Simulation for Science and Engineering Problems”, T. K. Pal, D. Datta, INS Workshop on Advanced Engineering Mathematics, August 21-25, **2017**.

2. ”Theory of Random Walk and Continuous Time Random Walk and its Applications in Diffusion Process”, T. K. Pal, D. Datta, INS Workshop on Advanced Engineering Mathematics, August 21-25, **2017**.

Conferences

1. ”Numerical Solution of Model for Migration of Radionuclides in Geological Sorbing Media Using Lattice Boltzmann Method”, T. K. Pal, D. Datta, R. K. Bajpai, International Conference on Advancing Frontiers in Operational Research: Towards a Sustainable World (AFOR2017), Kolkata, December 21-23, **2017**.

2. ”Risk Management via Uncertainty Modeling of Reaction Diffusion Process in Geological Media using Fuzzy Lattice Boltzmann Scheme”, D. Datta, T. K. Pal, International Conference on Advancing Frontiers in Operational Research: Towards a Sustainable World (AFOR2017), Kolkata, December 21-23, **2017**.

3. ”Uncertainty Analysis of Retardation Factor Using Monte Carlo, Fuzzy Set and Hybrid Approach”, T. K. Pal, V. Arumugam, D. Datta, Springer Proceedings in Mathematics Statistics, **2015**, 125, 153-163.

Others

1. ”Multi-Scale Contaminant Transport Modeling in Geological Media - Case Study”, T. K. Pal, D. Datta, V. Arumugam, R.S. Soni, BARC Internal Report, **2015**, BARC/2015/I/022.

2. ”Lattice Boltzmann Simulation to Study Reaction-Diffusion Processes in Geological Media”, T. K. Pal, R.S. Soni, D. Datta, BARC Newsletter, **2015**, No. 343, 6-13.

Dedicated To
My loving MOTHER *and* SIBLINGS

In memory of
My beloved FATHER

Acknowledgments

It wouldn't have been possible to complete the thesis without help of people around me. So, I would like to acknowledge people who have in direct or indirect way helped me in completing the work.

First and foremost, with reverence I would like to express my deep sense of gratitude to my research guide, Prof. D. Datta for his continuous motivation and guidance throughout my dissertation work. His inspiring discussions, continuous support, great patience, and the freedom he gave to me in the research have helped me to shape this thesis. Because of the knowledge in advanced mathematics and computation that he shared with me during this research work, I have been able to adopt new numerical techniques, which were not part of my academic studies in college and university. His continuous encouragement and support to write my own computer programs to simulate various processes has increased my confidence in writing computer program. I consider myself fortunate in having the privilege of being guided by him.

Beside my supervisor, I would like to thank all the members of my doctoral committee [Prof. T.C. Kaushik (Chairman), Prof. B.N. Jagatap (Ex-Chairman), Prof. Anurag Gupta (member), Prof. Indranil Mukhopadhyay (member), Prof. R.K. Bajpai (technical guide)] for their time, critical discussions and constructive suggestions during this course of Ph.D. The thesis has taken this present structure due to their outstanding guidance. I would also like to thank present Dean Academic, Prof. B.K. Nayak for his help in administrative works related to this Ph.D.

This thesis work was a part of a collaborative doctoral work between BARC, India and ANDRA, France. Special thanks to Dr. Benoit Cochepin, ANDRA, France for his constant support during the research work. He provided various benchmark problems on multi-component reactive transport, which have been used for validation and verification of the computer programs written in this doctoral work. Their critical review comments on progress reports have helped me to improve the quality of this research work.

Special thanks go to computer division people who helped me in developing parallel program in Anupam supercomputing facility. I also acknowledge the help on parallel processing that I received from Shri D. Parulekar, TDD during this research work.

I would like to sincerely thank Dr. V. Arumugam, Ex-Head, RES, TDD for being as a mentor before as well as during my research work. He has taught me various aspects of geochemistry and groundwater hydrology. It was due to his faith and confidence on me I got the chance to pursue this research work. He is the one for whom I got the opportunity to work under the supervision of Prof. D. Datta. I can recall how dedicatedly he spent his important time to search for a suitable guide for this research work. Thank you, Sir, for being so supportive.

I would like to take this opportunity to thank my present division head and AD, NRG, Shri K. Agarwal and former division heads, directors/associate directors of NRG for their kind support and encouragements. Specially, I am thankful to Shri P.K Wattal, Ex. Director, NRG for nominating my name in this cooperative doctoral work. I thank Shri R.S. Soni, Ex. Head, TDD for his support and encouragements during the period when he was heading TDD. I thank Dr. R.K. Bajpai, Head, RES, TDD for his valuable guidance and support during this research work. My thanks go to Shri A. Acharya, TDD for teaching me various aspects of deep geological repository. I would also like to thank present and former senior colleagues of NRG, Dr. J. G. Saha, Head, PSDD, Dr. D.N. Yadav, Dr, R.R. Rakesh, Shri M.R. Joshi (Ex.), Dr. G. Sugilal, Shri R.S. Bhatia, Shri Sunil Joshi, Shri P.D. Maniyar for their help, encouragement and support during the course of the research work. I thank all colleagues of RES, Shri Prattek Srivastava, Shri Shiva Kumar, Shri S.P. Singh, in particular Shri Yuvraj Dhamapurkar for their help and support in this Ph.D. study. I would like to thank Shri S.B. Patil, TDD who is my senior colleague as well as landlord for providing me a specious apartment at reasonable rent during the entire period of this research work.

I would also like to thank all my childhood, school, college, university and BARC Training School friends with whom I shared memorable times and learned many things that have direct or indirect influences on my Ph.D. work.

I owe much to my mother for her unconditional love and support. Although I lost my father before enrolling myself in this PhD. work, his ideologies and advices still motivate me for pursuing higher studies. I am also grateful to my sister (Kajal) and brother (Mrinal) and their families for their unconditional love, support and taking care of me. I thank my cousin (Biswajit) and brother like friends (Shiba and Deba) who take care of my lonely mother, making me feel secure during my stay in Mumbai. Thanks are due to my nephews (Somu and Asesh) for their love which gave me strength to pursue this study. I would also like to thank my little niece (Rishona) with whom I spent my time whenever I visited my brothers home and she in her own way geared me up to reach the goal.

Lastly, I would like to thank all others who have contributed directly or indirectly to the successful realization of this thesis.

Contents

SUMMARY

Reprocessing of spent nuclear fuels generates high level radioactive waste (HLW) (activity$>$ $3.7 \times 10^{11}\ Bq/l$) containing long lived ($T_{1/2} \sim 10^6\ yrs.$) fission products and actinides. In order to protect human and environment from the toxicity of radioactive materials, stringent criteria implemented by regulatory bodies are need to be followed before their final disposal. The vitrified HLW canisters are planned to be disposed of in deep geological repository (DGR) at a depth of about 500 m below Earth's surface. Radiological safety evaluation and risk analysis of DGR require modeling transport of leached out radionuclides through the geological media and uncertainty analysis of model output. Transport of dissolved radionuclides (RNs) in pore water is governed by a set of processes, such as advection, diffusion, dispersion, geochemical reactions, radioactive decay etc. Migration of these radionuclides is mathematically modeled as advection-dispersion-reaction equation (ADRE) also termed as reactive transport equation. Since the dissolved RNs can stay in the form of various species, the governing ADRE is multi-component reactive transport equation.

Multi-component and long term reactive transport simulation demands for huge computational resources in terms of storage and computing speed. Communication overload between processors in a supercomputing platform reduces the efficiency of traditional numerical techniques, e.g., finite element method (FEM), finite difference method (FDM) etc. Lattice Boltzmann method (LBM) and differential quadrature method (DQM) are two relatively new and advanced numerical techniques. Parallelization of LBM based code is straightforward because collision process of LBM is localized. Also, simple bounce back boundary condition of LBM is ideal for porous media (complex geometry). Notable feature of DQM is that very small number of grid points (in the present study only 21 grid points were sufficient to achieve the results with 95$\%$ confident level of accuracy) are required for the numerical simulation while maintaining stability and providing very accurate results. Consequently, it requires much less computational effort and memory for storage.

The present thesis focuses on following three aspects (i) study of LBM and DQM for development of solute transport and reactive transport codes, (ii) development of an in-house computer code to interface the developed solute transport modules with commercial geochemical software (PHREEQC, a freeware developed by USGS), and (iii) Development of LBM and DQM based numerical schemes for uncertainty modeling. Detailed analysis of single relaxation time (SRT) LBM and DQM is carried out for development of computer codes for advection-dispersion equation (ADE). The in-house developed computer codes are verified and validated by solving 5 benchmark problems (1D and 2D). A comparative study between LBM, DQM and FDM is carried out by calculating L_2 errors of the solutions of a particular benchmark problem. This study shows that DQM based solutions are more accurate than the LBM and FDM based solutions and at the same time it takes smaller computing time. On the other hand, accuracy of LBM and FDM are same for same time step value, but LBM takes much smaller time than FDM. This study therefore justifies development of LBM/DQM codes for multi-component and long term reactive transport problems. The LBM based solute transport code is parallelized using OpenMP directives in a shared memory platform with Intel G1 quad-core processor. In order to increase computational load we reduced the grid size and achieved 2 times reduction in computing time. The in-house developed solute transport solver using LBM is further utilized for multi-component reactive transport. In order to increase the scope of incorporating complex geochemical reactions, such as ion exchange, dissolution/precipitation, surface complexation, into the multi-component reactive transport framework, LBM based solute transport code is interfaced with commercial geochemical software PHREEQC using operator splitting approach. This interfaced scheme is verified and validated by solving 3 benchmark problems.

This thesis proposes two innovative methodologies for solving ADE describing tracer transport through geological media in presence of imprecise measurement of model parameters such as tracer dispersion coefficient and groundwater velocity. Measurement around most likely value provides a spread causing an imprecision of the model parameters. Here imprecision is addressed as a fuzzy variable and the membership function of each such fuzzy variable is expressed in the form of triangular fuzzy number. The governing fuzzy ADE is numerically solved using LBM and DQM at various α-cut levels. Basically, LBM and DQM methods are amalgamated with fuzzy vertex theory of incorporating fuzziness of the fuzzy parameters in the model of interest for uncertainty analysis. Uncertainty quantification of the solute concentration as solution of the fuzzy differential equation is carried out. Advantage of LBM and DQM for obtaining numerical solution of fuzzy partial differential equation is shown. A supporting graphical user interface (GUI) computer code using Python programming language is developed during this research work to carry out the reported simulation studies.

List of Figures

List of Tables

List of abbreviations

$AD(E)$	Advection Dispersion (Equation)
$AAD(E)$	Anisotropic Advection Dispersion (Equation)
$ADR(E)$	Advection Dispersion Reaction (Equation)
AU	Aleatory Uncertainty
BGK	Bhatnagar Gross Krook
CA	Cellular Automata
CFD	Computational Fluid Dynamics
CGL	Chebyshev Gauss Lobatto
$(E)DF$	(Equilibrium) Distribution Function
DGR	Deep Geological Repository
DSA	Direct Substitution Approach
$DQ(M)$	Differential Quadrature (Method)
EU	Epistemic Uncertainty
FDM	Finite Difference Method
FDQ	Fourier Differential Quadrature
$FDQM$	Fuzzy Differential Quadrature Method
FEM	Finite Element Method
$FLBM$	Fuzzy Lattice Boltzmann Method
FN	Fuzzy Number
FS	Fuzzy Sets
FVM	Finite Volume Method
HDQ	Hermite Differential Quadrature
HLW	High Level Waste
ILW	Intermediate Level Waste
KGF	Kolar Gold Field
$LB(M/E)$	Lattice Boltzmann (Method/Equation)
$LGCA$	Lattice Gas Cellular Automata

LLW	Low Level Waste
LR	Leach Rate
MC	Monte Carlo
$NSDF$	Near Surface Disposal Facility
NSE	Navier Stokes Equation
$PDAE$	Partial Differential Algebric Equation
PDE	Partial Differential Equation
PDF	Probability Distribution Function
PDQ	Polynomial Differential Quadrature
RCT	Reinforced Concrete Treanch
REV	Representative Elementary Volume
RW	Radioactive Waste
SIA	Sequential Iterative Approach
SLT	Stone-lined Earth Treanch
SM	Safety Margin
$SNIA$	Sequential Non-Iterative Approach
SPH	Smoothed Particle Hydrodynamics
SRT	Single Relaxation Time

Chapter 1

Introduction

1.1 Research background

Multi-component and long term reactive transport has now become an active area of research in geosciences [Steefel et al., 2005; Xiao et al., 2018], particularly in the field of high level radioactive waste disposal in deep geological repository (DGR) [Grindrod et al., 1996; Steefel et al., 1998a,b; Spycher et al., 2003; Glynn, 2003; MacQuarrie et al., 2005]. Modeling groundwater flow and contaminants transport through geological media play a critical role in nuclear industry pertaining to geological disposal of hazardous nuclear waste generated at various stages of nuclear fuel cycle. Geological disposal of high level and long lived fission products and actinides generated inside nuclear reactors is considered to be one of the best solutions for long term containment and isolation of the radionuclides by preventing the ingress of water and providing retardation to their transport. In order to ensure the long term isolation, a multiple-barrier design of DGR, which includes metal canister containing high level vitrified waste glass or the spent fuel itself, bentonite barrier surrounding the canister and the host rock surrounding the repository, is adopted worldwide [Chapmann et al., 2012]. It is expected that the metal canister will start corroding over time in the repository environment [King, 2017]. Corrosion of canister ultimately leads to its failure and the radionuclides present inside the glass start leaching out due to diffusion and dissolution processes [Ledieu, et al.; Thorat et al., 2008]. It is worth mentioning here that canisters may also fail due to some accidental causes, such as seismic loads from earthquake, thermal load due to decay heat etc [Helnrik et al., 2009; Hernelind, 2010].

Multi-component reactive transport

Prediction of spatio-temporal spreading of leached out radionuclides is a prerequisite task for safety evaluation and risk assessment of a DGR system. In fact, this task demands for a through understanding of complex physico-chemical processes which can either retard or facilitate the migration of radionuclides from the disposal area. The leached out radionuclides in the pore water are subjected to a set of processes, such as advection, diffusion, dispersion, biogeochemical reaction etc. Due to speciation, radionuclides can stay in the solution in different chemical forms called species. Dissolved species can interact with other species present in the solution as well as with minerals of the solid phase during their transport due to advection, diffusion and dispersion. Considering the solution is dilute, transport due to charge imbalance and chemical potential are not considered in this work. The governing equations of migration of these species are therefore mass transport equations coupled with reaction terms representing various geochemical interactions. Mass transport equation is called advection dispersion equation (ADE), which is a second order partial differential equation (PDE) and geochemical reactions are represented by a set of nonlinear algebraic equations. In fact, transport of solutes and their geochemical interactions are not independent of each other, rather they are coupled processes. For example, geo-chemical reactions can modify the petrophysical properties, such as porosity, permeability, of the engineering clay barrier and natural host rock. These parameters are having overall control over fluid flow and solute transport processes. Therefore, small change in these petrophysical parameters alters the value of flow velocity and dispersion coefficient, which are the parameters of solute transport process. Similarly, change in water velocity has impact on residual time, which is an important parameter for reaction kinetics in an open system. Therefore, solute transport and geochemical reactions at the fluid-solid interface are coupled with each other. This coupled process of transport and geochemical reactions is called reactive transport and the equation modeling reactive transport is generally known as advection-dispersion-reaction equation (ADRE).

Uncertainty analysis

In order to have appropriate safety evaluation and risk analysis of radioactive waste disposal facilities, analysis of model uncertainty of various processes involved with the disposal system is required [Helton, 1994; Zio, 1996]. Simulation of these processes are carried out by formulating appropriate models, which are basically mathematical equations derived using physical principles, such as various conservation laws. Mathematical models can be considered having three components: inputs, operator, and output. Here operator is a closed form analytical solution of the model equation or some numerical solver. The outputs of such models are generally subjected to uncertainty because of the following three reasons: uncertainty in model parameters, uncertainty in model itself, and uncertainty in scenario. Here in this study we are interested in modeling uncertainty in solute transport/reactive transport model output due to uncertainty in model parameters, such as groundwater velocity, dispersion coefficient. The uncertainty associated with these parameters is due to the complexity of the DGR system and the large spatial and temporal scales involved. This type of uncertainty in model output is called parametric uncertainty. Estimation of parametric uncertainty in model output requires representation and aggregation of models inputs. The models parameters can be random in nature or they may be imprecise. Based on the nature of the parameters, parametric uncertainty are classified into two categories: one is called aleatory uncertainty which deals with random parameters and the other one is called epistemic uncertainty which deals with imprecise parameter [Hoffman et al., 1994; Helton, 1994; Ayyub et al., 2006]. Aleatory uncertainty is due to random variability of the model parameters which cannot be reduced or eliminated and can only be quantified, whereas epistemic uncertainty is due to insufficiency or vagueness of the model parameters and can be reduced with more information [Hoffman et al., 1994; Ferson et al., 1996; Hora, 1996; Helton, 1994]. Probabilistic uncertainty is quantified using Monte Carlo simulation in which sample values of the input parameters are taken from their probability distribution functions and uncertainty in the model output is expressed in terms of the 5^{th} and 95^{th} percentiles of the cumulative distribution of the probabilistic output of the model [Kushwaha, 2009; Datta, 2014]. On the other hand epistemic uncertainty is quantified using fuzzy logic [Datta, 2011]. Measurement around most likely value provides a spread, causing an imprecision of the model parameters. In geological media, the model parameters of ADRE are imprecise due to lack of experimental data (few measurements). Imprecise parameters are generally represented as fuzzy and therefore, the imprecision or fuzziness of the parameters of solute transport model results an uncertainty (epistemic) in the solute concentration. In this study imprecise parameters are represented as fuzzy variables and the membership function of each such fuzzy variables is expressed in the form of a triangular fuzzy number (TFN), because TFN encodes only most likely value (mean value) and the spread (standard deviation). Aggregation of all the fuzzy numbers in the estimation of uncertainty is carried out by using fuzzy vertex method (FVM) which is based on α-cut concept of fuzzy set and interval analysis [Dong et al., 1987]

Requirement for fast and parallel algorithm

The long term prediction of alteration of various components of DGR and modeling uncertainty associated with reactive transport with uncertain model parameters are challenging in the sense that the system is multi-species, time period required for the simulation is very large, and various complicated homogeneous and heterogeneous reactions are involved with the model equation. Hence, multi-component and long term reactive transport simulation demands huge computational resources in terms of storage and computational speed. Though both the demands of storage and computational speed can be achieved by availing present day supercomputing facility with clusters of CPUs, there has always been an active research to develop efficient numerical methods than can better utilize such facilities. Traditional numerical methods, such as finite difference method (FDM), finite element method (FEM), finite volume method (FVM), have been successfully deployed to solve multi-component and long term reactive transport in parallel platform, but huge communication overheads reduce their performance efficiency. Lattice Boltzmann method (LBM), which is relatively new in the field of numerical methods, is one such technique that has negligible communication overheads because of inherent localized property of its algorithm. Other desirable features of LB that has attracted many researchers for implementing this technique for solving partial differential equations (PDE) representing various science and engineering problems are its simple algorithm and easy bounce back algorithm for boundary conditions that has made it ideal for complex geometry (porous media). Another numerical method called differential quadrature method (DQM) [Bellman et al., 1971; Datta et al., 2016a], which approximates partial derivative of a piecewise continuous function at a grid point as weighted sum of functional values of the solution at all grid points along a grid line, has some suitable features like use of very few grid points in calculation while maintaining the stability without any condition and providing very accurate result [Datta et al., 2016a]. Because of this unique feature, DQ requires less storage and increases computational speed[Bellman et al., 1972].

On the onset of this chapter we will touch upon the background of this study by emphasizing the requirement of nuclear energy and how the nuclear industry is coping with radioactive wastes generated during reactors operation. Then special emphasis is given on literature survey on multi-component and long term reactive transport and traditional numerical techniques used for reactive transport simulation. Later on we will cover theoretical background and general implementation of two numerical simulation methods: LBM and DQM. The chapter will also highlights the relevant gap areas, objective and scope of the thesis. Finally the chapter presents the research strategy and outline of this thesis.

1.2 Energy resources

The level of development of a society is the indicator of the quality of life in that society. Electricity is the basic and important input for the overall development process. The per capita electricity consumption is generally used as measure of the standard of living. At present, there is a large discrepancy in the amount of annual per capita electricity consumption., from $>$ 12000 MW-h in developed countries, such as, Canada, USA, to $<$ 100 kW-h in some developing or under developed countries in Asia and Africa. In India, the present annual per capita electricity consumption is about 957 kW-h, which is very small compared to that of developed countries. Therefore, like other developing countries India too has a growing appetite for electricity. Energy resources are categorized as fossil fuel, nuclear fuel and renewable resources. Fossil fuels such as coal, natural gas and oil based thermal electricity provided most of the energy being produced in India. Natural resources of these fossil fuel are being depleted gradually and at the same time thermal power plant fueled with fossil fuels emitting huge amount of green house gas, which is causing global warning. This ever increasing demand of electricity and continuous depletion of fossil fuel based energy resources (coal, oil, gas etc.) together with requirement for low carbon emission based energy to mitigate global warming has given tremendous impetus to search for renewable and clean energy resources. Although Nuclear energy is not a renewable energy resource, it is treated as a clean energy source because of negligible carbon emission to the environment by nuclear reactors. Because of the vast thorium resources and indigenous reactor technologies available in India, nuclear energy is envisaged to provide energy security in the coming decades. At present, India has a total of 6.78 GWe installed nuclear power capacity [Banerjee et al., 2017], which is about 3% of the total electricity and has conceived of to achieve

10% by early 2030s.

1.3 Practices of radioactive waste management

Nuclear power plants, that harness nuclear energy from fissile materials (e.g. ^{235}U, ^{233}U, ^{239}Pu etc.), produce actinides and fission products during their operation. Figure 1.1 shows how actinides are produced in reactors due to (n, γ) reactions and β decay process. These actinides and fission products as radioactive waste are associated with high level of activity and and heat output, and therefore, require stringent criterion for their handling, transportation, and disposal. In fact, radioactive wastes are generated at various stages of nuclear fuel cycle which includes mining and milling of uranium ore, fuel fabrication, irradiation of fuel in nuclear power plant, storage of spent fuels and their reprocessing. Small amount of RWs are also produced as a result of ever increasing use of radio-isotopes in health care, industry and research laboratory. Since India has adopted closed fuel cycle most of the RWs (95% of total activity produced in a full nuclear power cycle) are produced during the reprocessing of the spent fuel [Wattal, 2017]. Various stages of management of radioactive waste, such as waste characterization, treatment, conditioning, storage, disposal, surveillance/monitoring etc., are adopted in India's radioactive waste management practices [Raj et al., 2006].Characterization of RW, which included clas-

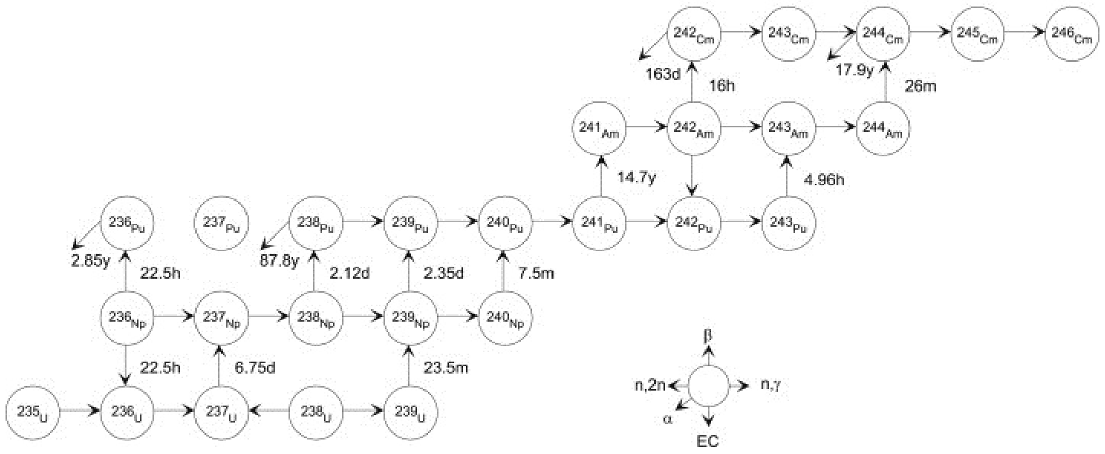

Figure 1.1: Actinide transmutation chain in ^{235}U fueled reactor (Salvatores et al., 2011)

sification and segregation, is an important step before their treatment and disposal. RWs are categorized based on their physical state, activity etc. Based on physical state, RWs are categorized as gaseous, liquid and solid waste. Based on activity level, liquid wastes are categorized in four categories: exempt waste, low-level waste (LLW), intermediate-level waste (ILW) and high-level waste (HLW). Table 1.1 shows the activity level of each of the categories of liquid waste. Solid wastes are also categorized in four categories, based on surface radiation dose: LLW, ILW, HLW and long-lived waste. Surface dose of each of the categories are shown in Table 1.2. Key radionuclides present in the various categories of the waste are given in Table 1.1. Considering the fact that safe management of RWs is vital for the successful deployment of nuclear programme for electricity production, various physico-chemical treatment on the radioactive waste is carried out in order to reduce its volume and stabilize in some suitable matrix [Raj et al., 2006]. The underlying objective behind these practices is to concentrate and contain the radioactivity associated with RWs as much as possible, and also to dilute and disperse the very low-level activity to the environment through aquatic root. The dischargeable activity limit is decided by regulatory bodies (in India Atomic Energy Regulatory Board is the authorized regulator).

Table 1.1: Categorization of liquid waste

Category	Activity (Bq/l)
Exempt waste	< 37
Low-level waste	$37 - 3.7 \times 10^6$
Intermediate-level waste	$3.7 \times 10^6 - 3.7 \times 10^{11}$
High-level waste	$> 3.7 \times 10^{11}$

Table 1.2: Categorization of solid waste

Category	Surface dose/activity
Low-level waste	$< 2mGy/h$
Intermediate-level waste	$2 - 20mGy/h$
High-level waste	$> 20mGy/h$
Long-lived waste	$> 4000Bq/g$ of α emitter and other long-lived β emitter

In India, LLW and ILW wastes are treated by chemical processes, ion exchange process, membrane process, thermal/solar evaporation process etc. and immobilized in cement/polymer. Details of treatment and vitrification processes adopted in India for LLW and ILW are given in [Raj et al., 2006]. Vitrified products of LLW and ILW are disposed of in Near Surface Disposal Facilities (NSDFs), which are co-located with nuclear power installations. There are four types of disposal modules in NSDFs, namely earth trench (ET), stone-lined earth trench (SLT), reinforced concrete trenches (RCT) and tile holes (TH). Details of each of the modules can be found elsewhere in literature [Raj et al., 2006].

HLW generated during reprocessing of spent nuclear fuel or the spent fuel itself is the most dangerous because it contains very high active fission products (FPs) as well as very long lived actinides and few long lived fission products. Key FPs and actinides present in HLW are given in Table 1.3. In India, a three stage program is adopted for management of liquid HLW generated during reprocessing of spent nuclear fuel. The liquid HLW is first immobilized in borosilicate glass after being properly treated by various radioactive waste treatment practices. Solidification of the mixture of HLW and glass additives happens inside a SS canister.

Table 1.3: Key FP and actinides and their half-lives

	Isotope	Half-life (year)	Isotope	Half-life (year)
Fission products	^{137}Cs	30.12	^{90}Sr	28.78
	^{135}Cs	2.3×10^{6}	^{129}I	1.57×10^{7}
	^{99}Tc	2×10^{5}	^{106}Ru	1.02
Actinides	^{235}U	7.04×10^{8}	^{238}U	4.47×10^{9}
	^{238}Pu	87.1	^{239}Pu	2.41×10^{4}
	^{240}Pu	6.56×10^{3}	^{241}Pu	14.29
	^{237}Np	2.14×10^{6}	^{241}Am	432.6
	^{243}Am	7.37×10^{3}	^{244}Cm	18.1

These high level canister are stored and cooled in an interim storage facility for about 30-40 years [Sundar Rajan et al., 1980] and after that they are supposed to be disposed of in deep geological repository (DGR). To ensure long term isolation of the disposed radionuclides from the surrounding environment a multi-barrier concept is adopted [Chapmann et al., 1987]. In this design concept clay buffer materials are placed surrounding the canister in disposal pit in the host rock media. The clay being a very low water permeable material acts as a barrier for ingress of water from the surrounding host rock to the canister and thus prevent corrosion of canister material. The negatively charged clay minerals trap radionuclides which leached out from the canister by diffusion or dissolution process when canister becomes corroded or failed due to any accidental reason, such as earth quake. In addition to the above mentioned functionalities clay buffer also provides swelling pressure which helps to keep the canister in its initial disposal position. These canister and clay buffer are called engineered barrier and the surrounding host rock is called natural barrier, which provides additional confinement to the radionuclides when they come out from the clay buffer region. All the above mentioned activities involved with radioactive waste management practices in India are provided in a detailed report [Raj et al., 2006] as shown in Figure 1.3.

1.4 Deep geological repository program in India

Disposal of high level vitrified waste forms into a specially designed DGR is the most feasible options available for long term isolation of HLW from the environment. In India, work on DGR in the form of experiments and site selection stated long back in early eighties. The first attempt towards this approach was to study the impact of heat emitted by radioactive waste on the properties of in-situ host rock. Researches carried out single and multiple heater test experiment in a generic underground research laboratory (URL) at a depth of 1000 m at Kolar gold field [Mathur et al., 1998]. The basic aims of this experiment were to examine thermal, mechanical, hydrological and chemical behavior of the host rock under simulated conditions and validation of in-house developed computational tools for simulation of various processes. Site selection for DGR is an ongoing research activity in Indian since the early 90s [Mathur et al., 1996]. In Indian context granite rock formation are considered to be suitable rock formation for hosting DGR [Mathur et al., 1996]. Details of site characterization criterion adopted in India can be found in the literature [Arumugam et al., 1994; Bajpai, 2008]. A schematic view of a disposal pit in Indian DGR is shown in Figure 1.2 [Goel et al., 2003]. Experimental and numerical studies on heat dissipation, solute transport and thermo-hydro-mechanical process in DGR are also being carried out actively [Verma et al., 2011, 2015].

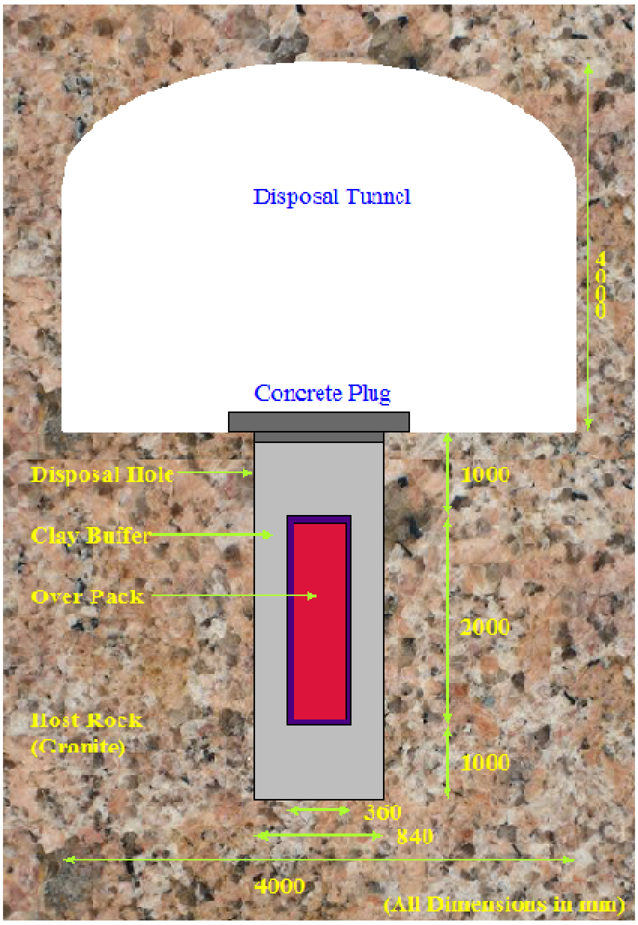

Figure 1.2: Schematic of a vertical disposal pit in DGR

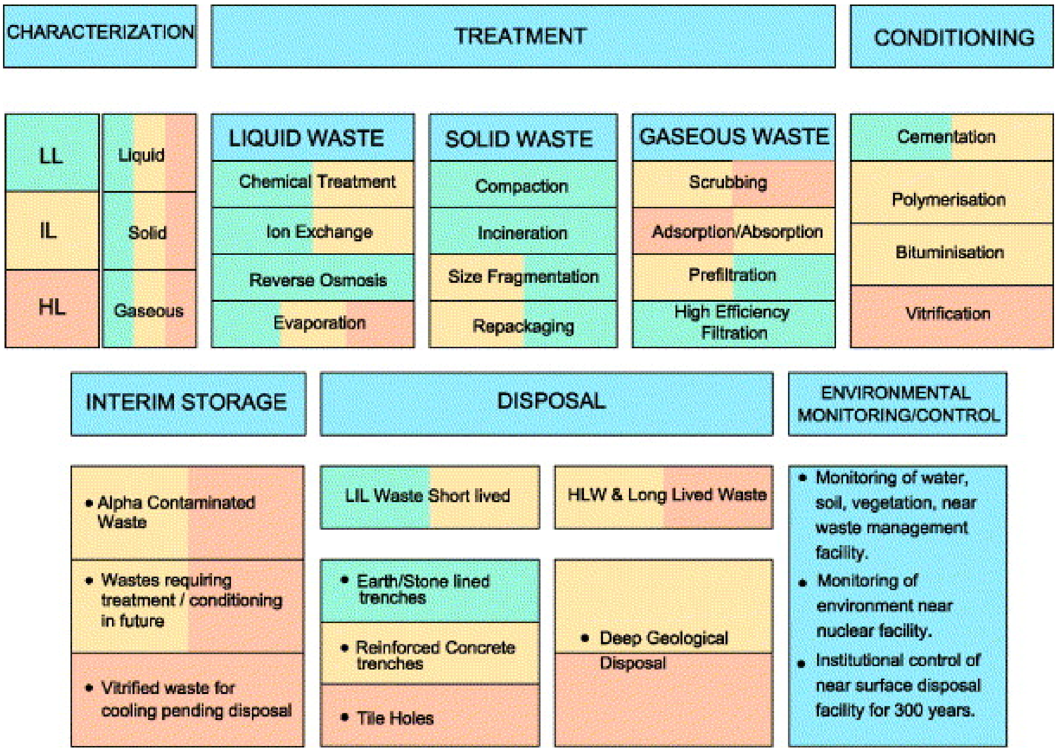

Figure 1.3: Management of radioactive waste in India (Raj et al., 2006)

1.5 Literature survey

1.5.1 Multi-component and long term reactive transport

There are two distinct scales at which multi-component and long term reactive transport are generally studied, which are (1) pore scale and (2) representative elementary volume (REV) scale [Bear, 1972; Zhang et al., 2000]. Pore scale studies are useful to understand the actual physical and chemical processes happening at microscopic level. Since most of the chemical reactions such as dissolution, precipitation, surface complexation and ion exchange occur at mineral surface and geological porous media are highly heterogeneous, pore scale study of reactive transport provide more realistic assessment of the actual process than REV scale study. For example, the above mentioned reactions at pore scale can modify the properties of the media, thereby altering the values of hydro-geological parameters (porosity, permeability), which has direct impact on flow and transport process at REV scale [Hoefner et al., 1998; Molins et al., 2012]. However, pore scale reactive transport simulation requires actual geometry of the porous media, which is generally obtained from tomographic images [Bultreys et al., 2016], and the domain size is limited to relatively small scale because of huge demand for computational storage and computing speed [Gao et al., 2015]. REV scale study is one type of upscaling of pore scale study. In this study pore scale heterogeneity of the media is not taken into consideration directly rather their existences are modeled as parameters of the macroscopic equations that are obtained via homogenization of pore scale model equations over the REV. In this study we have adopted REV scale study of multi-component and long term reactive transport.

Pore scale study

Though REV scale models are generally applied for large scale engineering problem, the unresolved heterogeneities at pore scale together with use of empirical parameters leads to its failure for modeling actual scenarios occurring even at laboratory scale experiments [Levy et al., 2003]. Since most of the chemical reactions, such as dissolution, precipitation, surface complexation, ion exchange, occur at mineral surface and geological porous media are highly heterogeneous, pore scale study of reactive transport provide more realistic assessment of the actual process than REV scale study. Pore scale study of flow and reactive transport through porous media are generally carried out using following three techniques (i) mesoscopic techniques such as LBM, (ii) smoothed particle hydrodynamics (SPH), and (iii) pore network method.

REV scale study

Transport of radionuclides through aquatic media due to physical processes (e.g., advection, molecular diffusion and mechanical dispersion) is affected by various chemical reactions, such as ion exchange, surface complexation, adsorption, desorption, absorption, precipitation, dissolution etc. There are generally two distinct modes for handling chemistry that play crucial role for modeling migration of radionuclides from the radioactive waste disposal area to the environment. In one mode of approach, effects of chemical reactions, such as ion exchange, surface complexation, adsorption, absorption etc., are treated together with the help of some empirical models known as sorption isotherms. Various empirical isotherms, such as linear, Freundlich and Langmuir isotherms, are generally used to model the impact of sorption on radionuclide migration. This formulation simplifies the mathematical complexity of multi-component reactive transport model as well as reduces the computation time drastically. Most frequently used isotherm in the study of migration of radionuclides is linear isotherm also known as K_d approach. The multi-component reactive transport equations with linear sorption coefficient have been solved by various authors using analytical [Bauer et al., 2001; Higashi et al., 1980; Lunn et al., 1996; Guerrero et al., 1996; Srinivasan et al., 2008a,b] as well as numerical techniques [Schwartz, 2009; Silveria et al., 2013]. But it has been reported by researchers that K_d-based approach provides results that are inconsistent with laboratory and fields observations [Bethke et al., 2000, and references there in]. The reason behind the inconsistency given by Brady and Bethke [Brady et al., 2000] and Bethke and Brady [Bethke et al., 2000] is that isotherm based approaches are not capable of accounting for the effects of variable chemical conditions, such as pH, presence of other competitive ions, on the sorption reactions.

The other mode for treatment of the above mentioned chemical reactions in a hydro-geological system (open system) is based on incorporation of model equation of the individual chemical reaction into the transport equation. This approach is more robust in modeling the actual geochemical condition prevailing at the waste disposal site. This kind of approach was initially formulated with the reference to reaction path model [Helgeson, 1968, 1971; Reed, 1982; Lasaga, 1984], which are applicable to chemical reactions in batch mode (closed system). The mathematical formulation of modern continuum multi-component reactive transport, which could model any kind of biogeochemical reactions in combination with various flow models in geological media, was developed during the mid-1980s [Lichtner, 1985; Lichtner et al., 1988; Krikner et al., 1998; Yeh et al., 1989; Lichtner, 1996]. These kind of models have widely been used in the past to simulate various processes in hydro-geological system [Steefel et al., 1994a,b, 1998a,b; MacQuarrie et al., 2005; Tartakovsky et al., 2008]. Important application of multi-component and long term reactive transport model could be found in the long term alteration study of bentonite barrier in presence of hyper-alkaline solution, generated due to use of cementitious materials in a DGR [Berner et al., 1992; Savage et al., 2002; Gaucher et al., 2004, 2006; Marty et al., 2014, 2015]

1.5.2 Traditional numerical methods for reactive transport

Reactive transport equation or ADRE is a nonlinear partial differential algebraic equation (PDAE). There are three approaches to solve REV scale PDAE [Steefel et al., 1996; Molins et al., 2004; de Simoni et al., 2005], which are (i) sequential non-iterative approach (SNIA) [Walter et al., 1994; Steefel et al., 1996], (ii) sequential iterative approach (SIA) [Yeh et al., 1991; Carrayrou et al., 2004] and (iii) direct substitution approach (DSA) [Saaltink et al., 1998, 2001; de Dieuleveult et al., 2009a,b]. SNIA and SIA are based on operator splitting approach generally used in multi-physics problems. In these approaches transport part, which is modeled as PDE, and reaction part, which is modeled as nonlinear algebraic equations, are treated separately for a given time step. The basic difference between the SNIA and SIA is that there is no iteration between the two solvers (transport and reaction) for SNIA, whereas in SIA the two solvers continue exchanging their solution unless until a given convergence criterion is fulfilled. One of the important drawbacks of SNIA and SIA approaches is that there is a limitation on time step size, which must be smaller than the reaction time of any reaction that need to be model kinetically. In DSA, transport and reaction equations are solved simultaneously. This approach has no time step limitation, but it becomes cumbersome to solve the global matrix for a large number of species [Guo et al., 2013].

In this study, we have adopted operator splitting approach (SNIA) for solving reactive transport equations, because this approach will facilitate the coupling of transport solver with commercial geochemical software. In both SIA and SNIA, the transport equations are generally solved using traditional numerical methods, such as FDM, FEM, FVM. In FDM, the computational model geometry is discretized by rectangular/square cells. The numerical values of parameters of governing equations are same in a single cell and the values of the parameters remain same over all the cells if the media is homogeneous. The nodes are usually set at the center of gravity of each cell and they represent the average concentration of the cell. Volumetric chemical reactions are carried out at each cell after the transport step. Numerical dispersion and numerical instabilities of FDM based solutions are avoided by a high-resolution discretization. The high resolution discretization, however, leads to very long computing times. The Grid-Peclet number and Courant number are used to select grid size and time interval. These criterion can be written as

$$P_e = \frac{|v|\Delta x}{D} \leq 2 \tag{1.1}$$

$$Co = |v\frac{\Delta t}{\Delta x}| \leq 1 \tag{1.2}$$

where D is dispersion coefficient, v is water velocity, Δx and Δt, are grid size and time interval, respectively. Stability of implicit FDM, which applies reverse differences in time, is better than explicit FDM. The time interval of an implicit FDM based solver for reactive transport is controlled by reaction time. Though FEM is more flexible for discretization of complex domain geometry, it also suffers from numerical dispersion and oscillation effects. Various commercial softwares are nowadays available to simulate multi-component reactive transport using traditional numerical methods. The list of such softwares includes PHREEQC [Parkhurst et al., 1999, 2013], OpenGeoSys [Kolditz et al., 2012], HYDROGEOCHEM [Yeh et al., 1990], PFLOTRAN [Hammond et al., 2010], CrunchFlow [Steefel et al., 1994a], TOUGHREACT [Xu et al., 2006, 2011], HYTEC [Van der Lee et al., 2003], HPx (HP1, HP2, HP3) [Jacques et al., 2005; Šimr̊nek et al., 2012, 2013], PHT3D [Prommer et al., 2003, 2010], ORCHESTRA

[Meeussen, 2003], MIN3P [Bea, 2011]. A brief summary of all the above mentioned reactive transport codes is given by Steefel et al. [Steefel et al., 2015] and Zhang et al. [Zhang et al., 2012]

1.5.3 Lattice Boltzmann method for solute and reactive transport

Numerical solution of PDAEs, representing reactive transport of a large number of species, becomes difficult to obtain when various equilibrium as well as kinetic reactions are involved. This becomes more challenging when the required simulation time period is very large. In order to overcome these difficulties researchers have attempted to develop efficient numerical algorithm for multi-component and long term reactive transport. LBM is a relatively new in the field of modeling and simulation method for complex system but has proven to be one of the powerful computational fluid dynamics (CFD) tools [Succi et al., 1991; Chen et al., 1998; Succi, 2001]. It has originated from Lattice Gas Cellular Automata (LGA) method [Frisch et al., 1986], which is a subset of cellular automata (CA) model [Chopard et al., 1998], with an urge to remove initial drawbacks (statistical noise) of the later one [McNamara et al., 1988]. The fundamental difference between the traditional numerical techniques and LBM is that traditional techniques focus on solving algebraic forms of macroscopic equation, whereas LBM solves discrete velocity Boltzmann equation, which models the dynamics of fictitious particles interacting on a lattice in such a way as to reproduce a desired physical or chemical process [Succi, 2001; Wolf-Gladrow, 2000]. Since Boltzmann equation governs the evolution of particle distribution function, which is mesoscopic variable representing particle density, the LBM is a mesoscopic technique. It has a finer description of the physical quantities than traditional schemes, because the later ones deal with macroscopic variables (such as density of fluid, solute concentration, temperature), which are various velocity moments of the distribution function. The inherent parallel structure of LBM algorithm has provided a fundamental scope of better utilizing modern computer architecture as in graphical processing units. Another major advantage of LBM is due to its simple bounce-back boundary condition, which can be easily implemented in a complex geometry such as porous media. The explicit nature of LB update scheme has attracted many researchers for applying LBM in various research domains.

Since its inception as a mesoscopic technique that can simulate fluid flow, particularly Navier-Stokes equation (NSE), LBM has been successfully applied to solve various kind of fluid dynamics problems, such as flow though complex boundary geometries (porous media), two phase flow, turbulence flow, microfluidics [Zhang, 2011; Guo et al., 2006] etc. In the last two decades, LBM has emerged as a promising numerical scheme that can solve a set of partial differential equations representing various other science and engineering problems, such as diffusion-reaction [Dawson et al., 1993; Qian et al., 1995; Chen et al., 1995], ADE[Flekky, 1993; Van der Sman et al., 2000; Zhang et al., 2002; Ginzburg, 2005; Stiebler et al., 2008; Zhou, 2009], electrochemical transport [He et al., 2000a; Wang et al., 2010], reactive transport [Kang et al., 2006, 2007, 2010b; Hiorth et al., 2013], wave motion [Yan et al., 2000], traffic flow [Yan et al., 2000], image analysis [Jawerth et al., 1999] etc. In the rest of this section, a comprehensive review of all popular works done thus far by researchers to simulate multi-component reactive transport using LBM is presented.

LBM has been applied to solve multi-component reactive transport in geological porous media at two different scales: pore scale and representative elementary volume (REV) scale [Bear, 1972; Zhang et al., 2000].

Kang et al. developed a LBM based multi-component reactive transport model at pore scale to study chemical dissolution in porous media [Kang et al., 2002]. They used their model to simulate dissolution of rock and subsequent formation of wormhole when acidic solution was injected into the media. They treated the heterogeneous dissolution reaction at solid surface through proper boundary conditions at solid surface. They further incorporated precipitation reaction into their model and studied impact of flow velocity on reaction rate [Kang et al., 2003]. In their recent progress on LBM based multi-component reactive transport, they considered both homogeneous reactions among aqueous species and heterogeneous reactions with solid surface [Kang et al., 2006, 2007] and applied the model for CO_2 sequestration [Kang et al., 2010a,b], changes in permeability and porosity of porous media due to dissolution reaction [Kang et al., 2014; Chen et al., 2014, 2015, 2018a]. Pore scale LB based multi-component reactive transport was further developed and used in CO_2 sequestration with experimental validation [Tian et al., 2014; Yoon et al., 2015; Gao et al., 2017; Tian et al., 2018; Chen et al., 2018b]. More sophisticated geochemical model, which includes ion exchange and surface complexation in addition to dissolution and precipitation, was developed by Hiorth [Hiorth et al., 2013]. All the above formulations modeled the heterogeneous reactions at the solid surface using boundary flux formulations and application of these type of LB based multi-component reactive transport was restricted to relatively simple geochemical reactions. In order to simulate more complex geochemical problems, there was a need to interface LB based solute transport model with commercial geochemical software. In this regard, Patel et al. developed a coupling scheme that was able to make use of geochemical software, PHREEQC, in the pore scale LB framework [Patel et al., 2013]. They considered the addition or removal of solute mass from the aqueous phase due to dissolution and precipitation reactions as source term and this concept facilitated the coupling with commercial geochemical software. They used the interfaced scheme to simulate degradation of concrete due to various chemical reactions [Patel et al., 2014, 2018; Fazeli et al., 2018].

Apart from the above mentioned development of LBM based reactive transport simulation, there has been another trend in development of reactive transport solver using mixed numerical techniques, such as LBM interfaced with FDM [Albuquerque et al., 2004; Van Leemput et al., 2003], LBM interfaced with FEM [Zhang et al., 2014a,b], LBM interfaced with FVM [Chen et al., 2012, 2013]. In this study, we have followed the previous development, i.e., LBM based transport solver interfaced with commercial geochemical software.

1.5.4 Differential quadrature method for solute and reactive transport

Differential quadrature method (DQM) is a numerical technique for solving linear and non-linear differential equations. Historically it was developed as an analogous to numerical integration technique called numerical quadrature. In numerical quadrature, definite integral over a closed domain is approximated by a linear weighted sum of the values of the integrand at a group of points in the domain of integration, similarly in DQM, partial derivative of a piecewise continuous function at any discrete point in the computational domain is approximated as weighted linear sum of functional values at all other discrete points along the line that passes through that point, which is parallel with coordinate direction of the derivative. This method was introduced by Richard Bellman and his associates in the early of 1970s [Bellman et al., 1971, 1972] while searching for a numerical method that can provide accurate solution of non-linear PDE with minimum number of grid points. It has further been advanced by the work of Shu [Shu, 2000] and has been successfully used to solve various linear and non-linear differential equations appear in science and engineering domain with faster computation and accurate solution[Jang et al., 1989; Shu, 1991; Sherbourne et al., 1991; Shu et al., 1992; Civan et al., 1983; Du et al., 1995, 1996; Laura et al., 1994; Bert et al., 1996; Shu, 2000].

The concept of DQM is very simple and it can be implemented straightforwardly. Since DQM requires very few grid points for solving differential equations with high accuracy, minimum computational efforts are required to implement it [Bellman et al., 1972; Malik et al., 1995; Bert et al., 1996]. The formulation of DQM is totally based on two important consideration which are (1) how the weight coefficients are determined and (2) how the grid points are selected. There are two approaches to determine the weight coefficients which are (1) solving a system of linear equations and (2) using approximation theory. The first approach was proposed by Bellman [Bellman et al., 1972] and the second one was formulated by Quan [Quan et al., 1989a,b]. In fact, Bellman proposed two methods which are based on same principle of solving a system of linear equations but with different options for grid point selections. In one of the Bellman's approach grid points can be selected arbitrarily, whereas in the other one grid points are roots of the shifted Legendre polynomial [Bellman et al., 1972]. Further development towards determination of weight coefficient was done by Shu [Shu, 1991, 2000]. In approximation theory based approach the unknown solution of the differential equation is first written in term of basis function, also called test function, using linear vector space analysis and function approximation theory. There are three frequently used bases which are polynomial basis, Fourier expansion basis, and harmonic basis [Shu, 2000]. Accordingly, considering the particular base function used for calculation of weight coefficient the related DQM is called polynomial differential quadrature method (PDQM), Fourier expansion based differential quadrature method (FDQM), and harmonic differential quadrature method (HDQM), respectively. Among the aforementioned DQMs, the most popular one is PDQM, because it is applicable for most of the engineering problems except those which have periodic and harmonic behaviors. FDQM and HDQM are generally used for engineering problems having periodic and harmonic behaviors, respectively. Various polynomial functions, such as Legendre polynomials [Bellman et al., 1972], Lagrange interpolation polynomials [Quan et al., 1989a,b; Shu et al., 1992], Hermite polynomials [Cheng et al., 2005], are used as a test function in PDQM. However, the most frequently used PDQM is based on Lagrange interpolation polynomials.

Since solution of ADE is not having any periodicity or harmonicity, PDQM with Lagrange polynomial as the basis function is used in this thesis for solving solute transport model equation. Kaya [Kaya, 2010] solved ADE using PDQM with Lagrange polynomial as the basis function and compared the results with the solutions obtained using explicit and implicit FDM. He concluded that DQM based results are more accurate than the results obtained using FDM schemes and same accuracy can be obtained if number of grid points for FDM are increased. His study also showed that DQM computation is 50-500 times faster than FDM computation. Aswin et al. solved convection diffusion equation using mixed FDM and DQM [Aswin et al., 2015]. They demonstrated three different numerical schemes, which includes finite difference in time and differential quadrature in space (FDTDQS), differential quadrature in time and finite difference in space (DQTFDS), and differential quadrature in time and differential quadrature in space (DQTDQS). They concluded that accuracy of results improves if more number of derivatives are approximated using DQM and therefore, DQTDQS scheme provides more accurate results than the other two schemes.

1.5.5 Modeling uncertainty analysis in solute transport and reactive transport model

The unresolved heterogeneities at pore scale together with use of empirical model parameters leads to uncertainty in model output of a REV scale solute transport and reactive transport model. This kind of uncertainty belongs to the category of model uncertainty. Another important source of uncertainty in the model output is special heterogeneity of geological media. Because of this spatial heterogeneity, the REV scale model parameters can not be represented by a single (crisp) value. In fact, single value of model parameters represent a homogeneous media, which is not true in general. One way to resolve this heterogeneity is to establish the relationship between the parameters and the spatial coordinate and use that relation in the numerical model. But, it is almost impractical to experimentally measure the values of the model parameters at each and every location. Another way of treating this spatial heterogeneity is to consider the model parameter as uncertain and propagate this parameter uncertainty through the model so that output of the model can be represented as a crisp value with an error bar. This kind of uncertainty is referred as parametric uncertainty. The objective of these type of models is to cast the processes in heterogeneous geologic media into an equivalent quasi-homogeneous processes. Now our next task is to represent these uncertain parameters with the help of some mathematical tool for uncertainty analysis. There are two broad classes of uncertainty analysis which are (i) aleatory uncertainty or stochastic uncertainty and (ii) epistemic uncertainty [Ayyub et al., 2006]. Quantification of stochastic uncertainty is done by Monte Carlo method, whereas epistemic uncertainty is quantified using fuzzy set theory.

Uncertainty analysis of solute transport simulation was carried out by Dou et al [Dou et al., 1997] using fuzzy set approach. They employed explicit FDM to solve both one- and two-dimensional ADE with imprecise model parameters such as groundwater velocity and dispersivity. Baraldi et al. calculated uncertainty in ground water flow model using both probability theory and Dempster-Shafer theory and compared the two results [Baraldi et al., 2010].

1.6 Lattice Boltzmann method

Since Lattice Boltzmann method has been adopted in this thesis as a numerical framework for multi-component and long term reactive transport, it is worth introducing the theoretical background and general implementation of lattice Boltzmann method (LBM) here, before applying it in the subsequent chapters. There are basically two distinct approaches to simulate the behavior of physical system, which are 'top down' and 'bottom up' approaches [Wolf-Gladrow, 2000]. The 'top down' approaches solve discretized forms of partial differential equations (PDEs), which model the macroscopic phenomena of the system of interest, whereas 'bottom up' approaches solve the microscopic equations, which model the dynamics of particles inside the system. Traditional numerical simulation techniques (FDM, FEM, FVM) fall under the category of 'top down' approaches, whereas Monte Carlo (MC) simulation of molecular dynamics, LBM falls under the category of 'bottom up' approach. In fact, the LBM is also described as a mesoscopic approach, because it solves the dynamics of mesoscopic variable called particle distribution function. In LBM discrete particles residing at regular lattice nodes stream towards a neighboring lattice node in a particular lattice direction and collide with the particle residing on that neighboring lattice node. The kinetics of these particles is governed by lattice Boltzmann equation, which is basically a finite difference scheme of the discrete velocity Boltzmann equation. Implementation of LBM is based on this concept of streaming and collision processes. This simple kinetic model of LBM is well enough to simulate various processes, such as fluid flow, mass transport, heat transport, wave motion etc [Chen et al., 1998; Succi, 2001]. In this section, we will cover a brief overview of the origin of LBM, derivation of lattice Boltzmann equation (LBE) and its general implementation.

1.6.1 Origin of lattice Boltzmann method

The lattice Boltzmann equation (LBE), which models the evolution of discrete velocity distribution function, can be derived from the continuum Boltzmann equation [He et al., 1997; Shan et al., 2006]. Historically, however, LBE was derived from discrete particle lattice gas cellular automata (LGCA) model [Wolf-Gladrow, 2000], which is a subset of cellular automata (CA) [Chopard et al., 1998]. A brief overview of the historical background of the LBM and its precursors, the CA and LGCA is presented in the following. For extended information, the reader may refer to the literatures [Chopard et al., 1998; Wolf-Gladrow, 2000; Succi, 2001].

Cellular automata

A CA model can be defined as a set of N number of cells placed in a regular grid, where each cell has a state from a finite number of possible discrete states [Wolf-Gladrow, 2000]. The states of all the cells get updated simultaneously after each discrete time step following some deterministic rules. This updating rule operates locally i.e. the new state of a cell depends upon the states of the neighboring cells including its own [Datta et al., 2016b]. As an illustrating example, we consider a one-dimensional CA consisting of 100 cells with only two possible states

(0 or 1) for each cell. The boundary cells are set to 0 and are not updated. The updating rule for the interior cells depends on the states of its neighbors and the cell itself. Therefore, each interior cell can be characterized by a local configuration in the form of a triplet s_{i-1}, s_i, s_{i+1}, where s_i is the state of the cell itself and s_{i-1}, s_{i+1} are the state of the left hand side cell and right hand side cell, respectively. For the two state CA there will be following 8 possible local configuration of each interior cell.

$$\begin{array}{cccc} (0,0,0), & (0,0,1), & (0,1,0), & (0,1,1) \\ (1,0,0), & (1,0,1), & (1,1,0), & (1,1,1) \end{array}$$

Therefore, any update rule r can assign any one of the above configuration to a local configuration. Since each state has two independent states (0,1), the total number of possible update rule for a one-dimensional CA is therefore $2^8 = 256$. The state s_i of the i^{th} interior state is then updated to a new state $s_i^{'}$ as

$$s_i^{'} = r(s_{i-1}, s_i, s_{i+1}), \quad i = 2, 3, ..., 99$$

Lattice gas cellular automata

LGCA are derivative of classical CA. The main difference between the CA and the LGCA lies in the update rule, which for the LGCA is split into two parts usually called collision and propagation. Furthermore, the LGCA conserve explicitly mass and momentum and because of these conservation LGCA simplify the construction and application of automata to given physical processes [Wolf-Gladrow, 2000]. LGCA aims to simulate fluid flows with simple fluid model. In LGCA, the fluid is treated as a set of simulated particles residing on a regular lattice with certain symmetry properties, where they collide and stream following some prescribed rules that satisfy some necessary physical laws. The philosophy behind the LGCA is that fluid behaviors at macro-scale are nothing but statistical collective results of the micro-dynamics of fluid molecules, and are insensitive to the detailed information of the individual molecules. In other words, fluids with different micro structure and interactions may have the same macroscopic phenomena. Therefore, it is possible to simulate macroscopic flows with a fictitious micro fluid model which has simple micro-dynamic but satisfies some necessary physical laws. In 1973, LGCA was proposed for the first time by three French scientists, Hardy, de Pazzis and Pomeau and the model is known as HPP model [Hardy et al., 1973]. They proposed the LGCA as a new technique for the study of Navier-Stokes equation (NSE) by simulating very simple microscopic system, where particles are allowed to move in a regular lattice, and a set of local collision rules are introduced on the nodes which conserve the mass and momentum. Mathematically, the motion of the particles in HPP model can be described as a set of discrete kinetic equations as

$$\begin{gathered} n_i(\vec{r}+\vec{e_i}\Delta t, t+\Delta t) = n_i(\vec{r},t) + \Omega_i\left(n\left(\vec{x},t\right)\right), \text{with} \\ \left(n\left(\vec{x},t\right)\right) = \left(n_1\left(\vec{x},t\right), n_2\left(\vec{x},t\right), ..., n_k\left(\vec{x},t\right)\right)^T \end{gathered} \tag{1.3}$$

where $n_i(\vec{x},t)$ is having two states represented by the binary digits 0 and 1, where state value 0 represents that cell i is not occupied by a particle and state value 1 signifies that cell i is occupied by a particle which is moving with discrete velocity $\vec{e_i}$ at node x and time t, Δt is the time step, and Ω_i is the collision operator that model the influence of particle collision. The collision operator is chosen in such a way that it conserve the number of particle and momentum. The particle evolution equation (1.3) can be decomposed into two sub-process, called collision and streaming, as

$$\begin{aligned} &\text{Collision:} \qquad n_i^{'}(\vec{r},t) = n_i(\vec{r},t) + \Omega_i\left(n\left(\vec{x},t\right)\right) \\ &\text{Streaming:} \qquad n\left(\vec{x}+\vec{e_i}\Delta t, t+\Delta t\right) = n_i^{'}(\vec{r},t) \end{aligned} \tag{1.4}$$

Macroscopic flow variables such as density, velocity, and temperature are calculated from the ensemble average of the Boolean variable, $f_i =< n_i >$ as

$$\begin{aligned} \rho &= \sum_{i=1}^{k} m f_i \\ \rho \vec{u} &= \sum_{i=1}^{k} m \vec{e_i} f_i \\ \rho E = \rho R T &= \sum_{i=1}^{k} \frac{m}{2} \left(\vec{e_i} - \vec{u_i} \right)^2 f_i \end{aligned} \tag{1.5}$$

Although HPP model satisfies the conservation of mass and momentum, it fails to represent the correct form of momentum flux tensor as required by Navier-Stokes equations (NSE). This failure is due to the square lattice used in the HPP model. This kind of lattice is not able to produce specific isotropic tensor of rank four which is required to obtain the correct form of NSE [Wolf-Gladrow, 2000]. In 1986, Frisch, Hasslacher and Pomeau used triangular lattice in their LGCA model and they were able to overcome the limitation of the HPP model. Their LGCA model, which was a milestone that motivated further developments of the LGA and their application in a wide range of real problems, is known as FHP model [Frisch et al., 1986].

Lattice Boltzmann method from lattice gas cellular automata

Although FHP model of LGCA is able to simulate correct hydrodynamic equations (NSE), there are few drawbacks in LGCA which are: large statistical noise in the computed macroscopic parameters (1.5) due to the use of Boolean variable in LGCA, non-Galilean invariance, number of physical parameters that can be derived from LGCA are limited to few, and requirement of high computational effort to obtain reasonable macroscopic quantities by averaging procedure [Wolf-Gladrow, 2000; Succi, 2001]. To circumvent these drawbacks, McNamara and Zanetti replaced the binary populations of LGCA by average value having interval [0, 1]. These average values represent particle distribution functions and by this consideration they were able to avoid the averaging process required in LGCA. This remarkable consideration came to the scientific community in 1988 [McNamara et al., 1988] and their work is considered as the origin of LBM. At the same time Higuera and Jimenez also proposed the formulation [Higuera et al., 1989a]. In the original LBM, calculation of equilibrium distribution function (EDF) and relaxation matrix were carried out using the underlying LGCA models. Higuera et al. further suggested that LBE can be derived independently of underlying LGCA [Higuera et al., 1989a]. Further development of LBE was done by Qian et al. who suggested that the collision term of LBE can be replaced by a linear term with a single relaxation parameter [Qian et al., 1992] similar to one proposed by Bhatnagar et al. [Bhatnagar et al., 1954]. This model of LBM is known as Bhatnagar-Gross-Krook (BGK) LBM, which is the most popular LB scheme till date due to its algorithmic simplicity. In this BGK LBM, the governing equation for LGCA (1.3) is changed into the LBE

$$f_i\left(\vec{x}+\vec{e_i}\Delta t, t+\Delta t\right) = f_i\left(\vec{x},t\right) + \frac{\Delta t}{\tau}\left(f_i\left(\vec{x},t\right) - f_i^{eq}\left(\vec{x},t\right)\right) \tag{1.6}$$

with lattice vector $\vec{e_i}$ and equilibrium distribution function (EDF), $f_i^{eq}\left(\vec{x},t\right)$, which can be derived from Maxwell-Boltzmann velocity distribution function (discussed in second chapter). The macroscopic quantities are the velocity moments of the distribution function

$$\begin{aligned}
\rho &= \sum_{i=1}^{k} f_i \\
\rho\vec{u} &= \sum_{i=1}^{k} \vec{e_i} f_i \\
\rho E = \rho RT &= \sum_{i=1}^{k} \frac{1}{2}\left(\vec{e_i}-\vec{u_i}\right)^2 f_i
\end{aligned} \tag{1.7}$$

Since after collision particle distribution function relaxes towards EDF, the required mass and momentum conservation are achieved by enforcing following conditions

$$\begin{aligned} &\text{Mass conservation:} && \sum_{i=1}^{k} f_i\left(\vec{x},t\right) = \sum_{i=1}^{k} f_i^{eq}\left(\vec{x},t\right) \\ &\text{Momentum conservation:} && \sum_{i=1}^{k} f_i\left(\vec{x},t\right)\vec{e_i} = \sum_{i=1}^{k} f_i^{eq}\left(\vec{x},t\right)\vec{e_i} \end{aligned} \tag{1.8}$$

This BGK LBM scheme is also known as single relaxation time (SRT) LBM. This scheme of LBM has some limitations in terms of stability of numerical solution. Stability of SRT LBM scheme is a function of its relaxation parameter and for stable solution the value of this parameter should be in the interval [0.5, 2]. Also this scheme of LBM is not able to simulate anisotropic processes. Further research to overcome these limitation has developed following two schemes: two relaxation time (TRT) LBM and multi relaxation time (MRT) LBM.

1.6.2 Boltzmann equation

In the previous section we have discussed about the historical origin of LBM from LGCA. After the work by He et al. [He et al., 1997], LBM is treated as a special finite difference scheme of Boltzmann equation. Therefore, it is worth having discussions on Boltzmann equation before using the same for the derivation of LBE. Boltzmann equation also known as Boltzmann transport equation, formulated by Austrian physicist Ludwig Boltzmann, is the governing equation for the evolution of particle distribution function with time.

The Boltzmann equation also known as the Boltzmann transport equation, devised by Ludwig Boltzmann, describes the statistical distribution of particles in a fluid. It is an equation for the time evolution of $f(\vec{x},\vec{p},t)$,the particle distribution function in the phase space. Phase space here can be viewed as a space in which coordinates are given by the position and momentum vectors at the time. The distribution function, $f = f(\vec{x},\vec{p},t)$, gives the probability of finding a particular molecule with a given position and momentum.

In this section, derivation of Boltzmann equation using the principle of conservation of particle in collision is given. The particle distribution function f is a function of space, time and particle velocity and therefore written as $f = f(\vec{x}, \vec{e}, t)$. The number of particle within a phase space volume $\Delta\vec{x}\Delta\vec{e}$ at phase space location $(\vec{x}, \vec{e})$ at time t is denoted as $f(\vec{x}, \vec{e}, t)\Delta\vec{x}\Delta\vec{e}$. These particles move according to the equation of motion of the system and after a time interval of Δt reach to the location $(\vec{x}+\vec{e}\Delta t, \vec{e}+\frac{\vec{F}}{m}\Delta t)$, where m is the mass of a single particle, $\vec{F}$ is external force, such as gravity, acting on the particles. Collisions between the particles are the cause of lose of particles during this period of time (Δt). Therefore, using the principle of conservation of particle we can write

$$f\left(\vec{x} + \vec{e}\Delta t, \vec{e} + (\vec{F}/m)\Delta t, t + \Delta t\right) - f\left(\vec{x}, \vec{e}, t\right) = \Omega \tag{1.9}$$

where Ω is called collision operator. Now using Taylor series expansion we get

$$\frac{\partial f\left(\vec{x}, \vec{e}, t\right)}{\partial t} + \vec{e}.\vec{\nabla}_{\vec{x}} f\left(\vec{x}, \vec{e}, t\right) + \frac{\vec{F}}{m}.\vec{\nabla}_{\vec{e}} f\left(\vec{x}, \vec{e}, t\right) = \Omega \tag{1.10}$$

where repeated indices follow Einstein summation convention. In absence of external force ($\vec{F} = 0$), we can simplify the above equation as

$$\frac{\partial f\left(\vec{x}, \vec{e}, t\right)}{\partial t} + \vec{e}.\vec{\nabla}_{\vec{x}} f\left(\vec{x}, \vec{e}, t\right) = \Omega \tag{1.11}$$

The above two equations (1.10 and 1.11) are the famous Boltzmann equations in presence of external force and in absence of external force, respectively [Chapman et al., 1991].

1.6.3 Implementation of lattice Boltzmann method

In this section, we have discussed the lattice Boltzmann algorithm and its implementation. We first rewrite the LBE (1.6)

$$f_i\left(\vec{x}+\vec{e_i}\Delta t, t+\Delta t\right) = f_i\left(\vec{x},t\right) + \frac{\Delta t}{\tau}\left(f_i\left(\vec{x},t\right) - f_i^{eq}\left(\vec{x},t\right)\right) \tag{1.12}$$

If we decompose the time step involved with the above equation into two (one for collision process and another for streaming) then Eq. (1.13) can be solved in two steps. One step represents collision process and other one represent streaming process. The two steps can be written in mathematical form as

Collision

The collision process update the equilibrium distribution function locally as

$$f_i^{\star}\left(\vec{x},t\right) = f_i\left(\vec{x},t\right) + \frac{\Delta t}{\tau}\left(f_i\left(\vec{x},t\right) - f_i^{eq}\left(\vec{x},t\right)\right) \tag{1.13}$$

where $f_i^{\star}\left(\vec{x},t\right)$ is the post collision distribution function.

Streaming

In the streaming process post collision distribution function reach to its nearest neighbor through a given velocity direction as

$$f_i\left(\vec{x}+\vec{e_i}\Delta t, t+\Delta t\right) = f_i^{\star}\left(\vec{x},t\right) \tag{1.14}$$

It can be observed from the above two equations (1.13 and 1.14) that out of the two processes only collision process involves algebraic calculations, whereas streaming process is just swipe in memory. Both the collision and streaming process are executed in a single operation, known as ”collide-and-stream” operation. This consideration is very advantageous for the implementation as it allows better performance and a optimization in memory requirement [Wellein et al., 2006; Mattila et al., 2007, 2008]

1.7 Differential quadrature method

In this section, we have briefly reviewed the mathematical formulations of PDQM. More detailed formulations are given in standard text books on DQM [Shu, 2000; Zong et al., 2009; Wang et al., 2015]. Since weight coefficients and grid point selections are the two most important steps for formulation of DQM, it is worth reviewing these aspects.

1.7.1 Differential quadrature equation

The DQ approximation of the k^{th} order derivative of a continuous function, $f(x)$, at i^{th} node point is given by weighted linear sum of the function values at all discrete node points along the direction of x as

$$f_x^k\left(x_i\right) = \frac{\partial^k f}{\partial x^k}\mid_{x=x_i} = \sum_{j=1}^{N} A_{ij}^{(k)} f\left(x_j\right), \quad i,j = 1,2,3,...,N \tag{1.15}$$

where x_j are the discrete nodes in the domain at which function values are known, $f(x_j)$ are the function values at these nodes, N is the total number of such nodes, and $A_{ij}^{(k)}$ are the weight coefficients for the k^{th} order derivative of the function, therefore for a N point DQM, $A_{ij}^{(k)}$ are the elements of a $N \times N$ matrix. DQ equation of a PDE is formulated by substituting the derivatives of the PDE with these approximate values. Using the above formula (1.15) first order and second order derivatives of $f(x)$ with respect to x can be written as

$$\begin{aligned} f_x^1\left(x_i\right) &= \frac{\partial f}{\partial x}\mid_{x=x_i} = \sum_{j=1}^{N} A_{ij}^{(1)} f\left(x_j\right), \quad i = 1,2,3,...,N \\ f_x^2\left(x_i\right) &= \frac{\partial^2 f}{\partial x^2}\mid_{x=x_i} = \sum_{j=1}^{N} A_{ij}^{(2)} f\left(x_j\right), \quad i = 1,2,3,...,N \end{aligned} \tag{1.16}$$

where $A_{ij}^{(1)}$ and $A_{ij}^{(2)}$ are the weight coefficients for the first and second order derivatives of the function, $f(x)$, with respect to x, respectively.

1.7.2 Determination of weight coefficients for differential quadrature method

Here we have derived the weight coefficients, $A_{ij}^{(k)}$, using approximation theory which works on how well a function can be approximated with simpler functions. In this procedure the function, which need to be approximated, is first written in terms of basis functions of a linear vector space. For a PDQM, this linear vector space is a polynomial vector space and various polynomials, such as Lagrange polynomials, Legendre polynomials, Hermite polynomials, are the basis functions. We take here Lagrange polynomials as the basis functions. Lagrange polynomials are used for interpolating discrete data set of a function, e.g., if x_1, x_2, x_3, ..., x_{n-1}, x_n are n discrete nodes at which the functional values are known then the interpolating polynomial, p, is written using Lagrange interpolation formula as

$$p(x) = \sum_{k=1}^{n} \lambda_k(x) f(x_k) \tag{1.17}$$

where $f(x_k)$ is the value of the unknown function, f, at x_k node point and λ_k is called Lagrange basis polynomials, which is defined as

$$\begin{aligned} \lambda_k(x) &= \prod_{j=1, j\neq k}^{n} \frac{x - x_j}{x_k - x_j} = \frac{M_k(x)}{M_k(x_k)} \\ M_k(x) &= \prod_{j=1, j\neq k}^{n} (x - x_j) \end{aligned} \tag{1.18}$$

If we consider the initial values of the solution of a PDE, which are provided by the given initial condition of the problem being solved, as the known values of our unknown solution of the PDE, then the above formulas can be utilized to approximate the solution of the PDE.

Therefore, the solution of the PDE can be approximately written as

$$f(x) \approx \sum_{k=1}^{n} \lambda_k(x) f(x_k) \tag{1.19}$$

Now, first and second order derivatives of the above solution (1.19) can written as

$$\begin{aligned} \frac{\partial f(x)}{\partial x} &\approx \sum_{k=1}^{n} \frac{\partial \lambda_k(x)}{\partial x} f(x_k) = \sum_{k=1}^{n} A_k(x) f(x_k) \\ \frac{\partial^2 f(x)}{\partial x^2} &\approx \sum_{k=1}^{n} \frac{\partial^2 \lambda_k(x)}{\partial x^2} f(x_k) = \sum_{k=1}^{n} B_k(x) f(x_k) \end{aligned} \tag{1.20}$$

We can calculate the first order derivative of the Lagrange basis polynomials using Eq. (1.18) as [Shu, 2000; Zong et al., 2009]

$$\begin{aligned} a_k(x) = \frac{\partial \lambda_k(x)}{\partial x} &= \frac{1}{M_k(x_k)} \frac{\partial M_k(x)}{\partial x} \\ &= \frac{1}{x - x_k} \sum_{l=1, l\neq k}^{n} \frac{M_l(x_l)}{M_k(x_k)}, \quad if \;\; x \neq x_k \quad k = 1, 2, ..., n \\ &= \sum_{l=1, l\neq k}^{n} a_l(x) \frac{M_l(x_l)}{M_k(x_k)}, \quad if \;\; x = x_k \quad k = 1, 2, ..., n \end{aligned} \tag{1.21}$$

From the above Eq. (1.21), the coefficient of second order derivative can be calculated as [Shu, 2000; Zong et al., 2009]

$$\begin{aligned} b_k(x) = \frac{\partial^2 \lambda_k(x)}{\partial x^2} &= \frac{\partial A_k(x)}{\partial x} \\ &= \sum_{l=1, l\neq k}^{n} a_l(x) \frac{M_l(x_l)}{M_k(x_k)} - \frac{A_k(x)}{x - x_k}, \quad if \;\; x \neq x_k \quad k = 1, 2, ..., n \\ &= \frac{1}{2} \sum_{l=1, l\neq k}^{n} b_l(x) \frac{M_l(x_l)}{M_k(x_k)}, \quad if \;\; x = x_k \quad k = 1, 2, ..., n \end{aligned} \tag{1.22}$$

We can write the explicit formulas for the weight coefficients of first and second order derivatives using the above two Eqs. (1.21 and 1.22) as [Shu, 2000; Zong et al., 2009]

$$A_{ij}^{(1)} = \frac{M^{(1)}(x_i)}{(x_i - x_j)\, M^{(1)}(x_j)}, \quad for \quad i, j = 1, ..., N \, and \, i \neq j \tag{1.23}$$

$$A_{ii}^{(1)} = -\sum_{j=1 \;\; i \neq j}^{N} A_{ij}^{(1)} \tag{1.24}$$

$$M^{(1)}(x_j) = \prod_{k=1, \;\; k \neq j}^{N} (x_j - x_k) \tag{1.25}$$

$$A_{ij}^{(2)} = 2A_{ij}^{(1)} \left(A_{ii}^{(1)} - \frac{1}{x_i - x_j} \right) \quad for \quad i, j = 1, ..., N \; and \quad i \neq j \tag{1.26}$$

$$A_{ii}^{(2)} = -\sum_{j=1 \;\; i \neq j}^{N} A_{ij}^{(2)} \tag{1.27}$$

$$A_{ij}^{(m)} = m \left(A_{ii}^{(m-1)} A_{ij}^{(1)} - \frac{A_{ij}^{(m-1)}}{x_i - x_j} \right) \quad for \quad i, j = 1, ..., N \; and \quad i \neq j \tag{1.28}$$

$$A_{ii}^{(m)} = -\sum_{j=1 \;\; i \neq j}^{N} A_{ij}^{(m)} \tag{1.29}$$

1.7.3 Selection of grid points

The locations of grid points can be taken at uniform intervals or non uniform intervals. Previous studies reveal that non-uniform mesh generated from the roots of orthogonal polynomials of functions can greatly enhance the accuracy of the quadrature solution in comparison to uniform mesh [Shu, 2000; Zong et al., 2009]. Most frequently used non-uniform grid points are Chebyshev-Gauss-Lobatto (CGL) grid points which can be written as

$$r_i = \frac{a+b}{2} + \frac{a-b}{2} cos \frac{i-1}{N-1} \pi \qquad i = 1, 2, ..., N \tag{1.30}$$

For a closed interval [a, b]. The uniform grid points in the same interval can be written as

$$r_i = a + (i-1) \times \frac{b-a}{N-1} \qquad i = 1, 2, ..., N \tag{1.31}$$

1.7.4 Numerical values of weight coefficients

In this section, numerical values of weight coefficients are calculated for $N = 5$ nos of grid points and closed inter [0,1] using both uniform and non-uniform grid points. The uniform grid points calculated using Eq. (1.31) are $[0, 0.25, 0.5, 0.75, 1.0]$ and non-uniform grid points calculated using Eq. (1.30) are [0, 0.14644661, 0.5, 0.85355339, 1.0]. The corresponding weight matrices calculated using Eqs. (1.23-1.29) are given in the following.

Uniform grid points

$$A_{ij}^{(1)} = \begin{pmatrix} -19.0 & 27.3137 & -12.0 & 4.6863 & -1.0 \\ -1.7071 & -1.4142 & 4.2426 & -1.4142 & 0.2929 \\ 0.3333 & -1.8856 & 0 & 1.8856 & -0.3333 \\ -0.2929 & 1.4142 & -4.2426 & 1.4142 & 1.7071 \\ 1.0 & -4.6863 & 12.0 & -27.3137 & 19.0 \end{pmatrix}$$

$$A_{ij}^{(2)} = \begin{pmatrix} 388.0 & -664.9016 & 408.0 & -167.0984 & 36.0 \\ 28.1421 & -40.0 & 12.0 & 0 & -0.1421 \\ -1.3333 & 10.6667 & -18.6667 & 10.6667 & -1.3333 \\ -0.1421 & 0 & 12.0 & -40.0 & 28.1421 \\ 36.0 & -167.0984 & 408.0 & -664.9016 & 388.0 \end{pmatrix}$$

Non-uniform grid points

$$A_{ij}^{(1)} = \begin{pmatrix} -11.0 & 13.6569 & -4.0 & 2.3431 & -1.0 \\ -3.4142 & 1.4142 & 2.8284 & -1.4142 & 0.5858 \\ 1.0 & -2.8284 & 0 & 2.8284 & -1.0 \\ -0.5858 & 1.4142 & -2.8284 & -1.4142 & 3.4142 \\ 1.0 & -2.3431 & 4.0 & -13.6569 & 11.0 \end{pmatrix}$$

$$A_{ij}^{(2)} = \begin{pmatrix} 68.0 & -113.9411 & 72.0 & -46.0589 & 20.0 \\ 36.9706 & -56.0 & 24.0 & -8.0 & 3.0294 \\ -4.0 & 16.0 & -24.0 & 16.0 & -4.0 \\ 3.0294 & -8.0 & 24.0 & -56.0 & 36.9706 \\ 20.0 & -46.0589 & 72.0 & -113.9411 & 68.0 \end{pmatrix}$$

1.8 Research gap areas

Multi-component and long term reactive transport simulation and uncertainty analysis of the corresponding model output when the parameters of the governing equations are imprecise demand for huge computational resources in terms of computational storage and computing speed. Though traditional numerical techniques (FEM, FDM, FVM) have been successfully applied to solve such problems in the present day parallel platform, but huge communication overheads reduce their performance efficiency. LBM being a parallel algorithm has negligible communication overheads. Though LBM has been successfully applied to solve various flows, mass transport, and reactive transport problems, the chemical model in LBM is limited to simple chemical reactions. To get rid of this limitation researches have interfaced LB based solute transport model with geochemical software PHREEQC, but there is no commercial software available on this interfaced technique. Literature study also reveals that though uncertainty modeling of solute transport equation is an important part of safety analysis of waste disposal site, there are very few studies that have attempted to estimate uncertainty of solute transport model using numerical technique. It is also observed that no attempts have been made to numerically solve solute transport equation with imprecise parameters using LBM and DQM. Therefore, objective of this study is to develop an in-house computer code using LBM interfaced with geochemical software PHREEQQC which can simulate multi-component reactive transport in parallel context. The study also focuses on the development of numerical schemes to model uncertainty of solute transport equation with imprecise input parameters such as groundwater velocity, dispersion coefficient using LBM and DQM.

1.9 Research objectives

The specific objectives of this thesis are

1. Study of fast numerical algorithms such as lattice Boltzmann method (LBM) and differential quadrature method (DQM) to develop solute transport code that will be interfaced with geochemical software PHREEQC to simulate multi-component and long term reactive transport.
2. To develop a numerical scheme that can interface in-house developed LBM based solute transport module with PHREEQC for reactive transport simulation.
3. To develop LBM and DQM based numerical schemes for uncertainty modeling of solute transport and reactive transport when the parameters of the governing equations, such as groundwater velocity, dispersion coefficient etc., are imprecise.

1.10 Scope of the thesis

Though the developed computer codes for solute transport and reactive transport are validated by solving benchmark problems having closed form solution, provisions are there to simulate reactive transport processes having more practical applicability in the field of radioactive waste disposal in geological repository. The developed fuzzy lattice Boltzmann scheme and fuzzy differential schemes are applied to model uncertainty involved with solute transport process. These schemes can further be utilized to model uncertainty involved with reactive transport process with imprecise model parameters.

1.11 Research Strategy

Multi-component and long term reactive transport simulation are generally carried out at two different scales, which are (i) pore scale and (ii) REV scale. There exist a variety of numerical schemes, such as mesoscopic technique (LBM), SPH, pore network model, to simulate pore scale reactive transport. Since most of the chemical reactions, such as surface complexation, ion-exchange, dissolution, precipitation, occur at the mineral surface, pore scale study of reactive transport provide more realistic assessment of actual processes than REV scale study of the same. But, the requirement of actual porous geometry and huge demand for computational resources in terms of computational storage and speed of computation has limited the application of pore scale study to small domain. REV scale study of reactive transport does not incorporate pore scale heterogeneity to the model directly, rather their effects are incorporated through empirical parameters of the macroscopic equations. In this study REV scale model of the reactive transport are considered.

REV scale reactive transport equations are generally solved using traditional numerical schemes, such as FDM, FEM, FVM. These numerical schemes have been successfully applied to solve multi-component and long term reactive transport in both serial and parallel platforms. But, communication overload of their parallel schemes is one of the serious bottlenecks for performance improvement. Since LBM is a parallel algorithm, it better utilizes the modern day parallel computational resources. Another numerical scheme called DQM requires very few grid point, therefore DQM based solvers takes less time and less storage to solve PDE. Considering these useful properties of LBM and DQM these two method have been used in this thesis as numerical framework. Though TRT and MRT schemes of LBM are more stable than SRT scheme, the SRT scheme is simpler and computationally more attractive than the other two schemes. In this work SRT scheme of LBM has been adopted.

As discussed earlier, multi-component reactive transport equation is a non-linear PDAE and there are three approaches (SIA, SNIA, DSA) to solve PDAE. Here in this thesis we have taken SNIA, therefore our approach to solve the multi-component reactive transport is based on treatment of the transport and reaction processes separately. The transport process is mathematically governed by ADE, which is a second order PDE, while the reaction processes are mathematically modeled as non-linear algebraic equations. This operator splitting approach is very useful to harness the capabilities of commercial geochemical software to model various complex geochemical reactions in batch mode by utilizing them as reaction engines in the numerical framework. Two different versions of the geochemical software, PHREEQC, namely IPhreeqc and PhreeqcRM are utilized as reaction engines in this thesis. These two versions of the PHREEQC software were developed in order to simplify the coupling of them with other transport solvers. In this thesis, we have first developed LBM and DQM based transport solvers and validated the schemes by solving various benchmark problems. The LBM based transport solver is then interfaced with both IPhreeqc and PhreeqcRM. The interfaced scheme is also validated by solving benchmark problems.

Since uncertainty modeling of solute transport and reactive transport model output is an integral part of safety assessment work for DGR, our next approach has been towards solving solute transport/reactive transport in presence of uncertain model parameters. Two important parameters namely groundwater velocity and dispersion coefficient involved with these processes are taken as uncertain parameters. Since experimental data of these parameters are very few and sparse, they are generally classified as imprecise parameters. These imprecise parameters are represented by triangular fuzzy numbers and Zadeh's extension principle is utilized to propagate these parameter uncertainty through the models. Analytical solution of the resulting fuzzy ADE is generally used for uncertainty estimation. We have solved these fuzzy ADE using both LBM and DQM and uncertainty in model output is presented as interval of lower and upper bounds.

1.12 Outline of the thesis

The thesis is composed of five chapters. Outline of the thesis excluding the present chapter is as follows:

Chapter 2 provides the basis of the two numerical schemes, LBM and DQM , which are used in this thesis as numerical framework. For the shake of completeness of this thesis we briefly reviewed the important aspects of LBM, which are derivation of lattice Boltzmann equation (LBE) from continuous velocity Boltzmann equation, construction of equilibrium distribution function, lattice structure for LBM. Recovery of macroscopic ADE from LBE is given in details. DQM based numerical scheme for solute transport is designed. LBM and DQM based solute transport schemes are then validated by solving various benchmark problems.

In chapter 3, mathematical formulation of multi-component reactive transport with sorption isotherm and geochemical reaction model is provided. The LBM based solver for solute transport, which was developed in Chapter 2, is then interfaced with commercial geochemical software, PHREEQC. The coupling scheme is then tested by solving benchmark problems.

Chapter 4 presents LBM and DQM based numerical schemes for solute transport with imprecise model parameters. Basics of fuzzy set theory is first introduced. Then, developed solute transport model in presence of imprecise model parameters. The formulated fuzzy solute transport is derived from the proposed LBM based numerical scheme. DQM based numerical scheme for uncertainty modeling is provided. Finally, both the schemes are verified and validated by solving standard one-dimensional and two-dimensional benchmark problems.

Chapter 5 brings out summary and conclusions of this study. Outline of future work proposal is also included in this chapter.

Chapter 2

Solute Transport Simulation using Lattice Boltzmann method and Differential Quadrature Method

2.1 Introduction

In this chapter transport of solute through geological media due to advection-dispersion processes is comprehensively treated with two relatively new and promising numerical techniques, LB and DQ. The purpose of this study is to develop the mesoscopic scale based an efficient solver for solute transport that can be utilized for the development of multi-component reactive transport solver as described in subsequent chapter. In section 2.2 mathematical formulation of solute transport is first discussed. Though two-relaxation-time (TRT) and multi-relaxation-time (MRT) schemes of LBM are more stable than single-relaxation-time (SRT) scheme, user friendly and most popular scheme is SRT. Considering this, SRT-LB scheme is used in this thesis. Details of the SRT-LB scheme, including derivation of LB equation, discussion on equilibrium distribution function for the advection dispersion (AD), various lattices used for LBM, and recovery of AD equation from LB equation, are given in section 2.3. The LB scheme developed is verified and validated by solving benchmark problems as presented in section 2.4. Since DQ solver requires very few grid points for calculation compared to other numerical techniques, it requires less memory for storage which in fact make the computation fast. This property of DQ is one of the important characteristics of a fast algorithm. In order to a have a comparative study of performance of various numerical techniques, solute transport equation is solved using DQ method also. In section 2.5 numerical framework of DQ method with respect to solute transport is provided. The developed DQ based solver for AD equation is benchmarked in section 2.6. Finally summary of this study is presented in section 2.7.

2.2 Solute Transport Model Equation

A set of physico-chemical processes, including advection, molecular diffusion, mechanical dispersion, bio-geochemical reactions, and decay of radionuclide simultaneously operate on solutes dissolved in groundwater. As a consequence of these operations, solutes start transporting through the geological media. The mathematical model of this transport is known as reactive transport equation also called advection-dispersion-reaction equation (ADRE), which is a second order non-linear partial differential equation (PDE). The non linear terms are due to various bio-geochemical reactions occurring in the hydro-geological system through which the solutes are being transported . For non-reactive and non-radioactive solutes, reactive transport equation is second order linear PDE, which is known as advection-dispersion equation (ADE). Advection, diffusion and mechanical dispersion are the individual processes involved with ADE. In the advection process, solute dissolved in groundwater moves with the velocity of groundwater. Diffusion process takes place due to thermal agitation of molecules, whereas mechanical dispersion process is due to porous structure and inherent heterogeneity of the geological media. These two processes are generally lumped together into a single process called dispersion.

Considering all the above mentioned processes, the general form of an ADE for solute transport in geological media can be written as

$$\frac{\partial (C)}{\partial t} = \frac{\partial}{\partial x_j}\left(D_j \frac{\partial C}{\partial x_j}\right) - \frac{\partial (u_j C)}{\partial x_j} \tag{2.1}$$

where $x_j = x, y,$ and z for Cartesian coordinate system, repeated index j is the Einstein summation convention, meaning a summation over the space co-ordinates, C represents solute concentration in groundwater, D_j signifies dispersion coefficient in j^{th} direction, u_j is ground water flow velocity along j^{th} direction. Equation (2.1) can be simplified if the parameters of the equation e.g., D, and u are independent of spatial and temporal co-ordinates. The following assumptions are valid only for a homogeneous formation of rock mass and for a time frame which is considerably shorter than geological time scale, which is of the order of million years. Based on these assumptions Eq. (2.1) can be written in simplified form as

$$\frac{\partial C}{\partial t} = D_j \frac{\partial^2 C}{\partial x_j^2} - u_j \frac{\partial C}{\partial x_j} \tag{2.2}$$

There are three types of domain boundary conditions: Dirichlet, Neumann, and Cauchy boundary condition. The general form of the domain boundary condition can be written as

$$A_1 C + A_2 \hat{n} \vec{\nabla} C = A_3 \tag{2.3}$$

where A_1, A_2 and A_3 are constants. Special form of boundary condition is derived based on the values of A_1, A_2 and A_3. For $A_1 = 1$ and $A_2 = 0$ we have Dirichlet boundary condition, for $A_1 = 0$, $A_2 = 1$ Neumann and for $A_1 = \vec{u_b}$, $A_2 = -D_0$ we have the value of $A_3 = C_b \vec{u_b}$ and this type of boundary condition is called Cauchy boundary condition. Here C_b and $\vec{u_b}$ are solute concentration and pore water velocity at boundary of the geometry of problem under consideration.

2.3 Lattice Boltzmann Method for Solute Transport

Lattice Boltzmann (LB) method [Succi, 2001; Wolf-Gladrow, 2000; Krger et al., 2017] is based on kinetic model of discrete particles motion. It basically solves discrete velocity Boltzmann transport equation over a regular grid of spatial and temporal discretization. The LB method was first introduced in 1988 by McNamara and Zanettii [McNamara et al., 1988] in order to eliminate the numerical noises of its ancestor called lattice gas cellular automata (LGCA), proposed by Frish et al. [Frisch et al., 1986]. Initially LB was developed to solve Navier Stokes equation (NSE) in hydrodynamics [Qian et al., 1992; Chen et al., 1992, 1998]. Since its inception as a mesoscopic technique that can simulate fluid flow, particularly Navier-Stokes equation (NSE), LBM has been successfully applied to solve various kind of fluid dynamics problems, such as flow though complex boundary geometries (porous media), two phase flow, turbulence flow etc. In the last two decades, LBM has emerged as a promising numerical scheme that can be applied to solve a set of partial differential equations representing various other science and engineering problems, such as diffusion-reaction, reactive transport, wave motion, traffic flow, image analysis etc. In this section details of lattice Boltzmann (LB) techniques for solving solute transport equation (2.1) are presented.

2.3.1 Derivation of lattice Boltzmann equation from Boltzmann equation

In the previous chapter, we have discussed about the historical origin of LBM from LGCA. This derivation of LBM from LGCA was required to eliminate the drawbacks of the later one. Later on, He et al. showed that LBE can be derived from continuous velocity Boltzmann equation [He et al., 1997]. Detailed derivation of the LBE from the continuous velocity Boltzmann equation are given in this following. The Boltzmann transport equation, which is the governing equation for the evolution of single particle distribution function, is written as

$$\frac{\partial f}{\partial t} + \vec{e}.\vec{\nabla}_{\vec{x}} f + \frac{\vec{F}}{m}.\vec{\nabla}_{\vec{e}} f = \Omega \tag{2.4}$$

where f is single particle distribution function, $\vec{e}$ is the velocity of the particle, $\vec{F}$ is external force acting on the particle, m represents the mass of the particle, and Ω is collision operator. In the absence of external force Boltzmann equation takes the form

$$\frac{\partial f}{\partial t} + \vec{e}.\vec{\nabla}_{\vec{x}} f = \Omega \tag{2.5}$$

In the equilibrium state of the system of particles, the collision term vanishes and the solution of the above equation is the well known Maxwellian distribution.

$$f^{eq}\left(\vec{x}, \vec{e}, t\right) = \frac{\rho}{\left(2\pi RT\right)^{3/2}} exp\left(-\frac{\left(\vec{e} - \vec{u}\right)^2}{2RT}\right) \tag{2.6}$$

where $R = k_B/m$ is the universal gas constant with k_B the Boltzmann constant and m is the molecular mass, $\vec{u}$ is the macroscopic velocity of the particles. It is to be mentioned here that collision operator, Ω, conserve mass and momentum. These conservation principles can be mathematically expressed as

$$\rho = \int_{\vec{e}} f\left(\vec{x}, \vec{e}, t\right) d^3e = \int_{\vec{e}} f^{eq}\left(\vec{x}, \vec{e}, t\right) d^3e \tag{2.7}$$

$$\rho u = \int_{\vec{e}} \vec{e} f\left(\vec{x}, \vec{e}, t\right) d^3e = \int_{\vec{e}} \vec{e} f^{eq}\left(\vec{x}, \vec{e}, t\right) d^3e \tag{2.8}$$

where ρ is particle density. The non-equilibrium solution of the Boltzmann equation (2.5) is difficult to obtain because of the presence of complicated collision term, which is a double integral over velocity space. In order to simplify the above equation, various simplified form of the collision operator are generally used. One of these types of collision operator, known as BGK collision operator, which is used in the LBM is due to Bhatnagar, Gross and Krook. In the BGK collision operator non-equilibrium particle distribution function relaxes towards the equilibrium distribution function (EDF) at a rate which is defined by a time constant, known as relaxation time. The BGK collision operator can be written as [Bhatnagar et al., 1954]

$$\Omega_{BGK} = -\frac{1}{\tau}\left(f - f^{eq}\right) \tag{2.9}$$

where τ is the relaxation time. Using the BGK collision operator Boltzmann equation (2.5) can be written as

$$\frac{\partial f}{\partial t} + \vec{e}.\vec{\nabla}_{\vec{x}} f = -\frac{1}{\tau}\left(f - f^{eq}\right) \tag{2.10}$$

Our next task is to discretize the continuous velocity into a set of discrete velocities in such a way that the mass and momentum conservation equations (2.7 and 2.8) are preserved. For this purpose we first expand the equilibrium distribution function (2.6) in Taylor series as

$$\begin{aligned}
f^{eq}\left(\vec{x},\vec{e},t\right) &= \frac{\rho}{\left(2\pi RT\right)^{3/2}} exp\left(-\frac{\left(\vec{e}-\vec{u}\right)^2}{2RT}\right) \\
&= \frac{\rho}{\left(2\pi RT\right)^{3/2}} exp\left(-\frac{\vec{e}^2}{2RT} + \frac{\vec{e}.\vec{u}}{RT} - \frac{\vec{u}^2}{2RT}\right) \\
&= \frac{\rho}{\left(2\pi RT\right)^{3/2}} exp\left(-\frac{\vec{e}^2}{2RT}\right) \times exp\left(\frac{\vec{e}.\vec{u}}{RT} - \frac{\vec{u}^2}{2RT}\right) \\
&= \frac{\rho}{\left(2\pi RT\right)^{3/2}} exp\left(-\frac{\vec{e}^2}{2RT}\right)\left(1 + \frac{\vec{e}.\vec{u}}{RT} + \frac{1}{2}\left(\frac{\vec{e}.\vec{u}}{RT}\right)^2 - \frac{\vec{u}^2}{2RT} + \Theta\left(|u|/\sqrt{RT}\right)^3\right) \\
&\approx \frac{\rho}{\left(2\pi RT\right)^{3/2}} exp\left(-\frac{\vec{e}^2}{2RT}\right)\left(1 + \frac{\vec{e}.\vec{u}}{RT} + \frac{1}{2}\left(\frac{\vec{e}.\vec{u}}{RT}\right)^2 - \frac{\vec{u}^2}{2RT}\right)
\end{aligned} \tag{2.11}$$

Here it is considered that the Mach number (Ma), $|u|/\sqrt{RT}$, is a small parameter and hence the series is truncated at reasonable order $O(Ma^2)$. The truncated above equation can be written as

$$f^{eq}\left(\vec{x},\vec{e},t\right)=\psi\left(\vec{e}\right)\left(1+\frac{\vec{e}.\vec{u}}{RT}+\frac{\left(\vec{e}.\vec{u}\right)^2}{2\left(RT\right)^2}-\frac{\vec{u}^2}{2RT}\right) \tag{2.12}$$

where $\psi(\vec{e})=\frac{\rho}{(2\pi RT)^{3/2}}exp\left(-\frac{\vec{e}^2}{2RT}\right)$ can be treated as a continuous weight function and the EDF, $f^{eq}\left(\vec{x},\vec{e},t\right)$, is a polynomial in $\vec{e}$, multiplied by a weight function, $\psi(\vec{e})$. Therefore, Gaussian quadrature can be used to evaluate the following integral

$$\begin{aligned}\int_{\vec{e}}f^{eq}\left(\vec{x},\vec{e},t\right)d^3e&=\int_{\vec{e}}\psi(\vec{e})\left(1+\frac{\vec{e}.\vec{u}}{RT}+\frac{\left(\vec{e}.\vec{u}\right)^2}{2\left(RT\right)^2}-\frac{\vec{u}^2}{2RT}\right)d^3e\\&=\sum_i w_i\left(1+\frac{\vec{e_i}.\vec{u}}{RT}+\frac{\left(\vec{e_i}.\vec{u}\right)^2}{2\left(RT\right)^2}-\frac{\vec{u}^2}{2RT}\right)\\&=\sum_i f_i^{eq}\left(\vec{x},\vec{e_i},t\right)\end{aligned} \tag{2.13}$$

where w_i and $\vec{e_i}$ are the the weights and points of the numerical quadrature rule and $f_i^{eq}\left(\vec{x},\vec{e_i},t\right)$ is the discrete EDF, which can be written as

$$f_i^{eq}\left(\vec{x},\vec{e_i},t\right)=w_i\left(1+\frac{\vec{e_i}.\vec{u}}{RT}+\frac{\left(\vec{e_i}.\vec{u}\right)^2}{2\left(RT\right)^2}-\frac{\vec{u}^2}{2RT}\right) \tag{2.14}$$

The above points, $\vec{e_i}$, of the numerical quadrature are the discrete velocities of LBM. Since velocity discretization is done, we can define the discrete distribution function, $f_i(\vec{x},t)=w_if\left(\vec{x},\vec{e_i},t\right)$, which satisfies the following equation

$$\frac{\partial f_i}{\partial t}+\vec{e_i}.\vec{\nabla}_{\vec{x}}f_i=-\frac{1}{\tau}\left(f_i-f_i^{eq}\right) \tag{2.15}$$

The above equation is called discrete velocity Boltzmann equation. Here it is assumed that relaxation time is independent of direction of velocity, which is the basic ingredient of SRT-LB scheme. The general form of the above equation can be written as

$$\frac{\partial f_i}{\partial t} + \vec{e_i}.\vec{\nabla}_{\vec{x}} f_i = -\Omega_{ij}\left(f_j - f_j^{eq}\right) \tag{2.16}$$

where Ω_{ij} is the collision matrix of the relaxation time. Further discretization of Eq. (2.15) with respect to space and time results

$$\begin{aligned} \frac{f_i\left(\vec{x}, t+\Delta t\right) - f_i\left(\vec{x}, t\right)}{\Delta t} + \frac{\Delta \vec{x}}{\Delta t} \frac{f_i\left(\vec{x} + \vec{e_i}\Delta t, t+\Delta t\right) - f_i\left(\vec{x}, t+\Delta t\right)}{\Delta x} \\ = -\frac{1}{\tau}\left(f_j - f_j^{eq}\right) \end{aligned} \tag{2.17}$$

where Δx and Δt are spatial and time step, respectively. Since at each time step particle move to the next lattice point, particle velocity, $\vec{e_i}$, is written as $\Delta\vec{x}/\Delta t$. Simplifying the above equation we get

$$f_i\left(\vec{x} + \vec{e_i}\Delta t, t+\Delta t\right) = f_i\left(\vec{x}, t\right) + \frac{\Delta t}{\tau}\left(f_i\left(\vec{x}, t\right) - f_i^{eq}\left(\vec{x}, t\right)\right) \tag{2.18}$$

This is the working equation for LBM.

2.3.2 Equilibrium Distribution Function

Though the governing LBE (2.18) is same for different macroscopic equation, the particular equation being solved is decided by the EDF. The EDF for ADE is derived from Maxwell-Boltzmann distribution. The Linear part of Maxwell-Boltzmann distribution function with respect to velocity is generally used for ADE and quadratic part of EDF is used for Navier-Stokes equation. The discrete velocity EDF (2.14) with linear velocity terms can be written as

$$f_i^{eq}\left(\vec{x}, t\right) = w_i\left(1 + \frac{\vec{e_i}.\vec{u}}{e_s^2}\right) \tag{2.19}$$

where $e_s = \sqrt{RT}$ is called 'pseudo speed of sound' [Chen et al., 1998]. Similarly, EDF with second order velocity term is

$$f_i^{eq}(\vec{x}, t) = w_i \left(1 + \frac{\vec{e_i}.\vec{u}}{e_s^2} + \frac{(\vec{e_i}.\vec{u})^2}{2e_s^4} - \frac{\vec{u}.\vec{u}}{2e_s^2} \right) \tag{2.20}$$

For ADE conservation of mass is required during the collision process. Therefore, the particle distribution function and EDF must follow the following condition

$$\sum_i f_i = \sum_i f_i^{eq} = C \tag{2.21}$$

where C is the solute concentration. Substituting the value of the EDF (2.19) in the above equation (2.21) we get

$$\sum_i f_i^{eq} = \sum_i w_i \left(1 + \frac{\vec{e_i}.\vec{u}}{e_s^2} \right) = C \tag{2.22}$$

Since the lattices used in LBM are rotationally symmetric, the second term, $\frac{\vec{e_i}.\vec{u}}{e_s^2}$, inside the bracket of the above equation vanishes when summation is taken over all the lattice direction. Therefore, performing the summation we get

$$\sum_i w_i = C \tag{2.23}$$

From the above equation we can write $w_i = \omega_i C$, where ω_i is the weight factor corresponding to velocity $\vec{e_i}$, which satisfies the following condition

$$\sum_i \omega_i = 1 \tag{2.24}$$

Therefore, we can write EDF for ADE as

$$f_i^{eq}\left(\vec{x},t\right) = \omega_i C\left(\vec{x},t\right)\left(1+\frac{\vec{e_i}.\vec{u}}{e_s^2}\right) \tag{2.25}$$

2.3.3 Lattice structure for Lattice Boltzmann Method

Lattice Boltzmann method has three main components: LB equation, EDF and lattice. LB equation and EDF are explained in the previous sections. In this section a brief idea about various lattices used in LB method are given. The choice of EDF and type of lattice depends on the type of equation (physics) being solved. Particles in LB method are connected to its neighboring particles via lattice connectivity. Qian et al. introduced the name ”DnQm lattice” for a lattice structure with m lattice directions in n dimension [Qian et al., 1992]. The order of isotropy of a lattice, which is defined as the order of velocity moment and the symmetry of a lattice are the two important properties that need to be considered before selection of lattice for LB solution of a given equation. For mass conservation lattices should be at least second order isotropic and for mass and momentum conservation lattices with at least fourth order isotropy are required. Since ADE requires only mass conservation to be satisfied, the lattices for ADE should be at least second order isotropic. A second order isotropic lattice has following properties

$$\sum_i \omega_i = 1, \quad \sum_i \omega_i e_{i\alpha} = 0, \quad \sum_i \omega_i e_{i\alpha} e_{i\beta} = e_s^2 \delta_{\alpha\beta} \tag{2.26}$$

Calculation of weight factors

Weight factor corresponding to various velocity vectors can be calculated using the above mentioned (2.26) isotropic properties of lattices. In the following calculation of weight factor for commonly used lattices are given

(i) D1Q2

The velocity vectors of D1Q2 lattice are

Figure 2.1: D1Q2 lattice

$\vec{e_1}$= e

$\vec{e_2}$= -e

The sound speed for D1Q2 lattice is

$e_s = e/\sqrt{2}$

Using the first two isotropic properties we can write

$\omega_1 + \omega_2 = 1$

$e\omega_1 - e\omega_2 = 0$

Solving the above two equations we get $w_1 = \omega_2 = 1/2$

(ii) D1Q3

The velocity vectors of D1Q3 lattice are

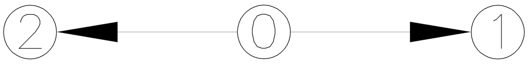

Figure 2.2: D1Q3 lattice

$\vec{e_0} = 0$

$\vec{e_1} = e$

$\vec{e_2} = -e$

The sound speed for D1Q3 lattice is

$e_s = e/\sqrt{3}$

Using the first two isotropic properties we can write

$$\omega_0 + \omega_1 + \omega_2 = 1$$

$$\omega_1 e - \omega_2 e = 0$$

Using the third property

$\omega_1 e^2 + \omega_2 e^2 = e_s^2 = e^2/3$

Solving the last two equations we get $w_1 = \omega_2 = 1/6$

Therefore, $\omega_0 = 1 - 2/6 = 4/6$

(iii) D2Q4

The velocity vectors of D2Q4 lattice are

$$\vec{e_1} = (e, 0) \qquad \vec{e_2} = (0, e)$$

$$\vec{e_3} = (-e, 0) \qquad \vec{e_4} = (0, -e)$$

The sound speed for D2Q4 lattice is $e_s = e/\sqrt{2}$

Using the first two isotropic properties we can write

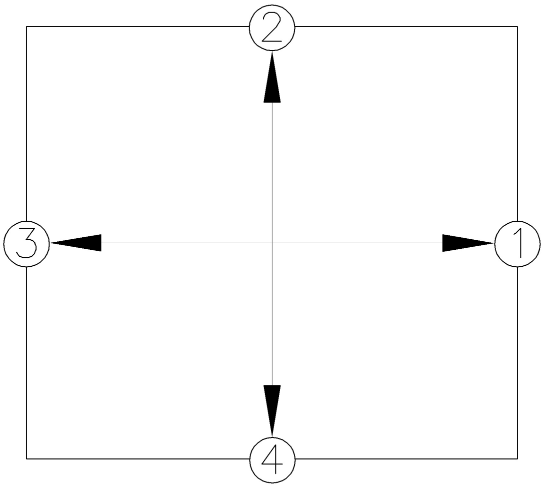

Figure 2.3: D2Q4 lattice

$$\omega_1 + \omega_2 + \omega_3 + \omega_4 = 1$$

$$\omega_1 e - \omega_3 e = 0$$

$$\omega_2 e - \omega_4 e = 0$$

From the last two equations we get

$$\begin{aligned} \omega_1 &= \omega_3 \\ \omega_2 &= \omega_4 \end{aligned} \tag{2.27}$$

Using the third isotropic property we obtain

$$\begin{aligned} \omega_1 e^2 + \omega_3 e^2 = e_s^2 = \frac{e^2}{2} \\ \omega_2 e^2 + \omega_4 e^2 = e_s^2 = \frac{e^2}{2} \end{aligned}$$

Simplifying the above two equations

$$\begin{aligned} \omega_1 + \omega_3 = 1/2 \\ \omega_2 + \omega_4 = 1/2 \end{aligned} \tag{2.28}$$

Solving Eqs. (2.27) and (2.28) we get $\omega_s = 1/4$, s = 1,2,3,4

(iv) D2Q5

The velocity vectors of D2Q5 lattice are

$$\begin{aligned} &\vec{e_0} = (0,0) \\ &\vec{e_1} = (e,0) \qquad \vec{e_2} = (0,e) \\ &\vec{e_3} = (-e,0) \qquad \vec{e_4} = (0,-e) \end{aligned}$$

The sound speed for D2Q5 lattice is $e_s = e/\sqrt{3}$

Using the first two isotropic properties we can write

$$\begin{aligned} &\omega_0 + \omega_1 + \omega_2 + \omega_3 + \omega_4 = 1 \\ &\omega_1 e - \omega_3 e = 0 \\ &\omega_2 e - \omega_4 e = 0 \end{aligned}$$

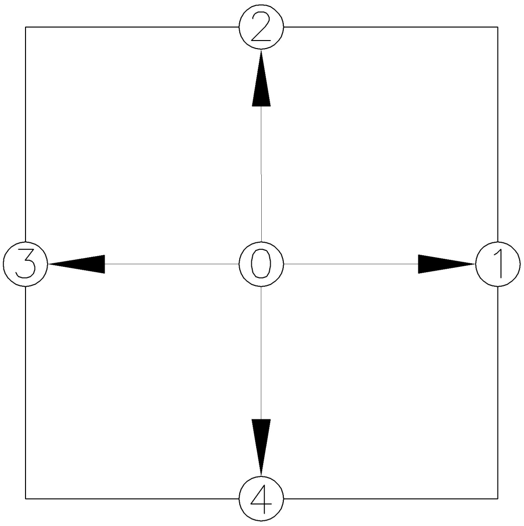

Figure 2.4: D2Q5 lattice

From the last two equations we get

$$\begin{aligned} \omega_1 &= \omega_3 \\ \omega_2 &= \omega_4 \end{aligned} \tag{2.29}$$

Using the third isotropic property we get

$$\begin{aligned} \omega_1 e^2 + \omega_3 e^2 = e_s^2 = \frac{e^2}{3} \\ \omega_2 e^2 + \omega_4 e^2 = e_s^2 = \frac{e^2}{3} \end{aligned}$$

Simplifying the above two equations

$$\begin{aligned} \omega_1 + \omega_3 = 1/3 \\ \omega_2 + \omega_4 = 1/3 \end{aligned} \tag{2.30}$$

Solving Eqs. (2.29) and (2.30) we get $\omega_s = 1/6,$ s = 1,2,3,4

Therefore, $\omega_0 = 1 - 4/6 = 2/6$

(v) D2Q9

The velocity vectors of D2Q9 lattice are

$\vec{e_0} = (0, 0)$

$\vec{e_1} = (e, 0)$ $\quad \vec{e_2} = (0, e)$ $\quad \vec{e_3} = (-e, 0)$ $\quad \vec{e_4} = (0, -e)$

$\vec{e_5} = (e, e)$ $\quad \vec{e_6} = (-e, e)$ $\quad \vec{e_7} = (-e, -e)$ $\quad \vec{e_8} = (e, -e)$

The sound speed for D2Q9 lattice is $e_s = e/\sqrt{3}$

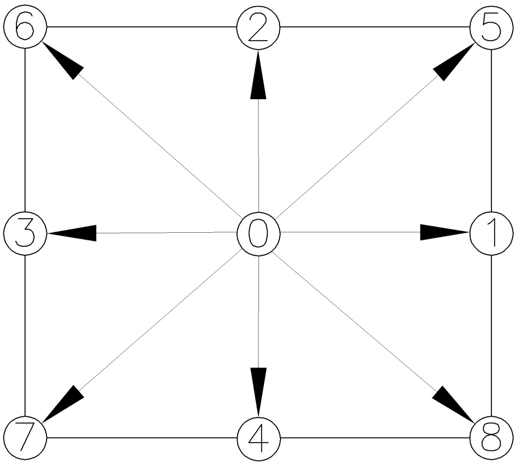

Figure 2.5: D2Q9 lattice

To simplify the calculation we make use of its 90^0 rotational symmetry property, i.e. weight of the horizontal and vertical velocities (ω_a) are same and weight of the diagonal velocities are same (ω_b). The weight of the stationary velocity is ω_0. Therefore, using the first isotropic property we get

$$\omega_0 + 4\omega_a + 4\omega_b = 1 \tag{2.31}$$

Using the third isotropic property we can write

$$\begin{aligned} &2\omega_a e^2 + 4\omega_b e^2 = e_s^2 = e^2/3 \\ &\Rightarrow 2\omega_a + 4\omega_b = 1/3 \end{aligned} \tag{2.32}$$

For calculation of weight factors for D2Q9 lattice we require another isotropic property of the lattice, which is fourth order velocity moments and can be written as

$$\sum_i \omega_i e_{i\alpha} e_{i\beta} e_{i\eta} e_{i\gamma} = e_s^4 \left(\delta_{\alpha\beta}\delta_{\eta\gamma} + \delta_{\alpha\eta}\delta_{\beta\gamma} + \delta_{\alpha\gamma}\delta_{\beta\eta}\right) \tag{2.33}$$

For the case $\alpha = \beta \neq \eta = \gamma$ we get the value of the left hand side of Eq. (2.33) as

$$\begin{aligned} \sum_i \omega_i e_{i\alpha} e_{i\beta} e_{i\eta} e_{i\gamma} &= \omega_a \sum_{i=1}^{4} e_{i\alpha} e_{i\alpha} e_{i\eta i\eta} + \omega_b \sum_{i=5}^{8} e_{i\alpha} e_{i\alpha} e_{i\eta} e_{i\eta} \\ &= 4\omega_b e^4 = e_s^4 = e^4/9 \\ \Rightarrow \omega_b = 1/36 \end{aligned} \tag{2.34}$$

Now, using Eq. (2.32) we get $\omega_a = 1/9$. Using Eq. (2.31) we obtain ω_0 = 1-4/9-4/39=4/9. Therefore, weight coefficients for D2Q9 lattice are $w_0 = 4/9,\quad \omega_s = 1/9,$ s = 1,2,3,4 $and \omega_l = 1/36,\ l = 5, 6, 7, 8, 9$

(vi) D3Q7

The velocity vectors of D3Q7 lattice are

$\vec{e_0} = (0, 0, 0)$

$\vec{e_1} = (e, 0, 0) \qquad \vec{e_2} = (0, e, 0) \qquad \vec{e_3} = (0, 0, e)$

$\vec{e_4} = (-e, 0, 0) \qquad \vec{e_5} = (0, -e, 0) \qquad \vec{e_6} = (0, 0, -e)$

The sound speed for D3Q7 lattice is

$e_s = e/\sqrt{3.5}$

To simplify the calculation we make use of its 90^0 rotational symmetry property, i.e. weight of the horizontal and vertical velocities (ω_a) are same. The weight of the stationary velocity is ω_0. Therefore, using the first isotropic property we get

$$\omega_0 + 6\omega_a = 1 \tag{2.35}$$

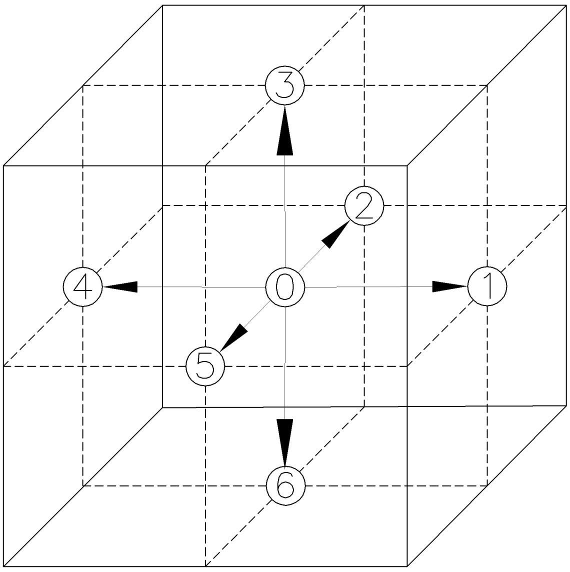

Figure 2.6: D3Q7 lattice

Using the second isotropic property we can write

$$2\omega_a e^2 = e_s^2 = e^2/7$$

$$\Rightarrow \omega_a = 1/7$$

From Eq. (2.35) $\omega_0 = 1 - 6/7 = 1/7$. Therefore, weight coefficient of all the velocities are same for D3Q7 lattice and it is equal to 1/7, i.e. $\omega_s = 1/7$,   s = 0,1,2,3,4,5,6

(vii) D3Q15

The velocity vectors of D3Q15 lattice are

$\vec{e_0} = (0, 0, 0)$

$\vec{e_1} = (e, 0, 0)$ $\vec{e_2} = (0, e, 0)$ $\vec{e_3} = (0, 0, e)$

$\vec{e_4} = (-e, 0, 0)$ $\vec{e_5} = (0, -e, 0)$ $\vec{e_6} = (0, 0, -e)$

$\vec{e_7} = (-e, -e, -e)$ $\vec{e_8} = (-e, -e, e)$ $\vec{e_9} = (-e, e, -e)$

$\vec{e_{10}} = (-e, e, e)$ $\vec{e_{11}} = (e, e, e)$ $\vec{e_{12}} = (e, e, -e)$

$\vec{e_{13}} = (e, -e, e)$ $\vec{e_{14}} = (e, -e, -e)$

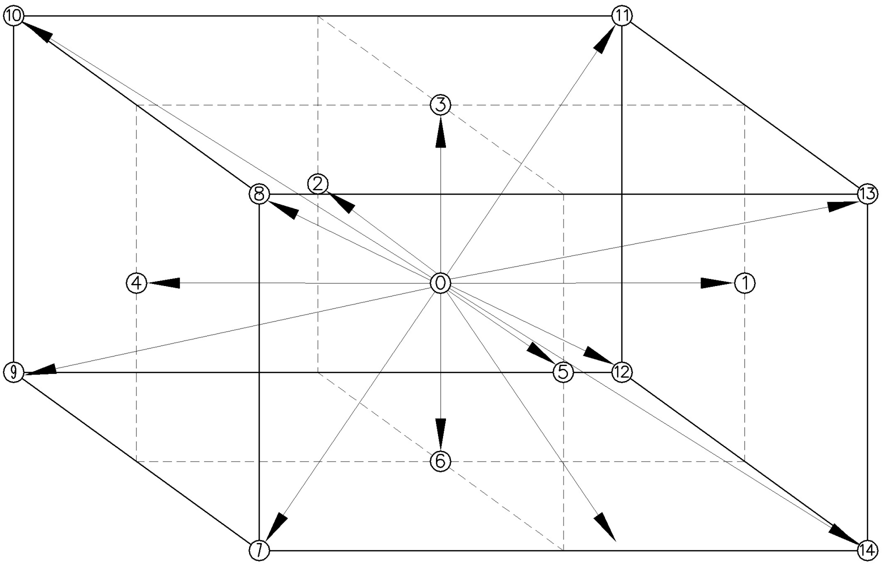

Figure 2.7: D3Q15 lattice

The sound speed for D3Q15 lattice is

$e_s = e/\sqrt{3}$

Similar to the previous derivation of weight coefficients, if we use the 90^0 rotational symmetry property then weight of the horizontal and vertical velocities (ω_a) are same and weight of the diagonal velocities are equal (ω_b). The weight of the stationary velocity is ω_0. Therefore, using the first isotropic property we get

$$\omega_0 + 6\omega_a + 8\omega_b = 1 \tag{2.36}$$

Using the second isotropic property we can write

$$\begin{aligned} &2\omega_a e^2 + 8\omega_b e^2 = e_s^2 = e^2/3 \\ &\Rightarrow 2\omega_a + 8\omega_b = 1/3 \end{aligned} \tag{2.37}$$

Similar to the calculation for D2Q9 lattice we require fourth order velocity moments and can be written as

$$\sum_i \omega_i e_{i\alpha} e_{i\beta} e_{i\eta} e_{i\gamma} = e_s^4 \left(\delta_{\alpha\beta}\delta_{\eta\gamma} + \delta_{\alpha\eta}\delta_{\beta\gamma} + \delta_{\alpha\gamma}\delta_{\beta\eta} \right) \tag{2.38}$$

For the case $\alpha = \beta \neq \eta = \gamma$ we get the value of the left hand side of Eq. (2.38) as

$$\begin{aligned} \sum_i \omega_i e_{i\alpha} e_{i\beta} e_{i\eta} e_{i\gamma} &= \omega_a \sum_{i=1}^{4} e_{i\alpha} e_{i\alpha} e_{i\eta i\eta} + \omega_b \sum_{i=5}^{8} e_{i\alpha} e_{i\alpha} e_{i\eta} e_{i\eta} \\ &= 8\omega_b e^4 = e_s^4 = e^4/9 \\ \Rightarrow \omega_b = 1/72 \end{aligned} \tag{2.39}$$

Now, using Eq. (2.37) we get $2\omega_a = 1/3 - 8/72 = 2/9$ or $\omega_a = 1/9$. Using Eq. (2.36) we obtain $\omega_0 = 1 - 4/9 - 8/72 = 2/9$. Therefore, weight coefficients for D3Q15 lattice are

$w_0 = 2/9, \quad \omega_s = 1/9$ s = 1,2,3,4,5,6 and $\omega_l = 1/72, \;\; l = 7, 8, 9, 10, 11, 12, 13, 14$

2.3.4 Recovery of Solute Transport Equation from Lattice Boltzmann Equation

In this section macroscopic ADE (2.1) is recovered from microscopic LBE (2.18) using multi-scale Chapman-Enskog expansion technique. We rewrite the LB equation derived in the previous section

$$f_i \left(\vec{x} + \vec{e_i}\Delta t, t + \Delta t \right) = f_i \left(\vec{x}, t \right) + \frac{1}{\tau} \left[f_i^{eq} \left(\vec{x}, t \right) - f_i \left(\vec{x}, t \right) \right] \tag{2.40}$$

Assuming Δt is a small parameter and equal to ε

$$\Delta t = \varepsilon \tag{2.41}$$

Substituting this value of Δt into Eq. (2.40) leads to

$$f_i \left(\vec{x} + \vec{e_i}\varepsilon, t + \varepsilon \right) = f_i \left(\vec{x}, t \right) + \frac{1}{\tau} \left[f_i^{eq} \left(\vec{x}, t \right) - f_i \left(\vec{x}, t \right) \right] \tag{2.42}$$

Now performing Taylor series expansion of the left side of the Eq. (2.42) with respect to time and space around point $(\vec{x}, t)$ we get

$$\sum_{n=1}^{\infty} \frac{\varepsilon^n}{n!} \left(\frac{\partial}{\partial t} + e_{ij} \frac{\partial}{\partial x_j} \right)^n f_i\left(\vec{x}, t\right) = \frac{1}{\tau} \left[f_i^{eq}\left(\vec{x}, t\right) - f_i\left(\vec{x}, t\right) \right] \tag{2.43}$$

Using Chapman-Enskog expansion technique, particle distribution function can be expanded as

$$f_i = f_i^{(0)} + \sum_{n=1}^{\infty} \varepsilon^n f_i^{(n)} = f_i^{(0)} + \varepsilon f_i^{(1)} + \varepsilon^2 f_i^{(2)} + \vartheta\left(\varepsilon^3\right) \tag{2.44}$$

Neglecting the higher order terms of ε and substituting the truncated value of f_i into Eq. (2.43) we get

$$\begin{aligned} \sum_{n=1}^{\infty} \frac{\varepsilon^n}{n!} \left(\frac{\partial}{\partial t} + e_{ij} \frac{\partial}{\partial x_j} \right)^n & \left(f_i^{(0)} + \varepsilon f_i^{(1)} + \varepsilon^2 f_i^{(2)} \right) \\ &= \frac{1}{\tau} \left[f_i^{eq} - \left(f_i^{(0)} + \varepsilon f_i^{(1)} + \varepsilon^2 f_i^{(2)} \right) \right] \end{aligned} \tag{2.45}$$

Grouping terms of the same order in ε yields the following successive approximations

$$\vartheta\left(\varepsilon^0\right) : f_i^{eq} = f_i^{(0)} \tag{2.46}$$

$$\vartheta\left(\varepsilon^1\right) : \left(\frac{\partial}{\partial t} + e_{ij} \frac{\partial}{\partial x_j} \right) f_i^{(0)} = -\frac{1}{\tau} f_i^{(1)} \tag{2.47}$$

$$\vartheta\left(\varepsilon^2\right) : \left(\frac{\partial}{\partial t} + e_{ij} \frac{\partial}{\partial x_j} \right) f_i^{(1)} + \frac{1}{2} \left(\frac{\partial}{\partial t} + e_{ij} \frac{\partial}{\partial x_j} \right)^2 f_i^{(0)} = -\frac{1}{\tau} f_i^{(2)} \tag{2.48}$$

Substituting Eq. (2.47) into Eq. (2.48) we get

$$\left(1 - \frac{1}{2\tau} \right) \left(\frac{\partial}{\partial t} + e_{ij} \frac{\partial}{\partial x_j} \right) f_i^{(1)} = -\frac{1}{\tau} f_i^{(2)} \tag{2.49}$$

Eq. (2.47) + $\varepsilon\times$ Eq. (2.49) leads to

$$\begin{aligned}\left(\frac{\partial}{\partial t}+e_{ij}\frac{\partial}{\partial x_j}\right)f_i^{(0)}+\varepsilon\left(1-\frac{1}{2\tau}\right)\left(\frac{\partial}{\partial t}+e_{ij}\frac{\partial}{\partial x_j}\right)f_i^{(1)}\\ =-\frac{1}{\tau}\left(f_i^{(1)}+\varepsilon f_i^{(2)}\right)\end{aligned}\tag{2.50}$$

Summing over i, Eq. (2.50) can be written as

$$\begin{aligned}\frac{\partial}{\partial t}\sum_i f_i^{(0)}+\frac{\partial}{\partial x_j}\sum_i e_{ij}f_i^{(0)}+\varepsilon\left(1-\frac{1}{2\tau}\right)\frac{\partial}{\partial t}\sum_i f_i^{(1)}\\ +\varepsilon\left(1-\frac{1}{2\tau}\right)\frac{\partial}{\partial x_j}\sum_i e_{ij}f_i^{(1)}=-\frac{1}{\tau}\sum_i f_i^{(1)}-\frac{\varepsilon}{\tau}\sum_i f_i^{(2)}\end{aligned}\tag{2.51}$$

Equilibrium distribution function (EDF) for ADE defined in the previous section has following properties

$$\sum_i f_i^{eq}\left(\vec{x},t\right)=C\left(\vec{x},t\right)\tag{2.52}$$

$$\sum_i e_i f_i^{eq}\left(\vec{x},t\right)=u_i C\left(\vec{x},t\right)\tag{2.53}$$

$$\sum_i e_{ix}e_{iy}f_i^{eq}\left(\vec{x},t\right)=e_s^2 C\left(\vec{x},t\right)\delta_{x,y}\tag{2.54}$$

where $\delta_{x,y}$ is the Dirac delta function, which is equal to 1 when $x=y$ and equal to 0 when $x\neq y$. Macroscopic particle density is the zero order velocity moment of the distribution function

$$C\left(\vec{x},t\right)=\sum_i f_i\left(\vec{x},t\right)\tag{2.55}$$

Using the above mentioned property of distribution function (2.55) and EDF (2.46 and 2.52) we can impose the following constraints on the fluctuating parts of the distribution function

$$\sum_i f_i^{(k)}\left(\vec{x},t\right)=0,\qquad k=1,2,3,...\tag{2.56}$$

$$\frac{\partial}{\partial t}\sum_i f_i^{(k)}\left(\vec{x},t\right)=0, \qquad k=1,2,3,... \tag{2.57}$$

Considering the above properties of the fluctuating parts of the distribution function we can simplify the Eq. (2.51) as

$$\frac{\partial}{\partial t}\sum_i f_i^{(0)}+\frac{\partial}{\partial x_j}\sum_i e_{ij}f_i^{(0)}+\varepsilon\left(1-\frac{1}{2\tau}\right)\frac{\partial}{\partial x_j}\sum_i e_{ij}f_i^{(1)}=0 \tag{2.58}$$

Substituting the value of $f_i^{(1)}$ from Eq. (2.47) into the above equation we get

$$\begin{aligned}\frac{\partial}{\partial t}\sum_i f_i^{(0)}+\frac{\partial}{\partial x_j}\sum_i e_{ij}f_i^{(0)}-\tau\varepsilon\left(1-\frac{1}{2\tau}\right)\frac{\partial}{\partial x_j}\sum_i e_{ij}\frac{\partial}{\partial t}f_i^{(0)}\\ -\tau\varepsilon\left(1-\frac{1}{2\tau}\right)\frac{\partial}{\partial x_j}\sum_i e_{ij}e_{ik}\frac{\partial}{\partial x_k}f_i^{(0)}=0\end{aligned} \tag{2.59}$$

The term containing time derivative of EDF is smaller compared to the other three terms and hence, it can be omitted and can be treated as error term. Using the properties of EDF as given in Eq. (2.52), (2.53), and (2.54), Eq. (2.59) can be written as

$$\frac{\partial C}{\partial t}+\frac{\partial\left(u_jC\right)}{\partial x_j}-\varepsilon\left(\tau-\frac{1}{2}\right)\frac{\partial}{\partial x_j}\left(e_s^2\frac{\partial C}{\partial x_j}\right)=0 \tag{2.60}$$

The above equation can be rearranged as

$$\frac{\partial C}{\partial t}=\frac{\partial}{\partial x_j}\left(D\frac{\partial C}{\partial x_j}\right)-\frac{\partial\left(u_jC\right)}{\partial x_j} \tag{2.61}$$

where

$$D=e_s^2\varepsilon\left(\tau-\frac{1}{2}\right) \tag{2.62}$$

Since $\varepsilon=\Delta t$ (2.41), Equation (2.62) can be written as

$$D=e_s^2\Delta t\left(\tau-\frac{1}{2}\right) \tag{2.63}$$

Equation (2.61) is the governing ADE for solute transport. Equation (2.63) correlates macroscopic parameter dispersion coefficient with microscopic parameter relaxation coefficient.

2.3.5 Conversion between lattice units and physical units

Lattice Boltzmann simulations are generally carried out in lattice units because in these units solution of LBE becomes more stable and accurate. Therefore, conversion between lattice units and physical units is required for solving practical problems. The lattice length unit is denoted as lu, whereas lattice time unit is denoted as ltu. In order to obtain various quantities, such as length, time, mass, amount of substance, in physical unit, the conversion factors obtained during the conversation are simply multiplied with the corresponding quantities in lattice units. This conversion process between the units is straightforward. Let us consider that Δx_{lbm} and Δt_{lbm} are the lattice length and time step in lattice units, respectively and Δx and Δt are the corresponding lattice length and time step in physical units. The length conversion factor (L_c) is the ratio between these two lattice lengths, i.e. $L_c = \Delta x/\Delta_{lbm}$. In this thesis simulations are carried out using $\Delta x_{lbm} = 1\ lu$ and $\Delta t_{lbm} = 1\ ltu$. Therefore, L_c is equal to the lattice spacing in physical units, i.e. $L_c = \Delta x$. Therefore, if L is the length of the physical domain and N is the total number of lattice points considered in the simulation then $L_c = \Delta x = L/(N-1)$. The corresponding time step in physical unit can be calculated in the following way

(2.63). If we take D1Q3, D2Q5 type of lattices for which the value of sound speed as already discussed in this chapter is $e_s = e/\sqrt{3} = 1/\sqrt{3}(e = \Delta x_{lbm}/\Delta t_{lbm} = 1)$ then substituting the values of e_s, Δt_{lbm} and τ (the value of τ is taken equal to 1 in this thesis), in Eq. (2.63) we get 1/6 as the value of diffusion coefficient in lattice units. Now, conversion factor for diffusion coefficient, D_c, can be calculated as

$$D_c = \frac{D_x}{D_{lbm}} = \frac{\Delta x^2}{\Delta t}\frac{\Delta t_{lbm}}{\Delta x_{lbm}^2} = \frac{L_c^2}{T_c} \tag{2.64}$$

where T_c is the conversion factor for time. Using Eq. (2.64) we can write diffusion coefficient in physical units in terms of diffusion coefficient in lattice units as $D_x = D_c \times D_{lbm}$. Since D_{lbm} is 1/6 we get

$$D_x = \frac{L_c^2}{6T_c} \tag{2.65}$$

Since we have $\Delta t_{lbm} = 1ltu$, the time step in physical units is equal to the time conversion factor, T_c. Therefore, using the above Eq. (2.65) we can write the time step in physical unit as

$$\Delta t = T_c = \frac{L_c^2}{6D_x} \tag{2.66}$$

Similar time step in physical unit for D1Q2, D2Q4 type of lattices for which the value of sound speed is $e_s = e/\sqrt{2} = 1/\sqrt{2}$ (e=1 in this case) would be

$$\Delta t = T_c = \frac{L_c^2}{4D_x} \tag{2.67}$$

2.3.6 Initial and boundary conditions

In this section procedures for implementation of initial and boundary conditions for solute transport equation are presented. Bounce back scheme of LBM is the most popular one among the various scheme available for the implementation of boundary conditions in LB framework [Zeigler, 1993]

Initial conditions

The initial conditions are usually provided in terms of macroscopic variables i.e. C and $\vec{u}$. The primary variables involved with lattice Boltzmann method are particle distribution functions, which can be initialized as EDF in beginning of simulation.

Zero flux boundary

The zero flux boundary condition can be implemented in LBM using bounce back condition.

The bounce back condition essentially implies that the unknown incoming $f_i^{'}s$ are set to the outgoing $f_i^{'}s$ in opposite lattice direction i.e.

$$f_i = f_{-1} \tag{2.68}$$

Periodic boundary conditions

Periodic boundary condition can be used in the case where solution pattern is repeating itself.

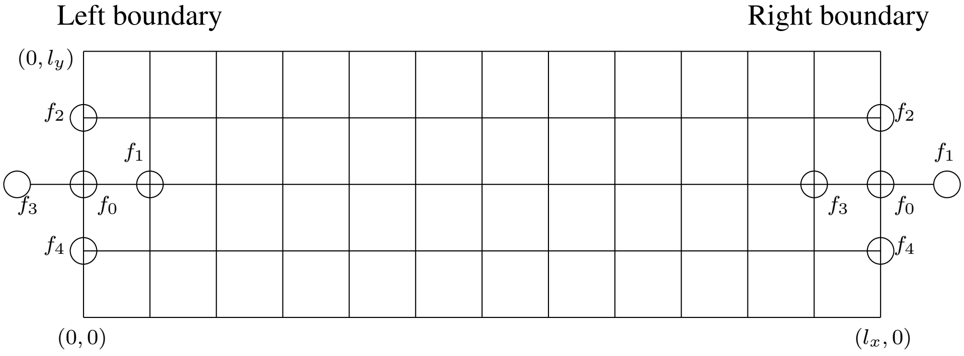

Figure 2.8: Sketch of the typical 2D domain with D2Q5 lattice. l_x and l_y are the length of the domain in x and y direction.

The periodic boundary condition can be imposed by assigning the outgoing distribution function to the incoming distribution function at other end. The typical two dimensional domain is shown in Fig. 2.8. The unknown distribution in the left boundary as shown in Fig. 2.8 is f_1. The unknown distribution in the right boundary as shown in Fig. 2.8 is f_3. Therefore the periodic boundary condition at left boundary can be written as

$$f_1(0, y, t + \Delta t) = f_1(l_x, y, t) \tag{2.69}$$

and correspondingly at the right boundary the periodic boundary is imposed as

$$f_3(l_x, y, t + \Delta t) = f_3(0, y, t) \tag{2.70}$$

2.4 Numerical Problems Solved

In this section standard one-dimensional and two-dimensional test problems are solved using the developed lattice Boltzmann scheme for solute transport and the results are compared with analytical/exact solution to demonstrate the stability and accuracy of the LBM based numerical scheme.

2.4.1 One-dimensional transport of solute in a finite width domain

Problem formulation

This test problem represents laboratory based column test where conservative solutes are introduced in a saturated soil column under steady flow with constant source at the inlet and zero flux at the outlet. The schematic of the model geometry is as shown in Figure 2.9. The transport of solutes through the column is modeled as one dimensional ADE which can be written from the general three dimensional ADE (2.1) as

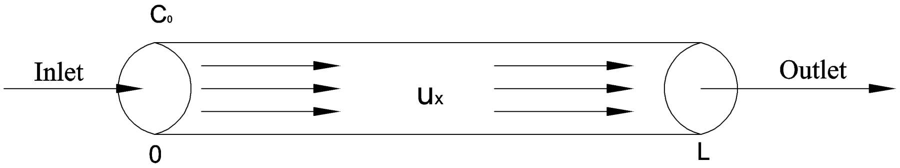

Figure 2.9: Solute transport in horizontal column

$$\frac{\partial C}{\partial t} = \frac{\partial}{\partial x}\left(D_x \frac{\partial C}{\partial x}\right) - \frac{\partial\left(u_x C\right)}{\partial x} \tag{2.71}$$

where C is concentration of solutes, D_x is dispersion coefficient along x direction, u_x represents velocity of the flow in the x direction, x is downstream distance and t is time of observation. The constant solute concentration at the inlet can be modeled as a Dirichlet boundary condition and zero flux at the outlet can be represented by Neumann boundary condition. As already discussed in this chapter, these boundary conditions can be written in mathematical forms as

$$\begin{aligned} C(x=0,t) &= C_0 \\ \frac{\partial C(x=L,t)}{\partial x} &= 0 \end{aligned} \tag{2.72}$$

where C_0 is the source concentration at the inlet and L is the column length. At t=0 concentration of solutes is zero everywhere except at x = 0. This initial condition can be written in mathematical form as

$$C(x,t=0) = C_0\delta(x) \tag{2.73}$$

where $\delta(x)$ is the Dirac delta function. $\delta(x) = 1$ when x=0 and $\delta(x) = 0$ when $x \neq 0$.

Numerical framework using LBM

LBM based simulation of the problem is carried out in lattice units and using D1Q3 lattice (Figure 2.2). The lattice length and time step in lattice units are $\Delta x_{lbm} = 1\ lu$ land $\Delta t_{lbm} = 1$ ltu. The relaxation parameter, τ, is fixed at 1. A total of 101 lattice points are considered in the simulation.

Values of input parameters used

Numerical values of the model parameters (u_x and D_x) are taken from [Zhang et al., 2002; Zhou, 2009] as benchmark problem. The domain length (L) is fixed at 0.3048 m. Since a total of 101 lattice points (n_x) are considered in LBM model, physical lattice length (Δx) is $\Delta x = L/100 = 0.3048/100\ m$ = 0.003048 m. The value of time step in physical units is calculated using Eq. (2.66) and its value is 14.4 s. The values of these physical and numerical parameters are provided in tabular form in Table 2.1.

Results and discussions

The lattice Boltzmann simulation is run at four different simulation times, e.g. 2.5 $hours$, 5 $hours$, 10 $hours$ and 15 $hours$ and corresponding spatial profiles of solute concentration are

Table 2.1: Values of input parameters used in the simulation of 1D test for solute transport in a finite domain

Parameter	Value
u$_x(m/s)$	4.23×10^{-6}
D$_x(m^2/s)$	1.075×10^{-7}
C$_0(Kg/m)$	0.001
L (m)	0.3048
n_x	101
Δx_{lbm} (lu)	1
Δt_{lbm} (ltu)	1
τ	1
Δx (m)	0.003048
Δt (s)	14.4

shown in Figure 2.10.

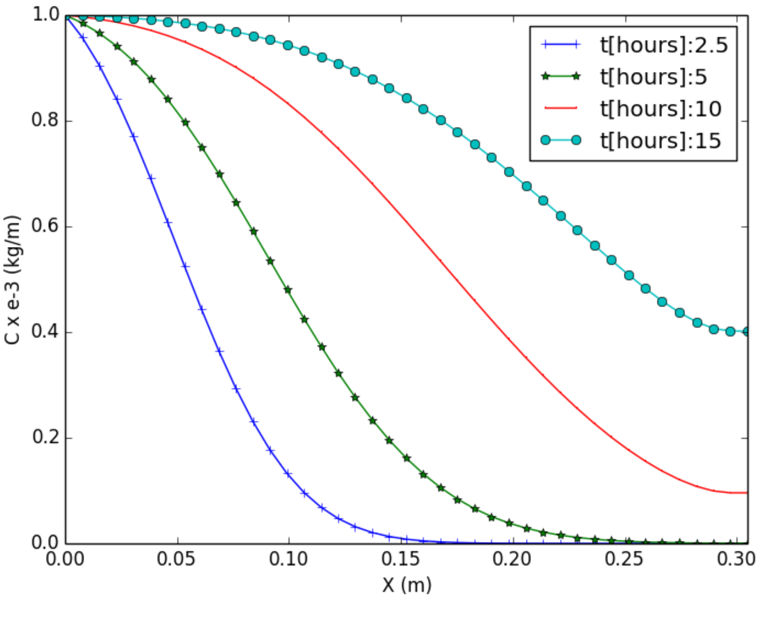

Figure 2.10: Spatial profile of solute concentration after $t = 2.5$ hours, 5 hours, 10 hours, and 15 hours using LBM

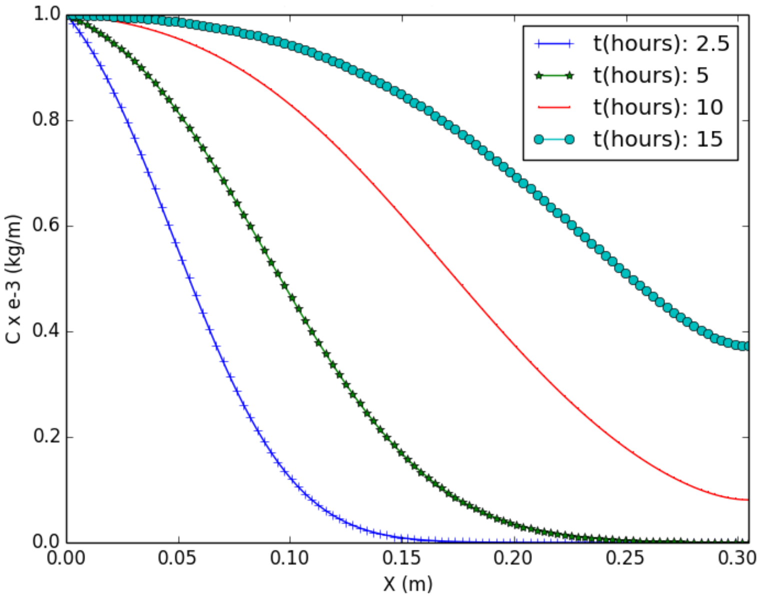

Figure 2.11: Spatial profile of solute concentration after t = 2.5 hours, 5 hours, 10 hours, and 15 hours using analytical solution

Verification and validation

The lattice Boltzmann scheme is verified and validated by comparing the numerical results with analytical solutions. The one-dimensional ADE (2.71) with the given boundary conditions (2.72) and initial condition (2.73) has closed form analytical solution of the form [Wexler, 1992]

$$C\left(x,t\right) = C_0 \left[1 - 2exp\left(\frac{xu_x}{2D_x} - \frac{u_x^2 t}{4D_x}\right) \sum_{i=1}^{\infty} \frac{\beta_i sin\left(\frac{\beta_i x}{L}\right) exp\left(-\frac{\beta_i^2 D_x t}{L^2}\right)}{\beta_i^2 + \left(\frac{u_x L}{2D_x}\right)^2 + \frac{u_x L}{2D_x}}\right] \tag{2.74}$$

where β_i are the roots of the equation

$$\beta cot\beta + \frac{u_x L}{2D_x} = 0 \tag{2.75}$$

The analytical solutions for the same simulation times are shown in Figure 2.11. The analysis of the Figures 2.10 and 2.11 shows that there is good matching between the numerical and analytical solutions.

2.4.2 One-dimensional transport of solute in an infinite domain

Problem formulation

This test problem represents transport of a point source in a very long aquifer having finite width and vertical depth. The solute source is instantaneously discharged into the aquifer and the duration of spreading along transverse and vertical directions are also instant. Therefore, the source term can be treated as an instantaneous point source which can travel only along longitudinal direction. This type of problems are generally solved in environmental hydraulics for measurement of groundwater velocity, solute dispersion coefficient etc. The solute source is discharged at a downstream distance of $x_0\ m$. The model geometry of problem is graphically shown in Figure 2.12. The transport of the discharged point is governed by 1D ADE, which is similar to that of the earlier problem and can be written as

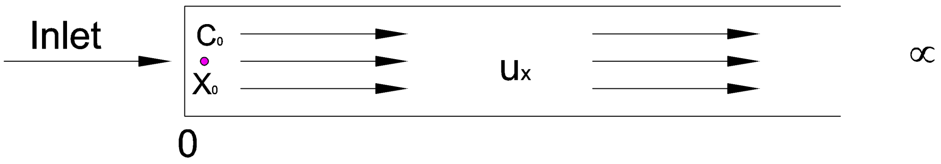

Figure 2.12: Solute transport in infinite domain

$$\frac{\partial C}{\partial t} = \frac{\partial}{\partial x}\left(D_x \frac{\partial C}{\partial x}\right) - \frac{\partial \left(u_x C\right)}{\partial x} \tag{2.76}$$

Initially the value of solute concentration is zero everywhere except at the point of discharge, therefore initial condition of the problem can be stated as

$$C(x, t = 0) = C_0 \delta(x) \tag{2.77}$$

where δ is the Kronecker delta function, C_0 is concentration of point source. Since the domain length is taken as very large, it is reasonable to consider following Dirichlet boundary

Table 2.2: Values of input parameters used in the simulation of 1D test for solute transport in an infinite domain

Parameter	Value
$u_x (m/s)$	0.01
$D_x (m^2/s)$	0.01
C_0(Kg/m)	1
L (m)	400
W (m)	10
x_0(m)	10
n_x	101
n_y	101
Δx_{lbm} (lu)	1
Δt_{lbm} (ltu)	1
τ	1
Physical lattice length along x-direction, Δx (m)	1.0
Physical lattice length along y-direction, Δy (m)	1.0
Δt (s)	16.67

conditions.

$$C(x = \pm\infty, t) = 0 \tag{2.78}$$

Numerical framework using LBM

LBM based simulation of the problem is carried out in lattice units and using D2Q5 lattice (Figure 2.4). The lattice length and time step in lattice units are $\Delta x_{lbm} = 1$ lu land $\Delta t_{lbm} = 1$ ltu. The relaxation parameter, τ, is fixed at 1. A total of 401 lattice points along x-direction (n_x) and 11 lattice points along y-direction (n_y) are considered in the simulation.

Values of input parameters used

Numerical values of the parameters involved with the above equations are taken from [Zhang et al., 2002; Zhou, 2009] as benchmark. In the simulation, the length (L) and width (W) of the model geometry are 400 m and 10 m, respectively. Therefore, the physical lattice lengths are 1.0 m along both the directions. The value of time step in physical units is calculated using Eq. (2.66) and its value is 16.67 s. Various physical and grid parameters used in the simulation are given in Table 2.2.

Results and discussions

The LBM based numerical simulation is carried out for two different simulation times via 10000 s and 30000 s. Results of the simulations in the form of spatial profiles of solute concentration are shown in Figure 2.13. It can be observed from the Figure 2.13 that the peak of solute concentration travel with the velocity of groundwater flow and due to diffusion and dispersion its peak height gets reduced with time. This spread of solute concentration is experimentally measured to calculate the value of dispersion coefficient.

Validation and verification

The lattice Boltzmann scheme is verified and validated by comparing the numerical results with analytical solutions. The analytical solution of the one-dimensional ADE (2.76) with the given initial condition (2.77) and boundary conditions (2.78) can be written as [Zhang et al., 2002]

$$C\left(x,t\right) = \frac{C_0}{\sqrt{4\pi D_x t}} exp\left[-\frac{\left(x-u_x t\right)^2}{4D_x t}\right] \tag{2.79}$$

Spatial profiles of solute concentration at simulation time $t = 10000\ s$ and 30000 s based on the analytical solution (2.79) are shown in Figure 2.14. From the interpretation of the two Figures 2.13 and 2.14 we can infer that LBM based simulation results are very close to that of analytical solutions.

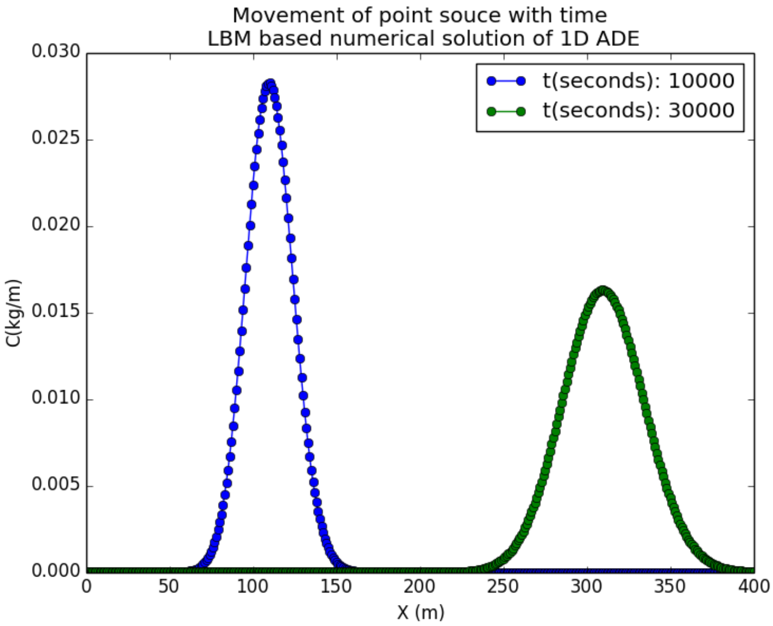

Figure 2.13: Spatial profile of solute concentration after 10000 s and 30000 s using LBM

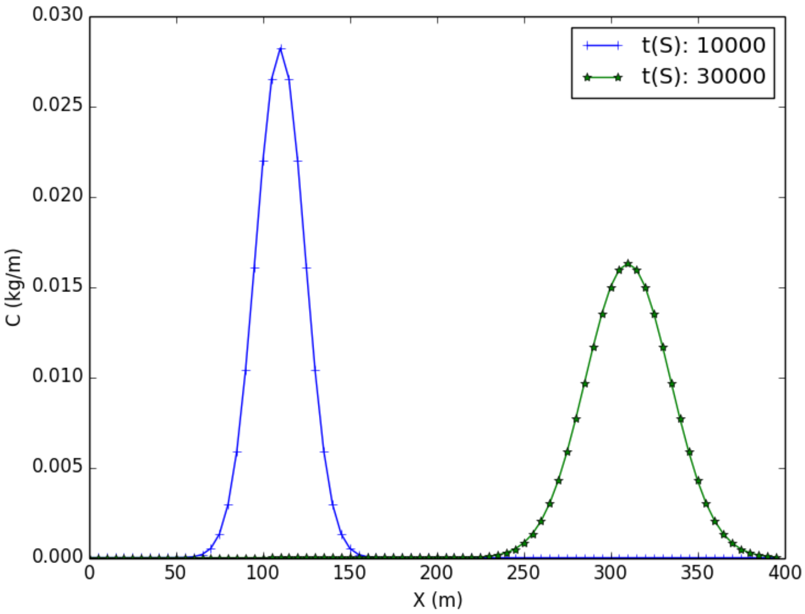

Figure 2.14: Spatial profile of solute concentration after 10000 s and 30000 s using analytical solution

2.4.3 Two-dimensional transport of solute

Problem statement

This standard test problem models migration of chloride ion in a landfill leachate through a narrow, relatively thin, valley-fill aquifer. Since the aquifer is thin, dispersion along vertical direction can be neglected and problem can be mathematically model as a two dimensional anisotropic ADE. The schematic of the model geometry is shown in Figure (2.15). Here we have considered that flow through the aquifer takes place along x-direction only. Therefore, the model equation (2D anisotropic ADE) can be written as

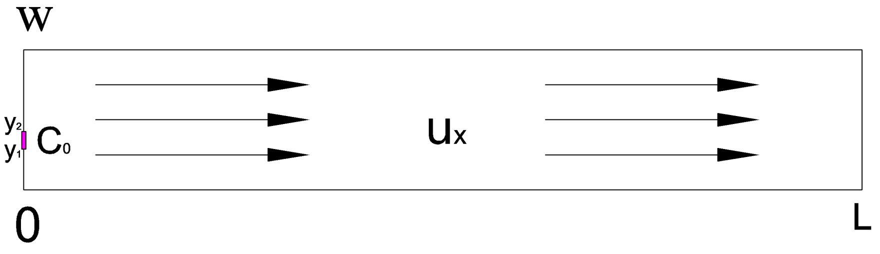

Figure 2.15: Two dimensional solute transport

$$\frac{\partial C}{\partial t} = \frac{\partial}{\partial x}\left(D_x \frac{\partial C}{\partial x}\right) + \frac{\partial}{\partial y}\left(D_y \frac{\partial C}{\partial y}\right) - \frac{\partial (u_x C)}{\partial x} \tag{2.80}$$

where D_x and D_y are the dispersion coefficients along x-direction and y-direction, respectively. Since the problem is anisotropic in nature, $D_x \neq D_y$. u_x is flow velocity along x-direction. The finite with constant source is defined by the following Dirichlet boundary condition (2.81)

$$C(x=0,y,t) = \begin{cases} C_0 & Y_1 < y < Y_2 \\ 0 & y < Y_1 \text{ or } y > Y_2 \end{cases} \tag{2.81}$$

where Y_1 and Y_2 are source position coordinate along y direction and source width is $Y_2 - Y_1$. The zero flux boundary conditions at all boundary locations except the inlet one (x=0 plane) are

Table 2.3: values of input data used in the simulation of 2D solute transport

Parameter	Value
$u_x (m/s)$	3.527777×10^{-6}
$D_x (m^2/s)$	2.150533×10^{-4}
$D_y (m^2/s)$	6.4516×10^{-5}
Length of the aquifer (L in m)	1500
Width of the aquifer (W in m)	900
Y coordinate of the source	$(Y_1 = 121.92\ m, Y_2 = 609.9\ m)$
Initial concentration kg/m^2	1

defined by Neumann boundary condition as

$$\begin{aligned}
&\frac{\partial C(x,y,t)}{\partial x}|_{x=L} = 0, \qquad 0 < y < W \\
&\frac{\partial C(x,y,t)}{\partial y}|_{y=0} = 0, \qquad 0 < x < L \\
&\frac{\partial C(x,y,t)}{\partial y}|_{y=W} = 0, \qquad 0 < x < L
\end{aligned} \tag{2.82}$$

where L is the length of the aquifer, W is the width of the aquifer. The initial solute concentration is considered to be equal to zero everywhere in the domain except at source positions. therefore, initial condition for the problem can be defined as

$$C\,(x, y, t = 0) = 0, \qquad 0 < x < L, \text{ and } 0 < y < W \tag{2.83}$$

Lattice Boltzmann simulation

Since the problem is anisotropic in nature, the standard SRT LBM scheme with square lattice is unable to simulate this process. In this regard, Zhang et al. considered rectangular lattice and directional dependent relaxation parameters (τ) to simulate anisotropic ADE [Zhang et al., 2002]. Later on Zhou developed a SRT LBM scheme with rectangular lattice and modified the standard EDF in order to embed the feature of a rectangular lattice [Zhou, 2009]. Both this formulations are complicated due to consideration of directional dependent relaxation parameters in the first one and due to difficulties involved in estimation of proper EDF. In this study we propose a new formulation that is capable of simulating such anisotropic ADE in a square lattice [Datta et al., 2018a,b]. This formulation is based on diffusion velocity lattice Boltzmann scheme developed by Perko et al. [Perko et al., 2014]. They used their formulation to simulate ADE in heterogeneous media having spatial dependency in dispersion coefficient. The basic steps involved with diffusion velocity lattice Boltzmann formulation is to write the total physical dispersion coefficient as a combination of two parts as

$$D = D_{ref} + D_{fluc} \tag{2.84}$$

where D is the total physical dispersion coefficient, D_{ref} is called reference dispersion coefficient and D_{fluc} is called fluctuating part of the dispersion coefficient. Perko et al. converted the diffusion flux due to D_{fluc} into an equivalent velocity flux and calculated the corresponding velocity term as [Perko et al., 2014]

$$u_d = -\frac{D_{fluc}\frac{\partial C}{\partial x}}{C} \tag{2.85}$$

where u_d is called diffusion velocity. They added this velocity term with the advective velocity term and then followed the same procedures as used in SRT LBM scheme. Using this concept we can write the longitudinal dispersion coefficient as a sum of transverse dispersion coefficient and fluctuating term as

$$D_x = D_y + D_{fluc} \tag{2.86}$$

Substituting this value in Eq. (2.84) and rearranging we get

$$\frac{\partial C}{\partial t} = \frac{\partial}{\partial x}\left(D_y \frac{\partial C}{\partial x}\right) + \frac{\partial}{\partial y}\left(D_y \frac{\partial C}{\partial y}\right) - \frac{\partial \left(u_t C\right)}{\partial x} \tag{2.87}$$

where $u_t = u_x + u_d$ is the total velocity. The above Eq. (2.87) is an isotropic ADE which can easily be solved using the standard the LBM scheme already used for solving one-dimensional solute transport problems. In the lattice Boltzmann simulation we have taken D2Q5 square lattice (Figure 2.4). The lattice length and time step in lattice units are $\Delta x_{lbm} = 1\ lu$ land $\Delta t_{lbm} = 1\ ltu$. The relaxation parameter, τ, is fixed at 1. The physical lattice length used in this simulation is 25 m. The domain length and width of the aquifer are 1500 m and 900 m, respectively. Therefore, a total of 61×41 lattice points are used in the simulation. The value of time step in physical units is calculated using Eq. (2.66) with D_y as the value of the dispersion coefficient.

Values of input parameters used

The values of the physical parameters are taken from the literature [Zhou, 2009]. The numerical values of these parameters and grid parameters used in the simulation are given in Table 2.3.

Results and discussions

Spatial profiles of solute concentration are calculated using the developed LBM scheme after 1500 $days$ and 1500 $days$. Results of the simulations in the form of spatial profiles of solute concentration are shown in Figures 2.16 and 2.18, respectively.

Validation and verification

The analytical solution of the model equation (2.80) using the given initial and boundary conditions (2.82, 2.83) can be written as [Wexler, 1992]

$$\begin{aligned} C\left(x,y,t\right) = &C_0 \sum_{n=0}^{\infty} L_n P_n cos\left(\eta y\right) \left\{ exp\left[\frac{x\left(u_x-\beta\right)}{2D_x}\right] erfc\left[\frac{x-\beta t}{2\sqrt{D_x t}}\right] \right. \\ &\left. + exp\left[\frac{x\left(u_x+\beta\right)}{2D_x}\right]\left[\frac{x-\beta t}{2\sqrt{D_x t}}\right]\right\} \end{aligned} \tag{2.88}$$

where

$$L_n = \begin{cases} \frac{1}{2}, & n = 0 \\ 1, & n > 0 \end{cases} \tag{2.89}$$

$$P_n = \begin{cases} \frac{y_2 - y_1}{W}, & n = 0 \\ \frac{[sin(\eta y_2) - sin(\eta y_1)]}{n\pi}, & n > 0 \end{cases} \tag{2.90}$$

$$\eta = \frac{n\pi}{W}, \qquad n = 0, 1, 2, 3, ... \tag{2.91}$$

$$\beta = \sqrt{u_x^2 + 4\eta^2 D_x D_y} \tag{2.92}$$

Analytical solutions after 1500 $days$ and 3000 $days$ are shown graphically in Figures 2.17 and 2.19, respectively. The similarities of the LBM and corresponding analytical solutions confirms the accuracy of the proposed model.

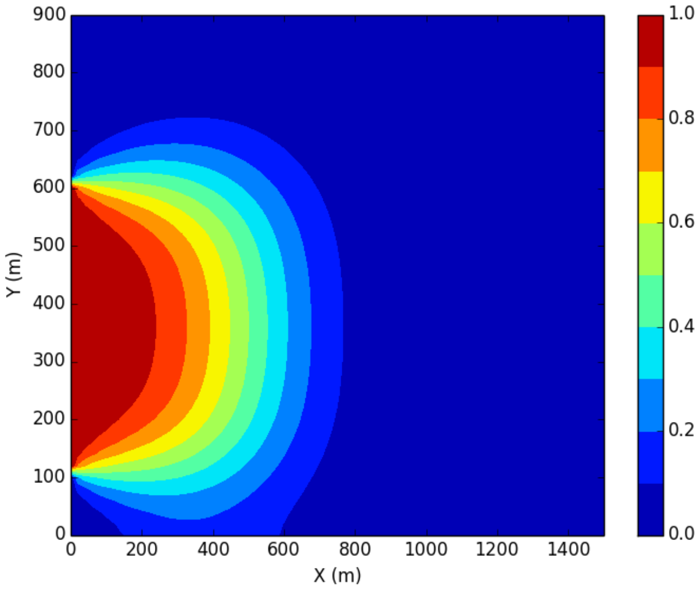

Figure 2.16: Solute concentration contours after 1500 days for 2D ADE: Numerical Solution

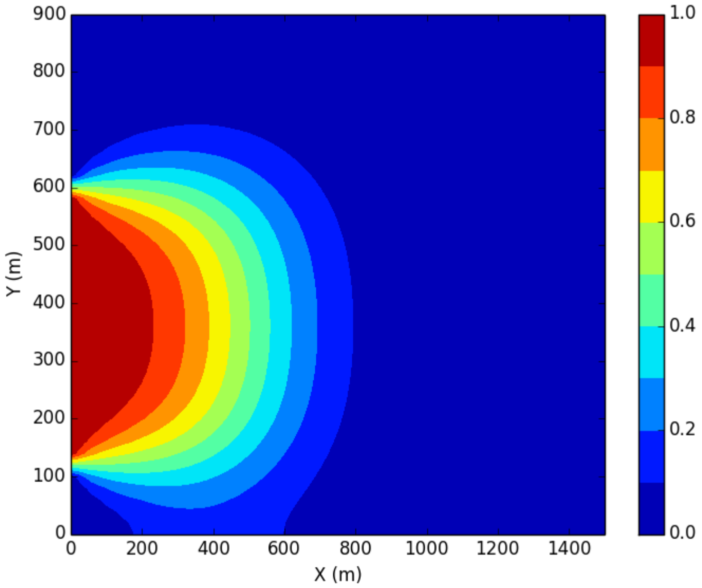

Figure 2.17: Solute concentration contours after 1500 days for 2D ADE: Analytical Solution

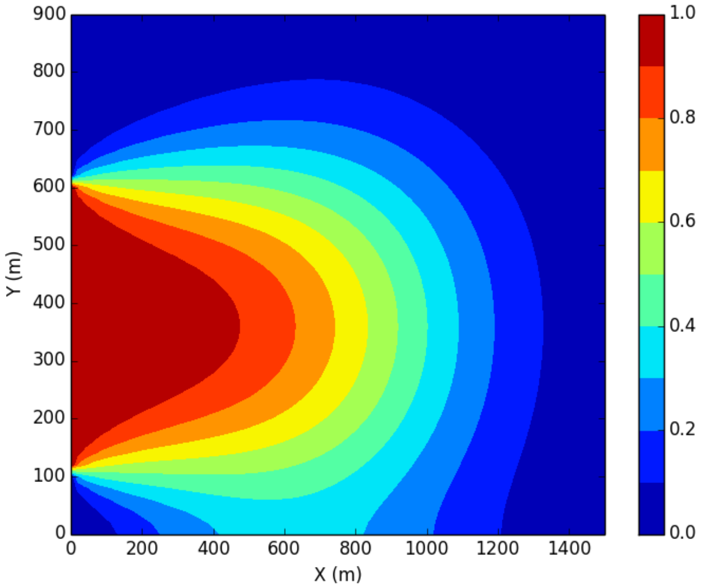

Figure 2.18: Solute concentration contours after 3000 days for 2D ADE: Numerical Solution

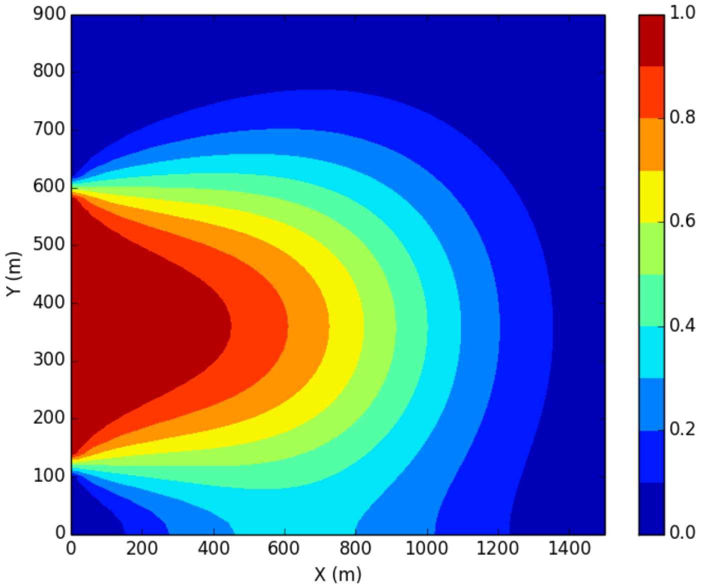

Figure 2.19: Solute concentration contours after 3000 days for 2D ADE: Analytical Solution

2.5 Limitation of Lattice Boltzmann Method for High Peclet Number Flow

Since LBM is an explicit scheme, it suffers from numerical instability at high Peclet number flow. In order to create sharp (step) jump in dependent variable in the domain, the benchmark problem in Section 2.4.1 One-dimensional transport of solute in a finite width domain is solved at higher velocity. The velocity is increased 100 times to that of the previous value listed in Table 2.1. The grid Peclet (Pe) number, which is the ration between diffusive time step and advective time step, is defined as

$$Pe = \frac{u_x \Delta x}{D_x} \tag{2.93}$$

For the same lattice length ($x = 0.003048\ m$) as used in Section 2.4.1, the value of Peclet number is 12 and LBM based solution is unstable. Figure 2.20 shows the results of the simulation. Since the value of the Peclet number reduces with decrease in lattice length, further simulations with smaller lattice lengths are carried out. It has been observed that LBM based results are stable only when $Pe < 2.4$. The spatial profiles of solute concentration at $Pe = 6, 4, 3,$ and 2.4

are shown in Figs. 2.21, 2.22, 2.23.

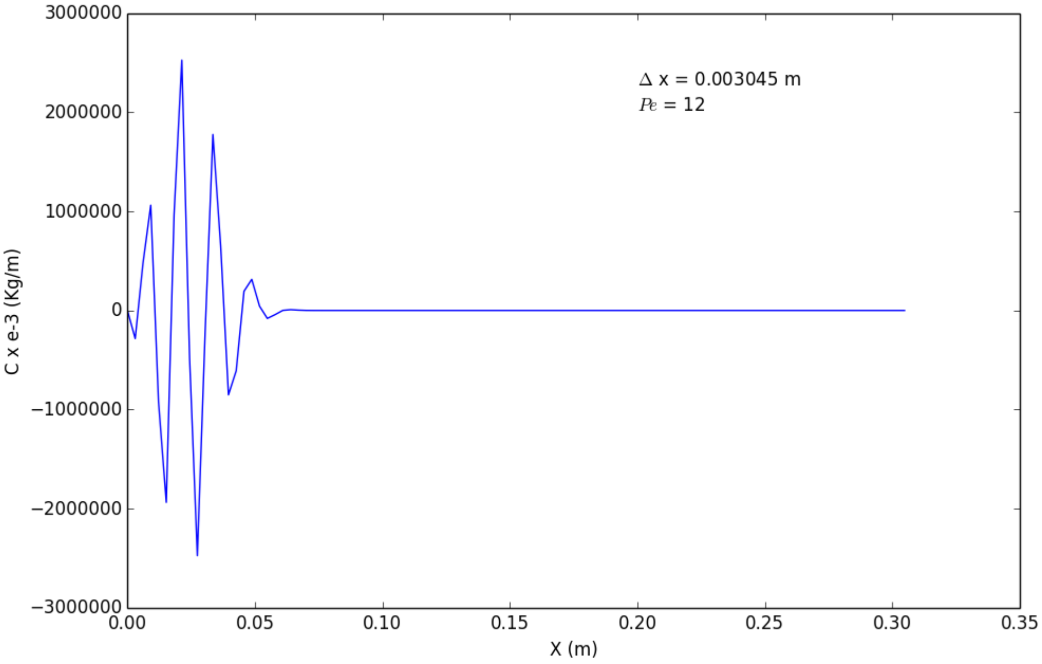

Figure 2.20: Unstable solution with Pe=12 after 0.1 hour

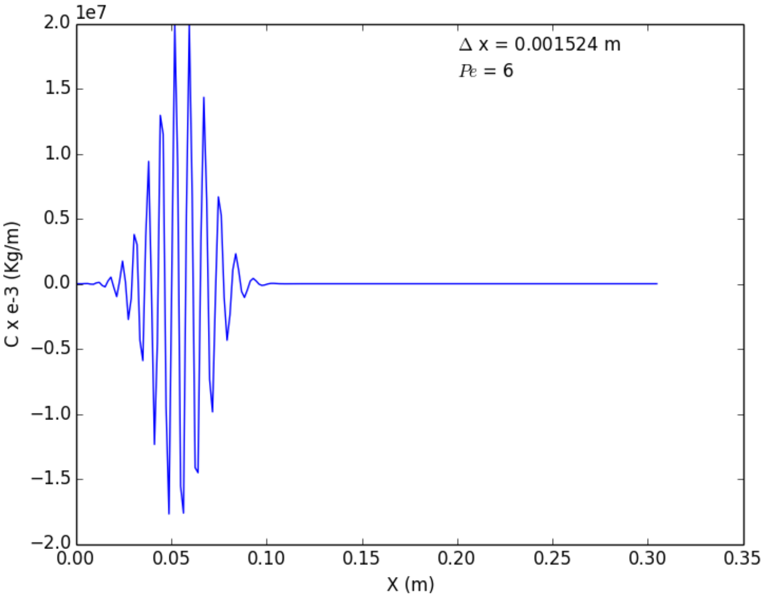

Figure 2.21: Unstable solution with Pe=6 after 0.1 hour

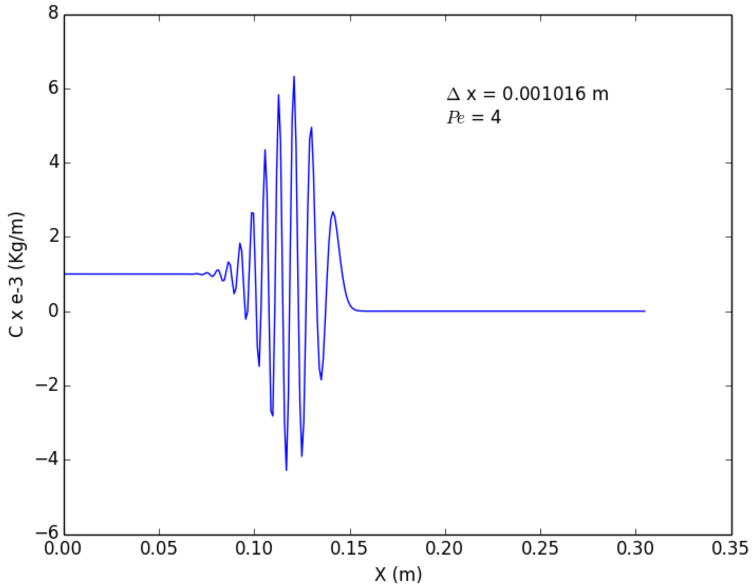

Figure 2.22: Unstable solution with Pe=4 after 0.1 hour

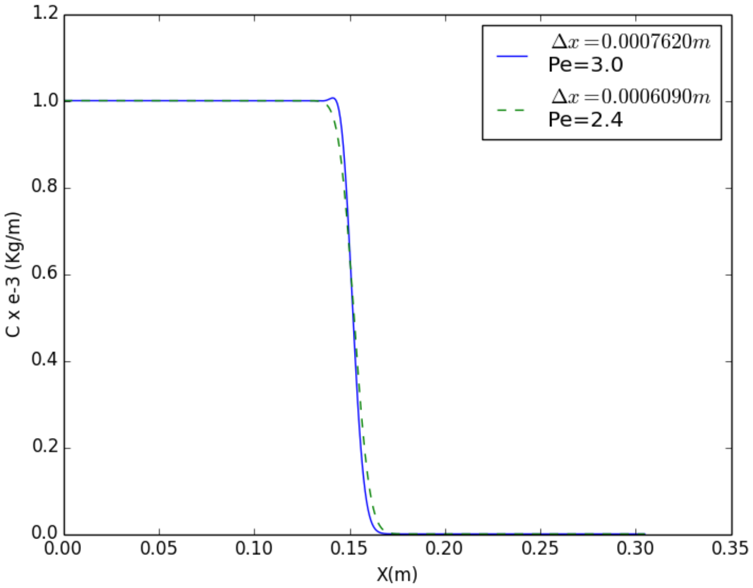

Figure 2.23: Solution is approaching towards stability Pe=3 and 2.4 after 0.1 hour

2.6 Differential Quadrature Method for Solute Transport

In this section an alternate numerical technique called differential quadrature method (DQM) [Bert et al., 1996; Shu, 2000; Zong et al., 2009] is utilized to solve solute transport equations.

The concept of DQM is simple and it can be implemented straightforwardly. Since DQM requires very few grid points for solving differential equations with high accuracy, minimum computational efforts are required to implement it [Bellman et al., 1972; Malik et al., 1995; Bert et al., 1996]. Historically DQ method was developed as an analogous to numerical integration technique called numerical quadrature. In numerical quadrature, definite integral over a closed domain is approximated by a linear weighted sum of integrand values at a group of points in the domain of integration, similarly in DQ method, partial derivative of a piecewise continuous function at a grid point is approximated as weighted sum of functional values of the solution at all grid points along a grid line [Bellman et al., 1972]. The DQ method was introduced by Richard Bellman and his associates in the early of 1970s [Bellman et al., 1971, 1972]. Currently, the DQ method has been extensively applied in various engineering domains for the rapid and accurate solution of various linear and non linear differential equations [Zong et al., 2009].

As discussed in chapter 1, the DQ approximation of n^{th} order derivative of a continuous function at a given node with respect to x is written as

$$f_x^k\left(x_i\right) = \frac{\partial^k f}{\partial x^k}\,|_{x=x_i} = \sum_{j=1}^{N} A_{ij}^{(k)} f\left(x_j\right), \quad i = 1, 2, 3, ..., N, \quad j = 1, 2, ..., N-1 \tag{2.94}$$

where x_j are the discrete nodes in the domain at which function values are known, $f(x_j$ are the function values at these nodes, N is the total number of such nodes, and A_{ij}^k are the weighting coefficients for the k^{th} order derivative of the function, therefore for a N point DQM, A_{ij}^k are the elements of a $N \times N$ matrix. The value of weighting coefficients of DQM is not influenced by the type of problem being solved rather it depends upon the type of base function or the approximate solution of the differential equation. Three frequently used bases are polynomial basis, Fourier expansion basis, and harmonic basis. For polynomial basis the DQM is called polynomial differential quadrature (PDQ), for Fourier expansion basis DQM is named as

Fourier Expansion based Differential Quadrature (FDQ), and it is called Harmonic Differential Quadrature (HQM) when harmonic based are used [Zong et al., 2009]. In this study PDQ is used because the polynomial approximation is suitable for most of the engineering problems except those which have periodic and harmonic behaviors. In a PDQ, the solution of a partial differential equation is approximated as an N-th degree polynomial.

2.7 Numerical Problems Solved

In this section test problems are solved using DQ method and numerical results are compared with analytical solution to demonstrate the capability and efficiency of DQ method for solution of solute transport equation.

2.7.1 Diffusion of solute in soil column

Problem formulation

This test problem simulates the diffusion of chloride ion in a 0.4 m long column composed of grains of soil samples. In the configuration, the chloride ion does not interact with the composition of soil and water and only diffuses into the column. The diffusion of chloride ion will follow the following 1-D diffusion equation

$$\frac{\partial C\left(x,t\right)}{\partial t} = D\frac{\partial^2 C\left(x,t\right)}{\partial x^2} \tag{2.95}$$

where D is the diffusion coefficient of chloride ion in the soil column, C is concentration of chloride ion in solution, x is the distance from the inlet of the column, t represent observation time. The simulation time is kept lower than the diffusive time in order to avoid the effect of outlet boundary condition. Initial and boundary conditions at the inlet are

$$C\left(x, t=0\right) = 0 \tag{2.96}$$

$$C\left(x=0, t\right) = C_0 \tag{2.97}$$

In order to keep the analytical solution simple following outlet boundary condition is taken into consideration

$$\frac{\partial C\left(x,t\right)}{\partial x} \mid_{x=\infty} = 0 \tag{2.98}$$

Formulation of DQ scheme

To solve the Eq. (2.95) using DQ method, the spatial derivative at the grid points is replaced by the DQ discretization method and temporal derivative is replaced by explicit finite difference scheme. The discretized equation can be written as

$$\frac{C_i^{k+1} - C_i^k}{\Delta t} = D \sum_{j=1}^{N} A_{ij}^{(2)} C_j^k \qquad i = 1, 2, ..., N \tag{2.99}$$

Rearranging the above equation, we get

$$C_i^{k+1} = C_i^k + D\Delta t \sum_{j=1}^{N} A_{ij}^{(2)} C_j^k \qquad i = 1, 2, ..., N \tag{2.100}$$

Values of input parameters used

The numerical values of dispersion coefficient and initial solute concentration are taken from literature. The values of these parameters and other parameters considered in the simulation are given in Table

Results and discussions

Numerical values of chloride ion concentration at various locations of the soil column are cal-

Table 2.4: Values of input parameters used in the simulation of diffusion of solutes in a soil column

Parameter	Value
D (m^2/s)	3×10^{-10}
C_0(mmol/l)	1
Number of grid points (n_x)	21

culated by solving the DQ Eq. (2.100) with 21 non-uniform grid points. The locations of the grid points are calculated using Eq. (1.30). The spatial profiles of chloride ion concentration are drawn for at $t =$ 10, 30 and 100 $days$.

Verification and validation

The analytical solution of the model Eq. (2.95) using the given initial and boundary conditions can be written as

$$C\left(x,t\right) = C_0\left[erfc\left(\frac{x}{\sqrt{4Dt}}\right)\right] \tag{2.101}$$

where $erfc(\alpha)$ is the complementary error function. The mathematical forms of error function and complementary error function are given in the following Eq. (2.102)

$$\begin{aligned} erf(\alpha) &= \frac{2}{\sqrt{\pi}}\int_0^{\alpha} e^{-t^2}dt \\ erfc(\alpha) &= 1 - erf(\alpha) \end{aligned} \tag{2.102}$$

The DQ based solutions of the problem are compared with the closed form solution (2.101) and a good agreement between the two results is established. The spatial plots of chloride ions are shown in Figure 2.24.

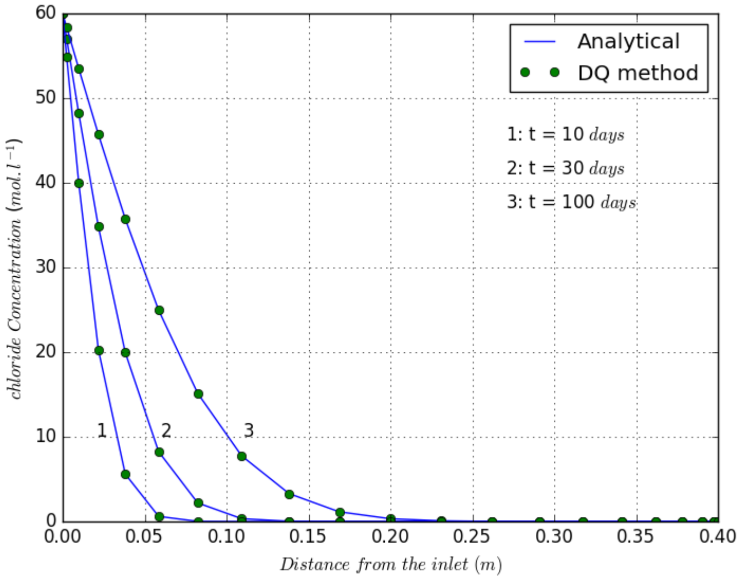

Figure 2.24: Time dependent spatial plots of chloride concentration in the soil column: comparison with analytical solution (No. of grid points = 21)

2.7.2 Leaching of radionuclide from radioactive waste form

Problem formulation

This test problem simulates leaching of radionuclides from a vitrified cementitious waste form. The geometry of the waste form is cylindrical. The leaching of radionuclides from the waste form take place due to diffusion and dissolution processes. Considering dissolution rate of the material is very slow, the process is mathematically modeled as an axisymmetric diffusion equation. The rate of change of concentration of radionuclides inside the cylindrical waste form due to diffusion process can be written as [Pal, et al.]

$$\frac{\partial C(r,t)}{\partial t} = \frac{D_r}{R_d}\frac{\partial^2 C(r,t)}{\partial r^2} + \frac{D_r}{R_d}\frac{1}{r}\frac{\partial C(r,t)}{\partial r} - \lambda C(r,t) \tag{2.103}$$

where $C(r,t)$ is concentration of radionuclides in waste form (Bq/ml), D_r is radial diffusion coefficient in waste form (cm^2/s), r is radial coordinate inside waste form (cm), λ represents radioactive decay constant (s^{-1}), t is time (s) of observation, R_d is retardation factor defined as $R_d = (1 + \frac{\rho}{\theta} K_d)$, ρ = bulk density of matrix used (gm/ml), θ = total porosity of the waste form, K_d = distribution coefficient of radionuclide for the matrix used (ml/gm). Eq. (2.103) is an axisymmetric diffusion equation with decay term. The diffusion leaching from the top and bottom surfaces is neglected considering thick barriers above and below the waste-form. The initial and boundary conditions for the problem can be written as

$$\begin{aligned} &C\left(r, t=0\right) = C_0 \\ &C\left(x=R, t\right) = 0 \\ &\frac{\partial C\left(r,t\right)}{\partial r}|_{r=0} = 0 \end{aligned} \tag{2.104}$$

where C_0 is initial concentration of radionuclides in the waste-form (Bq/ml), R is radius of the cylindrical waste-form, Boundary conditions described by Eq. (2.104) means that mass transfer external to the cylinder is so rapid relative to the internal transfer in the cylinder that the surface concentration is maintained at zero for any time greater than zero. The leach rate $(1/cm^2/s)$ of radioactivity can be evaluated using the relation

$$L_r\left(r,t\right) = -D_r \frac{\partial C\left(r,t\right)}{\partial r}|_{r=R} \tag{2.105}$$

Formulation of DQ scheme

The DQ equation of the leaching process defined mathematically in Eq. (2.103) with forward difference approximation of the time derivative and the spatial derivatives using PDQM can be written as

$$\begin{aligned} \frac{C\left(r_i, t+\Delta t\right) - C\left(r_i, t\right)}{\Delta t} &= D_r^* \left(\sum_{j=1}^{N} A_{ij}^{(2)} C\left(r_j, t\right) + \frac{1}{r_i} \sum_{j=1}^{N} A_{ij}^{(1)} C\left(r_j, t\right) \right) \\ &\qquad -\lambda C\left(r_i, t\right) \qquad i = 1, 2, ..., N \end{aligned} \tag{2.106}$$

Rearranging the above equation we get

$$
\begin{aligned}
C\left(r_i, t+\Delta t\right) = (1-\lambda\Delta t)\, C\left(r_i, t\right) + D_r^{*}\Delta t \Bigg(& \sum_{j=1}^{N} A_{ij}^{(2)} C\left(r_j, t\right) \\
& + \frac{1}{r_i}\sum_{j=1}^{N} A_{ij}^{(1)} C\left(r_j, t\right) \Bigg) \qquad i = 1, 2, ..., N
\end{aligned}
\tag{2.107}
$$

where Δt is discrete time step, N is the number of sampling grid points along radial direction. A^1, A^2 are the weighting coefficient matrices. In matrix form, Eq. (2.107) can be written as

$$
C\left(r, t+\Delta t\right) = (1-\lambda\Delta t)\, C\left(r, t\right) + D_r^{*}\Delta t \left[A^{(2)} C\left(r, t\right) + R A^{(1)} C\left(r, t\right)\right] \tag{2.108}
$$

where

$$
C\left(r, t+\Delta t\right) = \begin{pmatrix} \mathrm{C}(r_1, t+\Delta t) \\ \mathrm{C}(r_2, t+\Delta t) \\ . \\ . \\ . \\ \mathrm{C}(r_N, t+\Delta t) \end{pmatrix}, \qquad C\left(r, t+t\right) = \begin{pmatrix} \mathrm{C}(r_1, t) \\ \mathrm{C}(r_2, t) \\ . \\ . \\ . \\ \mathrm{C}(r_N, t) \end{pmatrix}
$$

$$A^{(2)}=\begin{pmatrix} \mathrm{A}_{11}^{(2)} & \mathrm{A}_{12}^{(2)} & . & . & . & \mathrm{A}_{1N}^{(2)} \\ \mathrm{A}_{21}^{(2)} & \mathrm{A}_{22}^{(2)} & . & . & . & \mathrm{A}_{2N}^{(2)} \\ . & . & . & . & . & . \\ . & . & . & . & . & . \\ . & . & . & . & . & . \\ \mathrm{A}_{N1}^{(2)} & \mathrm{A}_{N2}^{(2)} & . & . & . & \mathrm{A}_{NN}^{(2)} \end{pmatrix},\ A^{(1)}=\begin{pmatrix} \mathrm{A}_{11}^{(1)} & \mathrm{A}_{12}^{(1)} & . & . & . & \mathrm{A}_{1N}^{(1)} \\ \mathrm{A}_{21}^{(1)} & \mathrm{A}_{22}^{(1)} & . & . & . & \mathrm{A}_{2N}^{(1)} \\ . & . & . & . & . & . \\ . & . & . & . & . & . \\ . & . & . & . & . & . \\ \mathrm{A}_{N1}^{(1)} & \mathrm{A}_{N2}^{(1)} & . & . & . & \mathrm{A}_{NN}^{(1)} \end{pmatrix}$$

$$R=\begin{pmatrix} 1/\mathrm{r}_1 & 0 & . & . & . & 0 \\ 0 & 1/\mathrm{r}_2 & . & . & . & 0 \\ . & . & . & . & . & . \\ . & . & . & . & . & . \\ . & . & . & . & . & . \\ 0 & 0 & . & . & . & 1/\mathrm{r}_N \end{pmatrix}$$

where r_1, r_2, . . ., r_N are the radial co-ordinates of the discrete nodes. In the DQM computational algorithm, initial condition given in Eq. (2.104) is implemented explicitly by initializing the problem with an array of concentration as shown below

$$\begin{pmatrix} \mathrm{C}(r_1,0) \\ \mathrm{C}(r_2,0) \\ . \\ . \\ . \\ \mathrm{C}(r_N,0) \end{pmatrix} = \begin{pmatrix} \mathrm{C}_0 \\ \mathrm{C}_0 \\ . \\ . \\ . \\ \mathrm{C}_0 \end{pmatrix}$$

Since there are boundary conditions at the center and at the surface of the cylinder, we need to exclude these two grid points from DQM equation derived in Eq. (2.107). The modified equation can be written as

$$\begin{aligned} C\left(r_i, t+\Delta t\right) = \left(1-\lambda\Delta t\right) C\left(r_i,t\right) + D_r^*\Delta t \Bigg(\sum_{j=2}^{N-1} A_{ij}^{(2)} C\left(r_j,t\right) \\ + \frac{1}{r_i}\sum_{j=2}^{N-1} A_{ij}^{(1)} C\left(r_j,t\right)\Bigg) \qquad i = 2, ..., N-1 \end{aligned} \tag{2.109}$$

The Neumann boundary condition at the center of the cylinder given in Eq. (2.104) can also be written in the form of DQ equation as

$$\sum_{j=1}^{N} A_{ij}^{(1)} C\left(r_j,t\right) = 0$$

The above equation can be rearranged as

$$C\left(r_1,t\right) = -\sum_{j=2}^{N} A_{ij}^{(1)} C\left(r_j,t\right) \tag{2.110}$$

Table 2.5: Input data for leach rate calculation

Parameter	Value
$C_0 Bq/ml$	1.0
Half life (y)	30.1
$D(cm^2/s)$	1.8×10^{-6}
$\rho(gm/ml)$	1.3
θ	0.15
$K_d(ml/gm)$	30.0
R (cm)	100.0

The Eqs. (2.109) and (2.110) are the working equations for simulation of the leach process. Leach rate is estimated after calculating concentration profile in the waste form. DQM solution of leach rate as given in Eq. (2.105) can be written as

$$L_r\left(R,t\right) = -D_r\sum_{j=1}^{N} A_{Nj}^{(1)}C\left(r_j,t\right) \tag{2.111}$$

where $C(r_j,t)$ are the solutions of Eq. (2.109) and (2.110).

Values of input parameters used

The ^{137}Cs radionuclide which is supposed to be present with major percentage in cementitious nuclear waste form is taken as the studied radionuclide. The parameters used in the simulation are given in the table 2.5.

Results and discussion

The DQ solutions in terms of concentration of ^{137}Cs are calculated by solving the Eq. (2.109) with 30 nonuniform grid points. The locations of the grid points are calculated using Eq. (1.30). The radial concentration profiles of ^{137}Cs are drawn for total simulation times of 10, 30 and 100 years. From the radial concentration, calculation of leach rate is carried out using Eq. 2.111 and 11 nonuniform grid points.

Verification and validation

Analytical solution of the problem can be written as

$$C\left(r,t\right)=\sum_{n=1}^{\infty}\frac{2C_0}{\alpha_n J_1\left(\alpha_n\right)}J_0\left(\frac{\alpha_n r}{R}\right)\times exp\left[-\left(\lambda+\frac{\alpha_n^2 D_r}{R_d R^2}\right)t\right] \tag{2.112}$$

where J_0, J_1 are first kind of Bessel functions of order 0 and 1, respectively, α_n = roots of $J_0(\alpha) = 0$. Eq. (2.112) gives concentration of radionuclide at various radial distances and at various times. Analytical form of leach rate at the surface of the cylinder can be formulated by substituting the value $C(r,t)$ from Eq. (2.112) into the Eq. (2.105) as

$$L_R\left(r,t\right)=\sum_{n=1}^{\infty}\frac{2C_0 D_r}{R}\times exp\left[-\left(\lambda+\frac{\alpha_n^2 D_r}{R_d R^2}\right)t\right] \tag{2.113}$$

The DQ and analytical solutions of radial profile of concentration are shown in Figure 2.26. The comparison between calculated time dependent leach rate using DQM and analytical methods, are shown in Figure 2.26. The results are also given in tabular form in Table 2.6. The result shows that DQM based leach rate exactly matches with analytical results. The result also implies that leach rate gradually decreases with time and becomes almost zero after 300 $years$, i.e., after 10 half lives of ^{137}Cs..

Table 2.6: Leach rate calculated using DQ method and Analytical solution

Sr. No.	Time $(year)$	Leach Rate $(cm^{-2}s^{-1})$	
		DQM	Analytical
1	1	2.0388×10^{-06}	2.0953×10^{-06}
2	2	1.4570×10^{-06}	1.3839×10^{-06}
3	5	8.5991×10^{-07}	8.6108×10^{-07}
4	10	5.3982×10^{-07}	5.4106×10^{-07}
5	20	3.0153×10^{-07}	3.0143×10^{-07}
6	30	1.9473×10^{-07}	1.9469×10^{-07}
7	60	6.8342×10^{-08}	6.8338×10^{-08}
8	100	2.0869×10^{-08}	2.0867×10^{-08}
9	300	1.1659×10^{-10}	1.1656×10^{-10}
10	1000	5.9582×10^{-18}	5.9536×10^{-18}

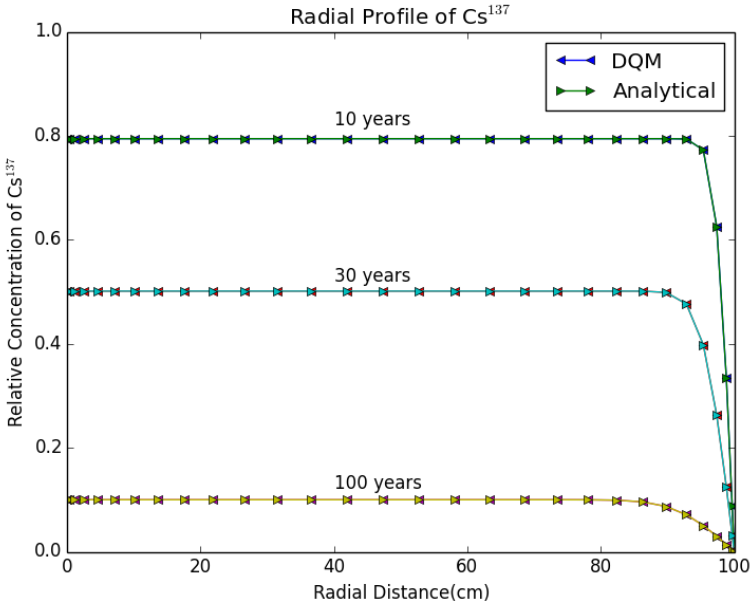

Figure 2.25: Radial Profile of Concentration of ^{137}Cs inside the waste form: Comparisons between DQM and Analytical Solution

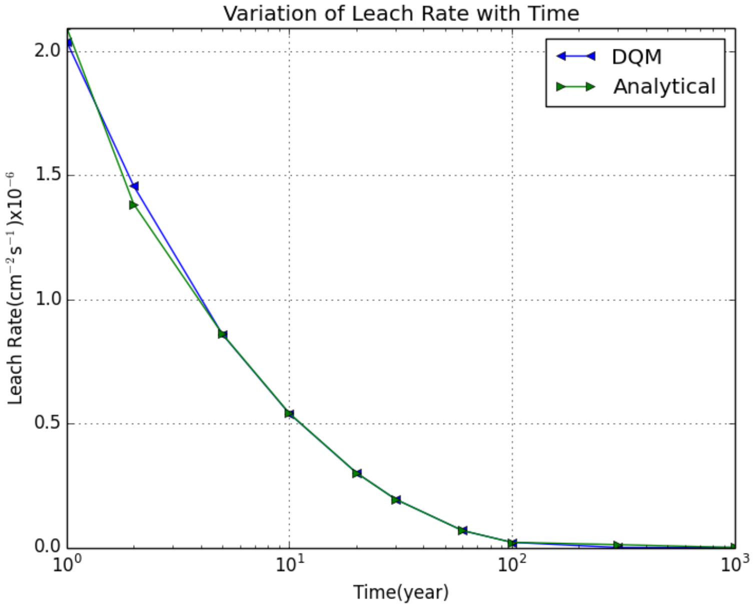

Figure 2.26: Time dependent leach rate: comparison with analytical solution (No. of grid points = 21)

2.8 Comparative Study of LBM, DQM, and FDM

In this section, a comparative study is carried out to assess selection of DQM and LBM as faster algorithms than FDM. The benchmark problem given in Section 2.4.1 ”One dimensional transport of solute in a finite width domain is solved using LBM, DQM and FDM. The simulations are carried out for two different lattice lengths and at three different simulation times. The results of the study are given in tabular forms in the Table 2.7 and 2.8. Accuracy of the techniques is assessed by comparing the results with analytical solution and calculating L2 error. It can be observed from the tables that DQM based solutions are more accurate than the LBM and FDM based solutions and at the same time it takes smaller computing time. On the other hand, accuracy of LBM and FDM are same for same time step value, but LBM takes much smaller time than FDM. One interesting fact that has been observed from this study is that computing time does not change substantially with increase in simulation time for DQM simulation. This fact is due to the fact that DQM based simulation requires very small number of grid points (11 no in this study).

Parallelization of LB code is done using OpenMP directives in a shared memory platform with Intel G1 quad-core processor. Since the problem is relatively simple, computing time required to solve it is small of the order of few minutes. Because of this, much efficiency in computing time using the parallel versions of the serial code has not been observed. As a test case, we increased the computational load by reducing the grid size and achieved up to 2 times reduction in computing time. Computing time required to solve the problem with different lattice lengths using serial and parallel LBM codes are shown in Table 2.9. From Table 2.9 and corresponding plot of computing time Vs computing load in Figure 2.27 it can be observed that efficiency of parallel LBM code increases with increase in computing load. Since computing load is huge for long term simulation of radioactive waste migration, this study therefore justifies development of LBM/DQM codes for such kind of problems.

Table 2.7: Relative performance of DQM, LBM and FDM (x = 0.003048 cm, lattice points = 101)

Sr. No.	Simulation time (h)	L_2 error			Computing time (s)		
		DQM	LBM	FDM	DQM	LBM	FDM
1	10.0	0.000354	0.000489	0.000489	0.2793	0.3417	1.5254
2	15.0	0.000361	0.001215	0.001215	0.294	0.4969	2.2965
3	20.0	0.00064	0.001105	0.001105	0.2993	0.6728	3.0586

Table 2.8: Relative performance of DQM, LBM and FDM (x = 0.0006096 cm, lattice points = 501)

Sr. No.	Simulation time (h)	L_2 error			Computing time (s)		
		DQM	LBM	FDM	DQM	LBM	FDM
1	10.0	0.000173	0.000237	0.000237	0.541	2.3172	12.2549
2	15.0	0.000039	0.000229	0.000229	2.6476	49.3152	290.4106
3	20.0	0.000035	0.000215	0.000215	5.2607	65.7328	386.0044

Table 2.9: Relative performance of serial and parallel LB algorithm

Sr. No.	Simulation time (h)	$\Delta x(\mu m)$	Computing time (s)	
			Serial LBM	Parallel LBM
1	10	15.24	0.2500	0.1846
2	10	7.62	1.125	0.9676
3	10	6.096	2.250	1.8075
4	10	3.801	9.625	5.8067
5	10	3.048	18.625	11.0877
6	10	1.524	148.25	74.9053
7	10	1.016	503.00	254.3118

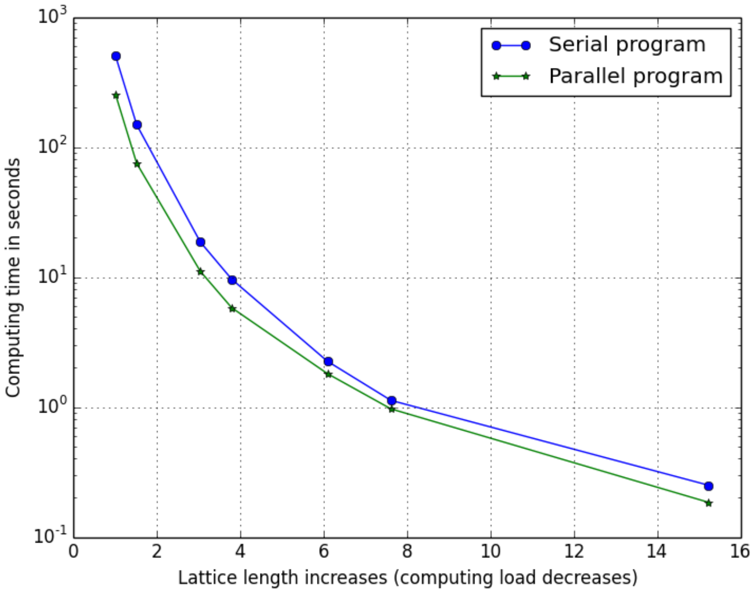

Figure 2.27: computing load Vs computing time for serial and parallel LB program

2.9 Summary

In this chapter, numerical simulation of ADE, which models the transport of solute through geological media by advection-dispersion process, is carried out using two relatively new and robust numerical techniques called LBM and DQM.

On the onset of the formulation of numerical scheme using LBM, we have derived LBE from continuous velocity Boltzmann equation then discussed about various lattice structures and shown how to calculate weight factor for different lattices. Derivation of macroscopic solute transport equation from microscopic LBE using Chapman-Enskog multi-scale expansion technique is shown in details. Discussion on conversion from lattice Boltzmann units to physical units is provided. The developed LBM based solute transport solver, which is being used in the following chapters for simulation of multi-component and long term reactive transport as well as for modeling uncertainty analysis of solute transport and reactive transport, is validated and verified by solving standard one-dimensional and two-dimensional solute transport problems. The accuracy of lattice Boltzmann based solutions of the problems is checked by comparing these solutions with closed form analytical solutions. The concept of diffusion velocity lattice Boltzmann scheme, which was developed by Perko et al. to simulate ADE in a specially heterogeneous media [Perko et al., 2014], has been applied to simulate two-dimensional anisotropic ADE. All the simulations are carried out in lattice units with $\Delta x_{lbm} = 1\ lu$ and $\Delta t_{lbu} = 1\ ltu$, and therefore the developed schemes are unconditionally stable.

We have also derived DQM based numerical scheme for solute transport equation. The developed scheme is validated and verified by solving two standard one-dimensional problems. The solutions of DQM show that very accurate results can be obtained using very few non-uniform grid points, thereby reduces the simulation time.

Chapter 3

Multi-component Reactive Transport Simulation using Lattice Boltzmann Method

3.1 Introduction

In the previous chapter, LBM and DQM were applied to develop an efficient solver for ADE describing transport of solute due to physical processes such as advection, molecular diffusion and hydrodynamic dispersion. In the formulation of solute transport model, it is assumed that solutes that are being transported through groundwater do not interact with the rock forming minerals. This assumption is rarely valid for practical problems. In fact, most of the radionuclides present in the vitrified radioactive waste product interact with the composition of groundwater as well as with the minerals present in the clay buffer and host rock media. These chemical reactions can modify the petrophysical properties, such as porosity, permeability, of the engineering clay barrier and natural host rock. Porosity and permeability are the key parameters that control the fluid flow and solute transport. In fact, changes in water velocity has impact on residual time which is an important parameter for reaction kinetics in an open system. Therefore, solute transport and geochemical reactions at the fluid solid interface are coupled with each other. This coupled process of solute transport and geochemical reactions is known as reactive transport process [Steefel et al., 2005; MacQuarrie et al., 2005]. Therefore, when geochemical interactions between solute and rock forming minerals take place special care needs to be taken to incorporate these geochemical interactions into the solute transport model equations. The equation that governs the transport of reactive solute is known as reactive transport equation, which is mathematically termed as advection-dispersion-reaction equation (ADRE) when electrochemical effects are negligible. In this chapter, in-house developed solvers for solute transport developed in the previous chapter are interfaced with a geochemical solver, PHREEQC, to simulate multi-component reactive transport. The coupling scheme is based on operator splitting approach, where transport and reaction operation are treated separately. Since the coupling of geochemical code PHREEQC with solute transport solver is based on operator splitting approach, the coupling scheme is insensitive of type numerical scheme used for the solute transport. Simulation of reactive transport in a chemically heterogeneous porous media requires large number of grid points in order to capture spatial heterogeneity of the media. Since DQM requires very few grid points for numerical simulation, we dont have much flexibility in placing of grid points in the chemically heterogeneous media. Therefore, it is obvious that this technique will not be able to take care of chemical heterogeneity of the domain. The developed DQM based solute transport solver can be used to solve inactive solute transport problems or reactive transport in a chemically homogeneous media. Since deep geological repository (DGR) will be having composition of different type of materials, such as clay barrier, host rock and geological media are themselves chemically heterogeneous, we have used LBM for reactive transport simulations.

There are basically two kind of approaches to model the geochemical interaction happening in groundwater system when solutes dissolved in groundwater moves through the rock formation. In the first method, called isotherm based model, effects of various geochemical interactions, such as ion exchange, adsorption, absorption, surface complexation etc., on the movement of the dissolved solute are treated together and an empirical relation between amount of solute present in the solid matrix and amount of solute present in the liquid phase is established. In the second method, called geochemical reaction based model, individual geo-chemical reactions are treated separately and reaction rate of all these reactions are directly used in the ADRE. Mathematical formulation of these reaction models and reactive transport models are presented in Section 3.2. LB scheme for single species and multi-species reactive transport simulation are discussed in Section 3.3 and Section 3.4, respectively. The interfaced model, consisting of LB based solute transport solver interfaced with geochemical software PHREEQC, is elaborated in Section 3.4.1. Finally the developed multi-component reactive transport solver is verified and validated by solving standard benchmark problems in Section 3.5.

3.2 Reactive Transport Model

There are generally two approaches to model reactive transport in geological media. In the first one, which is routinely used in environmental radionuclide migration, is based on empirical sorption isotherms. In the second one, which is more robust and demands more computational resources in terms of storage and speed of computation, individual geochemical interactions, such as dissolution/precipitation, ion exchange, surface complexation etc., are treated separately. Mathematical formulation of both the approaches are given in the following

3.2.1 Sorption Isotherms

While solutes are being transported in groundwater, their transport rate is generally slower than that of the groundwater. This is likely to be due to various sorption phenomena. In order to avoid the complexity and heterogeneity of geological formations, individual phenomena are not interpreted separately rather an empirical model of sorption of an element from the solution to a solid particles is used. This kind of model is based on the fact that solute concentration of an element C (mol/L) can be compared with the concentration of this element retained on solid particles S(mol/kg). The relation $S = f(C)$ is known as sorption isotherm. The isotherms based models reduces the mathematical complexity of a multi-component system in a chemically complex environment. The general form of a multi-component ADRE is

$$\frac{\partial\left(\theta C^j\right)}{\partial t} = \frac{\partial}{\partial x_i}\left(\theta D_i \frac{\partial C^j}{\partial x_i}\right) - \frac{\partial}{\partial x_i}\left(\theta u_i C^j\right) + R^j \quad j = 1, 2, 3, ..., N_t \tag{3.1}$$

where C^j represents the concentrations of j^{th} component in solution (mol/L^3), θ is porosity, t and x denote time (T) and space (L), respectively, u_i stands for average linear ground water velocity along i direction (L/T) and D_i is the i^{th} component of dispersion tensor (L^2/T). R^j ($mol/m^3rock/s$) is the reaction rate of the j^{th} component in solution, and N_t is total number of component present in the aqueous system. The reaction term in the ADRE (3.1) is written as

$$R^j = -\rho \frac{\partial S^j}{\partial t} \tag{3.2}$$

where S^j represents amount of j^{th} component absorbed onto unit mass of the rock and ρ is the bulk density of the rock mass (Kg/m^3). These are three different isotherms that are most widely used by researches: (i) Linear isotherm, (ii) Langmuir isotherm and (iii) Freundlich isotherm.

Linear isotherm

In the linear isotherm model it is assumed that adsorbed solute concentration (S^j) is related to the solution concentration (C^j) by linear and reversible isotherm of the form

$$S^j = K_d^j C^j \tag{3.3}$$

where K_d^j is the empirical distribution coefficients (m^3/Kg) of j^{th} component.

Langmuir isotherm

This is an equilibrium adsorption model taking into consideration of maximum adsorption capacity of the sorbing material. Mathematically Langmuir isotherm model is written as

$$S^j = \frac{b.C^j.Q^0}{1 + b.C^j} \tag{3.4}$$

where Q^0 is the maximum adsorption capacity of a forming single layer, b is a constant (L/mg).

Freundlich isotherm

Freundlich isotherm is empirical and is defined as

$$S^j = K_f(C^j)^{1/n} \tag{3.5}$$

where K_f is Freundlich adsorption constant and n is Freundlich exponent. If n = 1, the Freundlich isotherm reduces to the linear isotherm.

The schematic representation of the three isotherms are shown in Figure 3.1. In this study we have used linear isotherm model which is often practiced in contaminant transport modeling. Using the above formulations, the ADRE (3.1) with linear sorption isotherm can be written as

$$\frac{\partial\left(\theta C^j\right)}{\partial t} = \frac{\partial}{\partial x_i}\left(\theta D_i \frac{\partial C^j}{\partial x_i}\right) - \frac{\partial}{\partial x_i}\left(\theta u_i C^j\right) - \rho \frac{\partial C^j}{\partial t} K_d^j \tag{3.6}$$

Further simplification of Eq. (3.6) can be done if we consider that the rock mass is homogeneous and isotropic in nature and the hydrogeological parameters (porosity, permeability etc.) of the rock mass are time independent. Based on these assumptions, Eq. (3.6) can be simplified as

$$\frac{\partial C^j}{\partial t} = \frac{D_i}{R_d^j}\frac{\partial^2 C^j}{\partial x_i^2} - \frac{u_i}{R_d^j}\frac{\partial C^j}{\partial x_i} \tag{3.7}$$

where R_d^j is called retardation factor which has the form

$$R_d^j = 1 + \frac{\rho}{\theta} K_d^j \tag{3.8}$$

It can be observed here that the resulting ADRE (3.7) is similar to an ADE and therefore, LB and DQ based transport solvers developed in the previous chapter can be used to solve the equation numerically.

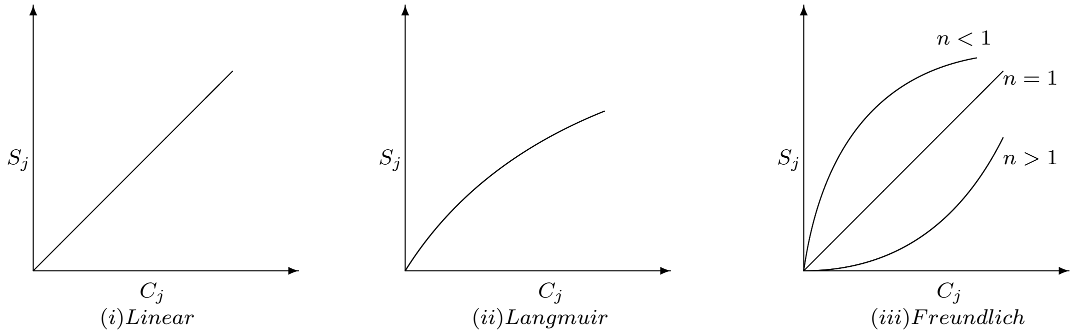

Figure 3.1: Various sorption isotherm models

3.2.2 Geochemical reaction based model

Geochemical reaction can be broadly classified into two categories: homogeneous reactions occurring in the fluid phase and heterogeneous reactions occurring at the interface of fluid and solid phases [Lasaga, 1984; Bethke, 1996]. Homogeneous reactions include both equilibrium reactions, such as aqueous complexation reactions and kinetically controlled reactions such as microbially mediated sulfate reduction, radioactive decay etc. Heterogeneous reactions are also can be equilibrium reactions, such as surface complexation, ion exchange and kinetic reactions, such as mineral dissolution/precipitation. Reactive transport of chemical species at continuum scale in absence of electro kinetic effect is mathematically governed by ADRE, which can be described as a set of partial differential equations on time and space scale in the form

$$\frac{\partial\left(\theta C^j\right)}{\partial t}=\frac{\partial}{\partial x_i}\left(\theta D_i\frac{\partial C^j}{\partial x_i}\right)-\frac{\partial}{\partial x_i}\left(\theta u_i C^j\right)+R^j \quad j=1,2,3,...,N_t \tag{3.9}$$

where C^j represents the concentrations of j^{th} species in solution (mol/L^3), θ is porosity, t and x denote time (T) and space (L), respectively, u_i stands for average linear ground water velocity along i direction (L/T) and D_i is the i^{th} component of dispersion tensor (L^2/T). R^j ($mol/m^3\ rock/s$) is the net reaction rate of the species j in solution, and N_t is the total number of aqueous species. The above equation is a multi-species ADRE. In the above formulation it is assumed that dispersion coefficient is species independent [Lichtner, 1996]. In most of the practical problems total number of aqueous species is a very large number and therefore, computational time required to solve the above equation will be very large. However, if we consider that the various aqueous species are in equilibrium then it is possible to define a set of independent species which can be used to define the concentration of the remaining species known as secondary species [Krikner et al., 1998; Lichtner, 1985; Reed, 1982]. The equilibrium chemical reactions between primary and secondary species is written as

$$A_k \rightleftharpoons \sum_{j=1}^{N_p}\nu_{kj}A_j \quad k=1,2,3,...,N_s \tag{3.10}$$

where A_j and A_k are the chemical formulas of primary and secondary species, respectively. ν_{kj} is stoichiometric reaction coefficient, N_p and N_s are number of primary and secondary species in the system. Total number of species is therefore, $N_t = N_p + N_s$. Now, concentration of secondary species can be written in terms concentration of primary species using the law of mass action

$$C_k=K_k^{-1}\gamma_k^{-1}\prod_{j=1}^{N_p}\left(\gamma_j C_j\right)^{\nu_{kj}} \quad k=1,2,3,...,N_s \tag{3.11}$$

where γ_j and γ_k are the activity coefficient for the primary and secondary species, respectively, and K_k is the equilibrium constant for the reaction. Now, total aqueous component concentration, which remain constant during reactive transport simulation, can be defined as [Lichtner1985, Steefel1994a]

$$T_j = C_j + \sum_{k=1}^{N_s} \nu_{kj} C_k \quad j = 1, 2, 3, ..., N_p \tag{3.12}$$

In term of total component concentration Eq. (3.9) can be written as

$$\frac{\partial \left(\theta T^j\right)}{\partial t} = \frac{\partial}{\partial x_i}\left(\theta D_i \frac{\partial T^j}{\partial x_i}\right) - \frac{\partial}{\partial x_i}\left(\theta u_i T^j\right) + R^{j,het} \quad j = 1, 2, 3, ..., N_p \tag{3.13}$$

where $R^{j,het}$ is the net heterogeneous reaction rate of j^{th} component per unit volume of the rock mass ($mol/m^3\ rock/s$). Here it is to be highlighted that the above formulation is valid only for equilibrium reactions in liquid phase and if heterogeneous reactions in liquid phase need to incorporate into the model equation then it is required to solve the original equation (3.9) for all the solution species [Krikner et al., 1998; Lichtner, 1985; Steefel et al., 1994a]. In this work kinetically controlled homogeneous reactions are not considered. Therefore, Eq. (3.13) is our governing equation for multi-component reactive transport. Now our task is to define the explicit form of the net heterogeneous reaction rate, $R^{j,het}$, which can be written as a sum of all the individual heterogeneous reaction that affect the concentration of j^{th} component [Lasaga, 1984; Reed, 1982].

$$R^{j,het} = -\sum_{m=1}^{N_m} \nu_{jm} r_m \quad j = 1, 2, 3, ..., N_p \tag{3.14}$$

where r_m is rate of m^{th} heterogeneous reaction per unit volume of rock., ν_{jm} is the stoichiometric coefficient of the m^{th} reaction and N_m is the number of heterogeneous reactions occurring in the system. Substituting the above reaction rate in Eq. (3.13) we get following equation for multi-component reactive transport

$$\frac{\partial\left(\theta T^j\right)}{\partial t}=\frac{\partial}{\partial x_i}\left(\theta D_i\frac{\partial T^j}{\partial x_i}\right)-\frac{\partial}{\partial x_i}\left(\theta u_i T^j\right)-\sum_{m=1}^{N_m}\nu_{jm}r_m \quad j=1,2,3,...,N_p \tag{3.15}$$

Mathematical form of the reaction rates appearing in the above equation can be derived from transition state theory as [Lasaga et al., 1994; Lasaga, 1984]

$$r_m=k_s\left(1-\frac{Q_s}{K_m}\right) \tag{3.16}$$

where k_s is the reaction rate for heterogeneous reactions and K_m are the equilibrium constants and Q_s is the ion activity products (IAP). The reaction rate k_s is function of reaction rate constant (k), mineral reactive surface area (S), concentration of reactant (C_s) on the mineral reactive surface, and reaction order (n). General form of kinetic rate (k_s) is written as

$$k_s=kS\prod_j C_{s_j}^{n_j} \tag{3.17}$$

Here, j stands for different species of ions.

3.3 Lattice Boltzmann Method for Single Component Reactive Transport

In this section single component reactive transport equation for both sorption isotherm and geochemical reaction based model is solved using LB scheme

Sorption isotherm based model

The single component reactive transport equation with isotherm based model for reaction term can be written following the Eq. (3.7) as

$$\frac{\partial C}{\partial t}=\frac{D_i}{R_d}\frac{\partial^2 C}{\partial x_i^2}-\frac{u_i}{R_d}\frac{\partial C}{\partial x_i} \tag{3.18}$$

The above equation can be written as

$$\frac{\partial C}{\partial t} = D_i^* \frac{\partial^2 C}{\partial x_i^2} - u_i^* \frac{\partial C}{\partial x_i} \tag{3.19}$$

where $D_i^* = D_i/R_d$ and $u_i^* = u_i/R_d$ are called effective dispersion coefficient and effective velocity, respectively along i-direction. The above equation (3.19) is an ADE and therefore the procedure of solving this equation using LB method is same as that explained in Chapter 2.

Geochemical reaction based model

The generalized equation for multi-component reactive transport (3.15) can be written for single component reactive transport equation with first order reaction term as

$$\frac{\partial (\theta C)}{\partial t} = \frac{\partial}{\partial x_i}\left(\theta D_i \frac{\partial C}{\partial x_i}\right) - \frac{\partial}{\partial x_i}(\theta u_i C) + k_s (C - C_{eq}) \tag{3.20}$$

Here heterogeneous reaction is considered as first order kinetics with reaction rate k_s. Ceq is equilibrium concentration in the liquid phase. Here it can be observed that the Eq. (3.20) is an ADE with additional source/sink term arising from geochemical reactions. LB method models the the source/sink term as additional operator called reaction operator [Dawson et al., 1993]. The Eq. (3.20) can be solved using standard LB scheme for ADE with an additional collision term which takes care of the reaction term. The LB equation with additional reaction collision operator is described as

$$f_i(\vec{x} + \vec{e_i}\Delta t, t + \Delta t) = f_i(\vec{x}, t) + \Delta t \Omega_i(\vec{x}, t) + \Delta t \Omega_i^{reaction}(\vec{x}, t) \tag{3.21}$$

where $\Omega_i(\vec{x}, t)$ is the same as given in Eq. (2.9) in Chapter 2 and $\Omega_i^{reaction}(\vec{x}, t)$ is called reaction collision operator and has the form $\Omega_i(\vec{x}, t) = w_i R$, where $R = k_s (C - C_{eq})$. In terms of equilibrium distribution function Eq. (3.21) can be written as

$$\begin{aligned} f_i\left(\vec{x}+\vec{e_i}\Delta t, t+\Delta t\right) = f_i\left(\vec{x},t\right) &+ \frac{\Delta t}{\tau}\left(f_i\left(\vec{x},t\right) - f_i^{eq}\left(\vec{x},t\right)\right) \\ &+ w_i k_s\left(\sum_{j=1}^{m} f_j - C_{eq}\right) \end{aligned} \tag{3.22}$$

3.4 Lattice Boltzmann Method for Multi-Component Reactive Transport

The single component LB scheme presented in the previous section can be extended to simulate multi-component reactive transport.

Sorption isotherm based model

The multi-component reactive transport equation with isotherm based model for reaction term can be written using Eq. (3.7) as

$$\frac{\partial C^j}{\partial t} = D_i^j \frac{\partial^2 C^j}{\partial x_i^2} - u_i^j \frac{\partial C^j}{\partial x_i} \quad j = 1, 2, 3, ..., N_c \tag{3.23}$$

where $D_i^j = D_i/R_d^j$ and $u_i^j = u_i/R_d^j$ are effective dispersion coefficient and effective velocity of j^{th} component along i-direction. It is shown in previous chapter that numerical time step is related to macroscopic dispersion coefficient. In order to keep same numerical time step for all the components of the system it is required to keep the apparent diffusion coefficient, which is the ratio between diffusion coefficient and retardation factor, same for all the components. This is achieved using diffusion velocity LB scheme [Perko et al., 2014; Patel et al., 2014]. The scheme was developed and applied to model solute transport in a heterogeneous media [Perko et al., 2014]. In this scheme, total physical diffusion coefficients is divided into reference (D_{ref}) and fluctuating ($\widetilde{D}$) parts.

$$D_i^j = D_i^{ref} + \widetilde{D_i^j} \tag{3.24}$$

Using Eq. (3.24), reactive transport Eqs. (3.23can be rewritten as

$$\frac{\partial C^j}{\partial t} = \left(D_i^{ref} + \widetilde{D_i^j}\right) \frac{\partial^2 C^j}{\partial x_i^2} - u_i^j \frac{\partial C_j}{\partial x_i} \quad j = 1, 2, 3, ..., N_c \tag{3.25}$$

D_i^{ref} is taken as the minimum of the apparent diffusion coefficients $min(D_i^j \quad j = 1, 2, 3, ..., N_c)$. It is seen in chapter 2 that time step value is inversely proportional to diffusion coefficient; therefore, consideration of minimum of the apparent diffusion coefficients as D_i^{ref} increases the time step value and consequently reduces the computational time. Diffusion flux corresponding to the fluctuating part of the diffusion coefficient is converted to corresponding diffusion velocity ($u_i^{d,j}$) using the following expression [Perko et al., 2014]

$$u_i^{d,j} = -\frac{\widetilde{D_i^j} \frac{\partial C^j}{\partial x_i}}{C^j} \tag{3.26}$$

Using Eq. (3.26), the reactive transport equation (3.25) can be written as

$$\frac{\partial C^j}{\partial t} = D_i^{ref} \frac{\partial^2 C^j}{\partial x_i^2} - u_i^{t,j} \frac{\partial C^j}{\partial x} \quad j = 1, 2, 3, ..., N_c \tag{3.27}$$

where $u_i^{t,j} = u_i^j + u_i^{d,j}$ is the total velocity. Equation (3.27) is solved using standard SRT scheme of LBM. The diffusion velocity as given in Eq. (3.26) is derived using the first order terms in the Chapman-Enskog expansion in the lattice Boltzmann framework. Details of the derivation are given by Perko et al [Perko et al., 2014]. Final expression for diffusion velocity can be written as

$$u_{\beta,i}^{d,j} = -\frac{\frac{\widetilde{D_i^j}}{\tau e_s^2}}{\left(1 + \frac{\widetilde{D_i^j}}{\tau e_s^2}\right)} \left(\frac{\sum_\alpha f_\alpha^j e_{\alpha,\beta}}{C^j} - u_{\beta,i}^{a,j}\right) \tag{3.28}$$

The diffusion velocity as given in Eq. 3.28 is incorporated into LBM through equilibrium distribution function (EDF). The EDF for ADE with diffusion velocity is written as

$$f_{\alpha}^{eq,j}\left(\overrightarrow{r},t\right) = w_{\alpha}C^{j}\left(\overrightarrow{r},t\right)\left(1+\frac{e_{\alpha,\beta}\left(u_{\beta,i}^{d,j}+u_{\beta,i}^{a,j}\right)}{e_s^2}\right) \tag{3.29}$$

The above equation is an ADE and therefore it's solution can be obtained using standard LB scheme for ADE. The LB equation for Eq. (3.23) is expressed as

$$f_i^j\left(\vec{x}+\vec{e_i}\Delta t, t+\Delta t\right) = f_i^j\left(\vec{x},t\right)+\frac{\Delta t}{\tau}\left(f_i^j\left(\vec{x},t\right)-f_i^{eq,j}\left(\vec{x},t\right)\right) \tag{3.30}$$

Geochemical reaction based model

Similar to single component reactive transport model, the LB equation for multi-component reactive transport equation (3.15) with geochemical reaction based model for reaction term can be written as

$$\begin{aligned} f_i^j\left(\vec{x}+\vec{e_i}\Delta t, t+\Delta t\right) = f_i^j\left(\vec{x},t\right)+\frac{\Delta t}{\tau}\left(f_i^j\left(\vec{x},t\right)-f_i^{eq,j}\left(\vec{x},t\right)\right) \\ + \Delta t\Omega_i^{reaction,j}\left(\vec{x},t\right) \end{aligned} \tag{3.31}$$

$$\Omega_i^{reaction,j}\left(\vec{x},t\right) = -w_i\sum_{m=1}^{N_m}\nu_{jm}I_m$$

In this work the LB solver for solute transport developed in the previous chapter is interfaced with a geochemical software, PHREEQC, to compute the geochemical reactions. The coupling scheme is based on operator splitting approach generally used for multi-physics problems. The coupling algorithm is elaborated in the following

3.4.1 Interfacing with Commercial Geochemical Solver

The source/sink term in the LB equation for multi-component reactive transport (3.25) is evaluated using commercial geochemical solver Phreeqc [Parkhurst et al., 1999], which has capabilities for simulating a broad range of equilibrium reaction between water and minerals, ion exchangers, surface complexes, solid solution, and gases. For the interfaces scheme, we have used the latest version of Phreeqc, called PhreeqcRM [Parkhurst et al., 2015] which was specifically designed for use as a reaction engine in reactive transport simulation using non-iterative operator splitting approach [Saaltink et al., 2001; Carrayrou et al., 2004]. The basic concept of operator splitting approach is to solve a multi-physics problem in a sequential way. More simply it can be said that at each time step LB based solute transport solver will solve the transport process and after that it will send the solution to an commercial software (PhreeqcRM), where the various reaction calculation will take place. After the reaction calculation, external reaction module will transfer the new solution composition to the client module where the solution of transport module is updated based on component loss or gain occurred due to geochemical interactions. Similar coupling scheme was used for pore scale reactive transport simulation by Ravi et al [Patel et al., 2014].

PhreeqcRM is basically a class of functionalities of Phreeqc that can be included in other programming language (C, C++, Fortran) to utilize the capabilities of Phreeqc in a dynamic way. The Phreeqc software takes input file, which is a geochemical model of the solution, from the user. The input file is composed of keyword data blocks. Before the release of PhreeqcRM in 2015, another version of Phreeqc called IPhreeqc [Charlton et al., 2011] was released. This IPhreeqc encapsulates all the capabilities of Phreeqc in a C++ class (with wrapper for C and Fortran) to facilitate integration of Phreeqc into other computer program. However, IPhreeqc relies primarily on processing strings that define keyword data blocks and arrays of selected-output to automate the use of Phreeqc. For reactive transport modeling, translating cell solutions to strings and processing output arrays item-by-item are tedious programming efforts. The latest version of Phreeqc, PhreeqcRM, is basically a C++ class that encapsulates IPhreeqc and it can perform on data array (instead of string) and there no requirement of keyword data blocks. In the reactive transport program an instance of PhreeqcRM is first created and a mapping operation is done where each grid cells are mapped into equivalent grid cells inside PhreeqcRM. The transport simulator provides new concentrations of each cell to PhreeqcRM at each time step after performing the transport operation and PhreeqcRM performs the geochemical operation on the new solution and returns the updated solution to transport solver. The structure of the multi-component reactive transport model is shown in Fig. 3.2.

Parallelization of PhreeqcRM code is done explicitly by providing the number of threads or processors to be used during run time. If only 1 thread or processor is used then the code will work in serial mode otherwise it will work in parallel mode. The code can be parallelized in both shared memory and distributed memory. In this study, parallelization was done in shared memory platform in Scientific Linux 7 with quad-core processor.

3.5 Numerical Problems Solved

The developed coupling scheme is tested by solving benchmark problems of single component and multi-component reactive transport in this section.

3.5.1 Diffusion and Kinetically Controlled Dissolution/Precipitation Reaction

Problem formulation

This benchmark problem has been received from ANDRA, France as a part of BARC-ANDRA co-operative doctoral work [COCHEPIN, 2014]. The aim of this test problem is to simulate the diffusion transport of an aqueous chemical element which is allowed to precipitate, following

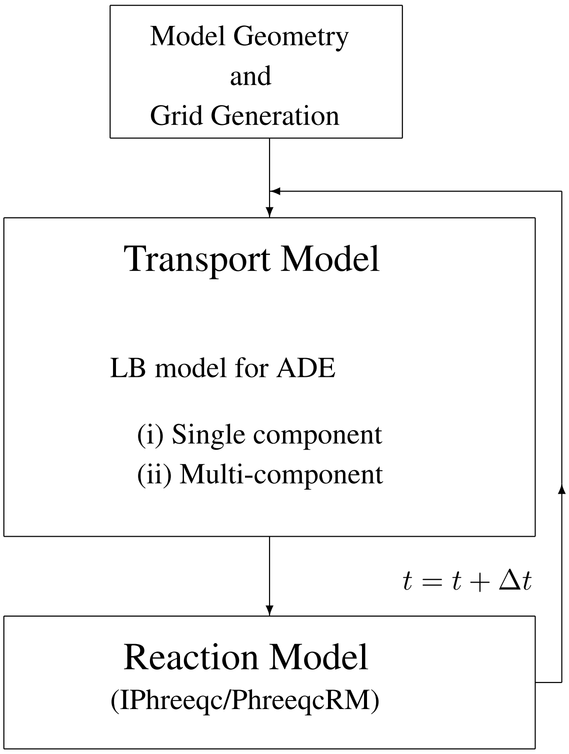

Figure 3.2: Schematic of the structure of reactive transport model

the reaction

$$A_{aqueous} \rightleftharpoons A_{solid} \tag{3.32}$$

The solubility constant of this reaction is $K_s = [A_{aqueous}]_{equil}$, where $[A_{aqueous}]_{equil}$ stands for the concentration of the element A in solution at equilibrium. We consider only one species exists in the solution, $A_{aqueous}$, and only one mineral, A_{solid}. The porous medium is only composed of inert material with a porosity θ and an effective diffusion coefficient D_e. Initially, the concentrations of A in solution and in the solid phase are

$$[A_{aqueous}] = C_0 \qquad [A_{solid}] = P_0 = 0 \tag{3.33}$$

We impose Dirichlet type boundary conditions with $[A_{aqueous}] = C_1$ on the left side of the domain, where C_1 is a constant with bigger value than the one imposed by the solubility limit

K_s of the solid A_{solid}, and $[A_{aqueous}]$ and $[A_{aqueous}] = C_2 = C_0$ on the right side of the domain. The model domain is shown in Figure 3.3. It is assumed no advection, i.e., the element, $A_{aqueous}$, is only transported by diffusion. This system, even though considerably simplified, can be met in the storage concept of nuclear waste. The progressive dissolution of vitrified waste leads to the release of silica in the environment. The dissolved silica may precipitate as quartz which has a low solubility. Transport equation for the diffusion of $A_{aqueous}$ can be written as

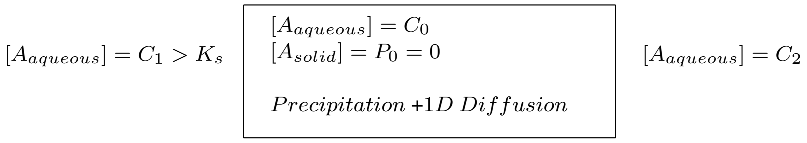

Figure 3.3: Model domain

$$\theta \frac{\partial C}{\partial t} = D_e \frac{\partial^2 C}{\partial x^2} - \frac{\partial P}{\partial t} \tag{3.34}$$

The above equation can be simplified as

$$\frac{\partial C}{\partial t} = D \frac{\partial^2 C}{\partial x^2} - \frac{1}{\theta} \frac{\partial P}{\partial t} \tag{3.35}$$

where C is the concentration of element A in the aqueous phase and P is its concentration in the solid phase (number of moles per total volume unit, i.e., solution volume + solid volume). In the case of kinetic reaction with an order of 1, we have

$$\frac{1}{\theta} \frac{\partial P}{\partial t} = kS \left(\frac{C}{K_s} - 1 \right) = \beta \left(C - K_s \right) \tag{3.36}$$

$$\beta = \frac{kS}{K_s}$$

In these equations, k and S are respectively the kinetic rate constant for the precipitation of the minerals (in $mol.l^{-1}.m.s^{-1}$) and the specific surface (in m^{-1}). Initial and boundary conditions are

$$\forall x \in [0, L], C(x, t=0) = C_0 \tag{3.37}$$

$$\forall t > 0 \begin{cases} C(x=0, t) = C_1 > k_s \\ C(x=L, t) = C_2 \end{cases} \tag{3.38}$$

Lattice Boltzmann simulation

The LBM based diffusion model interfaced with PhreeqcRM is used to solve the problem. Since LBM gives more stable and accurate results when the relaxation parameter, τ, is close to 1, we have performed our simulation considering τ = 1. It is also advantageous to perform simulation in LB units considering stability and convergence criterion. Therefore, unit lattice spacing and unit time step size, i.e., $\Delta x_{lbm} = 1$ lu, $\Delta t_{lbm} = 1\ ltu$ are considered in this simulation. The lattice diffusion coefficient, D_{lbm}, is calculated using Eq. (2.63) and it value is 1/6. Total 101 lattice nodes are considered for LB simulation using D1Q3 lattice.

Values of input parameters used

The various physical and chemical parameters used in the simulation are taken from the literature [COCHEPIN, 2014]. The values are tabulated in Table 3.1 ***Results and discussion***

Table 3.1: Values of input parameters used in the simulation of diffusion and kinetically controlled dissolution/precipitation reaction

D	Poral diffusion coefficient	$10^{-10}\ m^2/s$
θ	Porosity of the porous media	0.79
C_0	Initial concentration	$1.31\times10^{-4}\ mol.l^{-1}$
C_1	Concentration imposed on the left of the domain	$2.12\times10^{-3}\ mol.l^{-1}$
C_2	Concentration imposed on the right of the domain	$1.31\times10^{-4}\ mol.l^{-1}$
K_s	Solubility constant of the mineral	$1.31\times10^{-4}\ mol.l^{-1}$
k	Kinetic reaction rate of the mineral	$5\times10^{-11}\ mol.l^{-1}.m.s^{-1}$
S	Specific surface area	$1.6\times10^{4}\ m^{-1}$

Using the numerical values given in Table 3.1 we can calculate the value of β as

$$\beta = \frac{kS}{K_s} = 8 \times 10^{-7} S^{-1}$$

The characteristic time for the chemical phenomenon $t_{chemistry}$ (precipitation / dissolution) is of the order than $1/\beta = 1.25 \times 10^6\ s$, that is to say around 14.5 $days$. The diffusion length corresponding to $t_{chemistry}$ is

$$L_{diff} = \sqrt{2Dt_{chemistry}} = 1.6 \times 10^{-2} m$$

Grid size is chosen smaller than L_{diff} to keep the system diffusive. Therefore, physical lattice size is 0.1 cm and corresponding physical time step size can be calculated from the following expression

$$\Delta t = \frac{(\Delta x)^2}{6D} \tag{3.39}$$

where Δt is the physical time step size, Δx is the physical lattice size = 0.1 cm, D is the physical apparent diffusion coefficient. The domain length (L) is taken as 10 cm, time step value calculated from the above equation is 1666.67 s. The values of solute concentration are calculated for each grid points at 3.65 $days$, 10 $days$, 100 $days$ and 1 $year$. The results of the simulation shows that after 100 days the system remains in equilibrium state i.e. the amount of solute being precipitated or dissolved inside a given volume is equal to net solute concentration being entered in that domain due to diffusion process.

Verification and validation

The closed form analytical solution of Eq. (3.36) with the given initial and boundary conditions can be written as [COCHEPIN, 2014]

$$C(x,t) = C_\infty(x) - \sum_{n=1}^{\infty} b_n sin\left(\frac{n\pi}{L}x\right) exp\left(-\left(D\frac{n^2\pi^2}{L^2} + \beta\right)t\right) \tag{3.40}$$

In this expression, $C(x,t$, which is the stationary solution of the transport equation, can be written as

$$C\left(x\right) = Ae^{\Omega x} + Be^{-\Omega x} + K_s$$

$$\Omega = \sqrt{\frac{\beta}{D}}$$

With the boundary conditions A and B can be written as

$$\forall t > 0 \begin{cases} A = \frac{(C_2-K_s)-(C_1-K_s)e^{-\Omega L}}{2sinh(\Omega L)} \\ B = \frac{-(C_2-K_s)+(C_1-K_s)e^{\Omega L}}{2sinh(\Omega L)} \end{cases}$$

The b_n coefficients are the Fourier coefficients and can be written as

$$b_n = -2\frac{K_s - C_0}{n\pi}\left[(-1)^n - 1 - \frac{2n\pi}{\Omega^2 L^2 + n^2\pi^2} \times \right.$$
$$\left[A\left(e^{\Omega L}\left(-1\right)^n - 1\right) + B\left(e^{-\Omega L}\left(-1\right)^n - 1\right)\right]$$

The results of simulation in terms of spatial concentration profiles are shown in Figures 3.4 and 3.5. The results of numerical simulation are very close to the analytical solutions. This confirms the accuracy of the developed interfaced scheme.

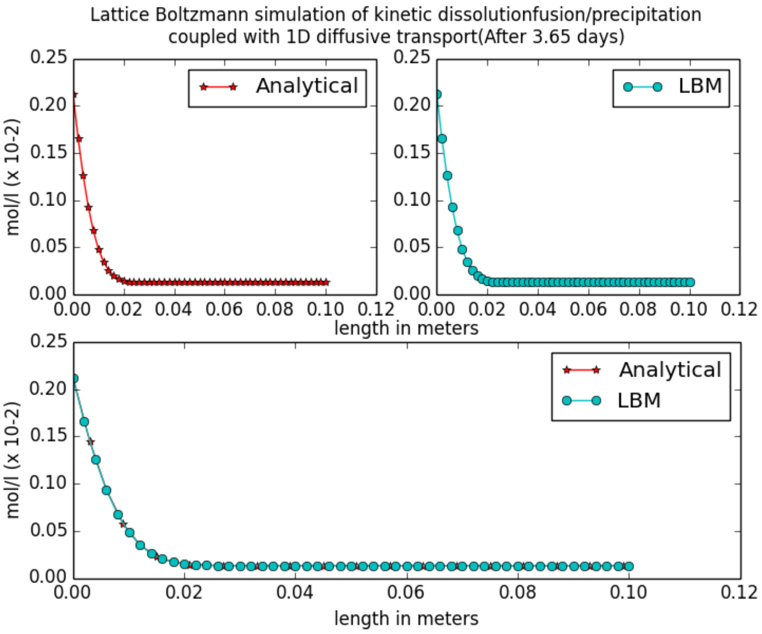

Figure 3.4: Solute concentration after 3.65 days: comparison between LB solution and analytical solution

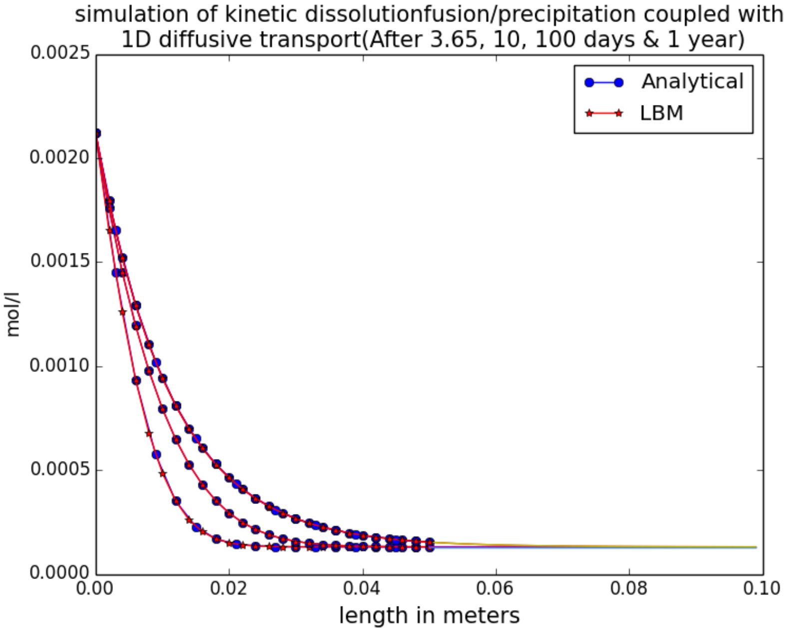

Figure 3.5: Solute concentration after 3.65, 10, 100 days and 1 year: comparison between LB solution and analytical solution

3.5.2 Diffusion of Alkaline Water in a Sand Column using Lattice Boltzmann Interfaced with Geochemical Solver

Problem formulation

This proposed model is used to simulate diffusion of alkaline water ($NaOH$) in a 0.4 m long column composed of grains of pure quartz, leading to acid/base reaction together with mineral dissolution. The dissolution reaction of quartz in presence of hydroxyl ions can be written as [Pal et al., 2016a]

$$quartz + OH^{-1} + H_2O \rightleftharpoons H_3SiO_4^{-1} \tag{3.41}$$

The above reaction can be decomposed in terms of four elementary chemical reactions as

$$\begin{aligned} NaOH &\rightleftharpoons Na^+ + OH^- \\ H_2O &\rightleftharpoons H^+ + OH^- \qquad (K_w) \\ H_4SiO_4 &\rightleftharpoons H^+ + H_3SiO_4^- \quad (K_a) \end{aligned} \tag{3.42}$$

$$quartz + 2H_2O \rightleftharpoons H_4SiO_4 \qquad\qquad (K_s) \tag{3.43}$$

where K_w, K_a and K_s are the equilibrium constant for the respective reactions. Assuming concentration to be identical to the activity and using elementary mass-action law we can write

$$\begin{aligned} K_w &= \left[H^+\right]\left[OH^-\right] \\ K_a &= \frac{\left[H^+\right]\left[H_3SiO_4^-\right]}{\left[H_4SiO_4\right]} \\ K_s &= \left[H_4SiO_4\right] \end{aligned} \tag{3.44}$$

where bracketed quantity signify activity of species. Equation (3.44) contains four unknown and three equations therefore, additional equations in the form of charge balance as given in Eq.

(3.45) is used to calculate pH value

$$\left[OH^-\right] + \left[H_3SiO_4^-\right] = \left[H^+\right] + \left[Na^+\right] \tag{3.45}$$

From Eqs. (3.44) and (3.45), activity of H^+ ion can be calculated as

$$H^+ = \frac{1}{2}\left(\sqrt{\left[Na^+\right]^2 + 4\left(K_w + K_a K_s\right)} - \left[Na^+\right]\right) \tag{3.46}$$

Therefore pH of the solution can be written as

$$pH = -log\left[H^+\right] = -log\left[\frac{1}{2}\left(\sqrt{\left[Na^+\right]^2 + 4\left(K_w + K_a K_s\right)} - \left[Na^+\right]\right)\right] \tag{3.47}$$

Eq. (3.47) implies that concentration of $[Na^+]$ ion is the controlling parameter for the pH of the pore water. In the system, the cation Na^+ is not reactive and only diffuses into the sand column. As a consequence, $[Na^+]$ concentration is governed by the following diffusion equation.

$$\frac{\partial\left[Na^+\right]}{\partial t} = D_e\frac{\partial^2\left[Na^+\right]}{\partial x^2} \tag{3.48}$$

Initial and boundary conditions are

$$\left[Na^+\right](x, t=0) = 0 \tag{3.49}$$

$$\forall t > 0 \begin{cases} \left[Na^+\right](x=0, t) = \left[Na^+\right]_0 \\ \frac{\partial\left[Na^+\right]}{\partial t}(x=\infty, t) = 0 \end{cases} \tag{3.50}$$

where $[Na^+]_0$ is the fixed concentration on the inlet boundary.

Lattice Boltzmann simulation

The developed interfaced scheme is utilized to simulate the problem numerically. The LB simulation is carried out using D2Q5 lattice and 101 lattice points.

Values of input parameters used

The physical and grid parameters used in the simulation are taken from literature [Mgler et al., 2004]. The grid is composed of 100 identical cells ($\Delta x = 4 \times 10^{-3}\ m$), with $D_e = 3 \times 10^{-10}$ $m^2.s^{-1}$ and $[Na^+]_0$ = 20 $mmol.l^{-1}$.

Results and discussions

The concentration of $[Na^+]$ ion is calculated using the developed interfaced scheme. From the LBM solution of solute concentration, the value of pH is calculated using Eq. 3.47. The simulations are run for 10, 30 and 100 $days$.

Verification and validation

Closed form solution of Eq. (3.48) can be written as

$$\left[Na^+\right](x,t) = \left[Na^+\right]_0 \left[erfc\left(\frac{x}{2\sqrt{D_e t}}\right)\right] \tag{3.51}$$

Calculation of spatial profiles of $[Na^+]$ ion and corresponding spatial profile of pH is carried out at 10, 30 and 100 $days$. Figures 3.6 and 3.7 give spatial profile of $[Na^+]$ and pH and compares the numerical solutions with the analytical solution 3.48.

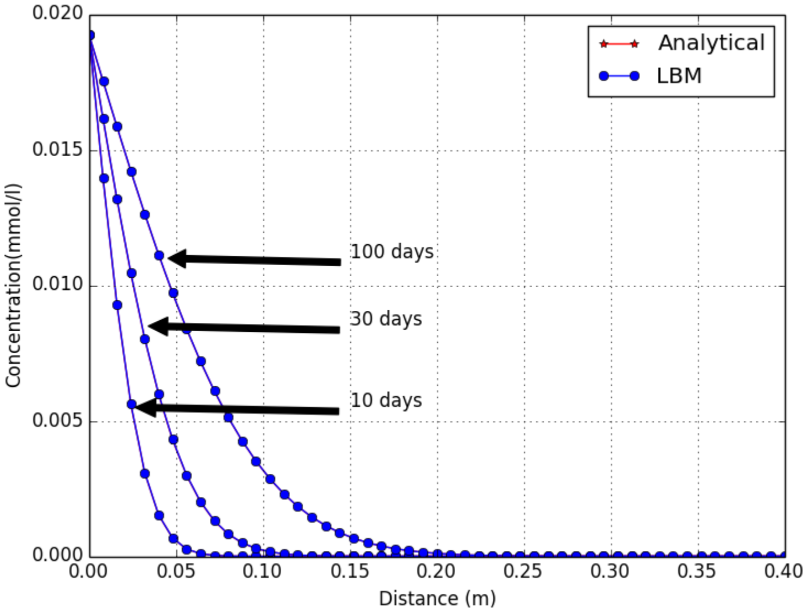

Figure 3.6: Spatial profile of concentration of Na^+ ion at various times: Comparison between LB solution and analytical solution

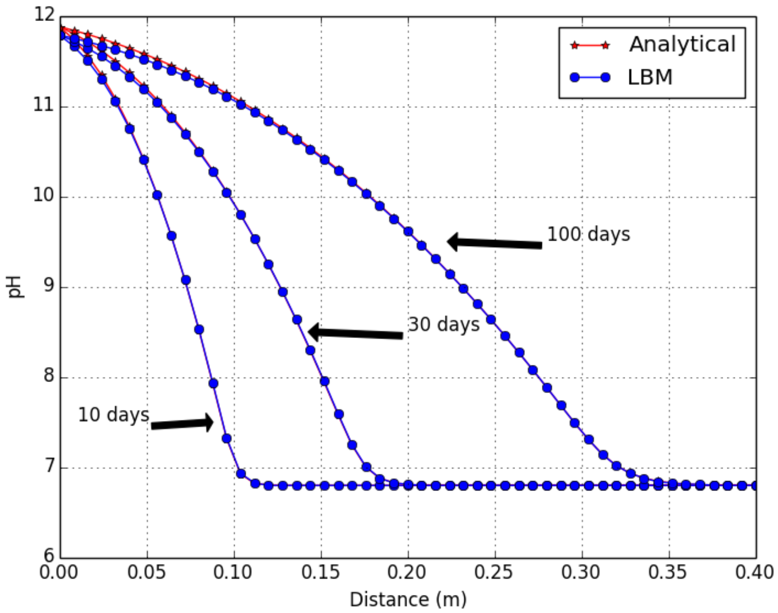

Figure 3.7: Spatial profile of pH at various times: Comparison between LB solution and analytical solution

3.5.3 Migration of Radionuclide Chain

Problem formulation

This test problem model the migration of radionuclide chain through groundwater. The model equations are coupled one dimensional advection dispersion reaction equations with decay term. A generic inventory of parent nuclide and leach rate are considered for source term. The problem attempted here involves three species comprising of parent radionuclide ^{241}Pu which successively decays to ^{241}Am and ^{237}Np. The governing equations for the migration of the radionuclide chain through the aquifer media can be written as

$$\frac{\partial C_1}{\partial t} = \frac{D}{R_1}\frac{\partial^2 C_1}{\partial x^2} - \frac{u}{R_1}\frac{\partial C_1}{\partial x} - \mu_1 C_1 \tag{3.52}$$

$$\frac{\partial C_2}{\partial t} = \frac{D}{R_2}\frac{\partial^2 C_2}{\partial x^2} - \frac{u}{R_2}\frac{\partial C_2}{\partial x} + \mu_1 C_1 - \mu_2 C_2 \tag{3.53}$$

$$\frac{\partial C_3}{\partial t} = \frac{D}{R_3}\frac{\partial^2 C_3}{\partial x^2} - \frac{u}{R_3}\frac{\partial C_3}{\partial x} + \mu_2 C_2 - \mu_3 C_3 \tag{3.54}$$

where D is the dispersion coefficient (L^2T^{-1}), u is average pore water velocity (LT^{-1}), $\mu_i = \lambda_i + \gamma_i$ is general decay coefficient (T^{-1}), λ_i is radioactive decay constant, and γ_i is leach rate (T^{-1}) of the i^{th} species. In the leach rate model it is assumed that amount of radionuclide leached out from the solidified waste from is proportional to the amount of radionuclide present in the waste. The retardation factor R_i is given by

$$R_i = 1 + \frac{\rho K_i}{\theta} \tag{3.55}$$

where ρ is the porous media bulk density (ML^{-3}), θ is volumetric water content which is equal to the porous media bulk porosity when the the media is fully saturated.

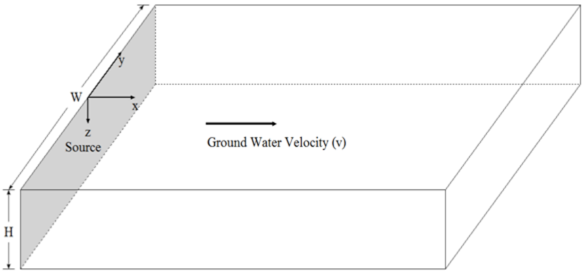

Figure 3.8: Model geometry for migration of radionuclide chain

Initially the concentrations of radionuclides are assumed to be zero everywhere therefore, the initial condition for the coupled differential equations (3.52,3.53, 3.54) can be written as

$$C_i\left(x, t=0\right)=0, \qquad i=1,2 \tag{3.56}$$

Lattice Boltzmann simulation

These coupled equations are solved numerically using diffusion velocity LB scheme developed in this chapter. Using the concept of diffusion velocity LBM scheme the total physical diffusion coefficients can be divided into reference (D_{ref}) and fluctuating ($\widetilde{D}$) parts as

$$D=D_{ref}+\widetilde{D} \tag{3.57}$$

Considering D/R as D_{app}, which is called apparent diffusion coefficient and u/R as u_{app}, which is called apparent groundwater velocity and utilizing Eq. 3.57, coupled Eqs. (3.52,3.53, 3.54) can be rewritten as

$$\frac{\partial C_1}{\partial t}=\left(D_{ref}+\widetilde{D_1}\right)\frac{\partial^2 C_1}{\partial x^2}-u_{app}^{1}\frac{\partial C_1}{\partial x}-\mu_1 C_1 \tag{3.58}$$

$$\frac{\partial C_2}{\partial t}=\left(D_{ref}+\widetilde{D_2}\right)\frac{\partial^2 C_2}{\partial x^2}-u_{app}^{2}\frac{\partial C_2}{\partial x}+\mu_1 C_1-\mu_2 C_2 \tag{3.59}$$

$$\frac{\partial C_3}{\partial t} = \left(D_{ref} + \widetilde{D_3}\right)\frac{\partial^2 C_3}{\partial x^2} - u^3_{app}\frac{\partial C_3}{\partial x} + \mu_2 C_2 - \mu_3 C_3 \tag{3.60}$$

D_{ref} is taken as the minimum of three apparent diffusion coefficients (D^1_{app}, D^2_{app}, D^3_{app}). Diffusion flux corresponding to the fluctuating part of the diffusion coefficient is converted to corresponding diffusion velocity (u_d) using the following formula.

$$u_d = -\frac{\widetilde{D}\frac{\partial C}{\partial x}}{C} \tag{3.61}$$

Using Eq. 3.61, the coupled Eqs. 3.58,3.59, and 3.60 can be written as

$$\frac{\partial C_1}{\partial t} = D_{ref}\frac{\partial^2 C_1}{\partial x^2} - u^1_{tot}\frac{\partial C_1}{\partial x} - \mu_1 C_1 \tag{3.62}$$

$$\frac{\partial C_2}{\partial t} = D_{ref}\frac{\partial^2 C_2}{\partial x^2} - u^2_{tot}\frac{\partial C_2}{\partial x} + \mu_1 C_1 - \mu_2 C_2 \tag{3.63}$$

$$\frac{\partial C_3}{\partial t} = D_{ref}\frac{\partial^2 C_3}{\partial x^2} - u^3_{tot}\frac{\partial C_3}{\partial x} + \mu_2 C_2 - \mu_3 C_3 \tag{3.64}$$

where $u_t = u_{app} + u_d$ the total velocity. Equations 3.62,3.63, and 3.64 are solved using standard SRT scheme of LBM. The diffusion velocity can be written as

$$u_{\beta,d} = -\frac{\frac{\widetilde{D}}{\tau e_s^2}}{\left(1 + \frac{\widetilde{D}}{\tau e_s^2}\right)}\left(\frac{\sum_\alpha f_\alpha e_{\alpha,\beta}}{C} - u_{\beta,a}\right) \tag{3.65}$$

The diffusion velocity as given in Eq. (3.65) is incorporated into LBM through equilibrium distribution function (EDF). The EDF for ADE with diffusion velocity can be written as

$$f^{eq}_\alpha\left(\overrightarrow{r}, t\right) = w_\alpha C\left(\overrightarrow{r}, t\right)\left(1 + \frac{e_{\alpha,\beta}\left(u_{\beta,a} + u_{\beta,d}\right)}{e_s^2}\right) \tag{3.66}$$

Values of input parameters used

The three members decay chain considered in this study is $^{241}Pu \rightarrow {}^{241}Am \rightarrow {}^{237}Np$. In this decay chain ^{241}Pu, which is considered as the parent radionuclide, decays to ^{241}Am via β-decay process. The daughter element, ^{241}Am, then decays to ^{237}Np vis α-decay process. It is reported that neptunium is the most mobile actinide in the NSDF environment and due to its long half-life, ^{237}Np possess long term radio-toxicity. Various physico-chemical parameters used in the simulation are given in Table 3.2. Half-lives and distribution coefficients of the decay-chain members for typical sandy soil are given in Table 3.3. Aquifer thickness is taken as 6.0 m.

Table 3.2: Physico-chemical parameters

D(m^2/s)	u (m/s)	Density (g/ml)	Porosity
5.79×10^{-5}	5.79×10^{-7}	1.35	0.30

Table 3.3: Half-lives and distribution coefficients of the decay-chain members

Nuclide	Half-life (yr)	$K_d(ml/g)$
^{241}Pu	14.29	3.4×10^{2}
^{241}Am	432.52	3.4×10^{2}
^{237}Np	2.144×10^{6}	5.0

Results and discussions

In the calculation, it is assumed as a basis that only the first nuclide (^{241}Pu) of 1 Bq is present in the disposal site at the start of the release. The second (^{241}Am) and third radionuclide (^{237}Np) are formed from ^{241}Pu in both of disposal area and during migration through geological media. Spatial profiles of the radionuclides after 400 $years$ and 1000 $years$ are shown in Figures 3.9 and 3.10 , respectively. The figures show that neptunium concentration moves faster than of the other two radionuclides. Temporal plot of concentration of the radionuclides at 500 m distance from the disposal area are shown in Figure 3.11. The spatial profiles of radionuclide concentration show that the time at which maximum peak of concentration will arrive at a given monitoring point not only depends on the physico-chemical properties of parent radionuclide, but also depends on physico-chemical properties of its progenies. The time dependent radionuclide concentration profile shows that though there is almost no concentration of parent radionuclide (^{241}Pu) at a distance of 500 m from the location of radionuclide disposal, considerable amount of daughter radionuclides (^{237}Np) are there. This result has considerable amount of application particularly, in the case of radiological dose calculation. In the traditional approach for determination of dose from radionuclides, having radioactive progeny, we first calculate concentration of parent radionuclide at the monitoring point by solving a single species (parent radionuclide) ADRE and then solve Bateman equation for calculation of concentration of progenies at the same location. The results of our study show that traditional method may lead to underestimation of calculated dose.

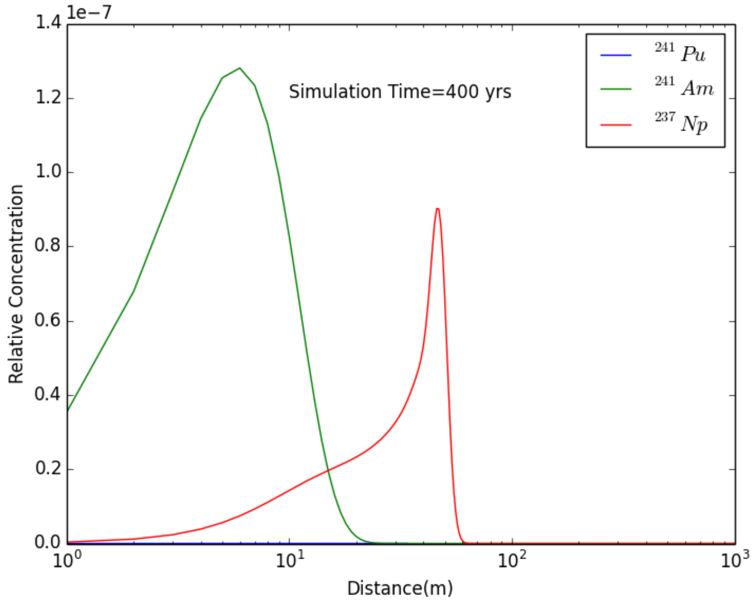

Figure 3.9: Spatial Profile of Radionuclides in the Decay Chain after 400 yrs

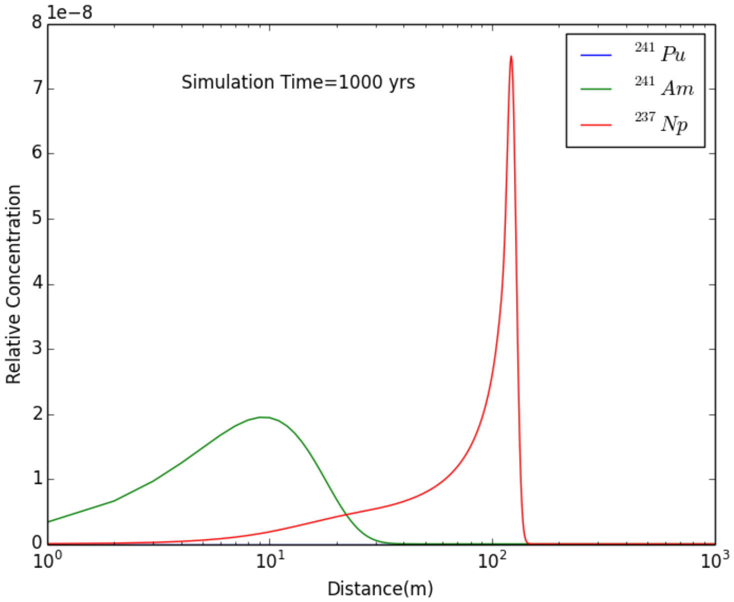

Figure 3.10: Spatial Profile of Radionuclides in the Decay Chain after 1000 yrs

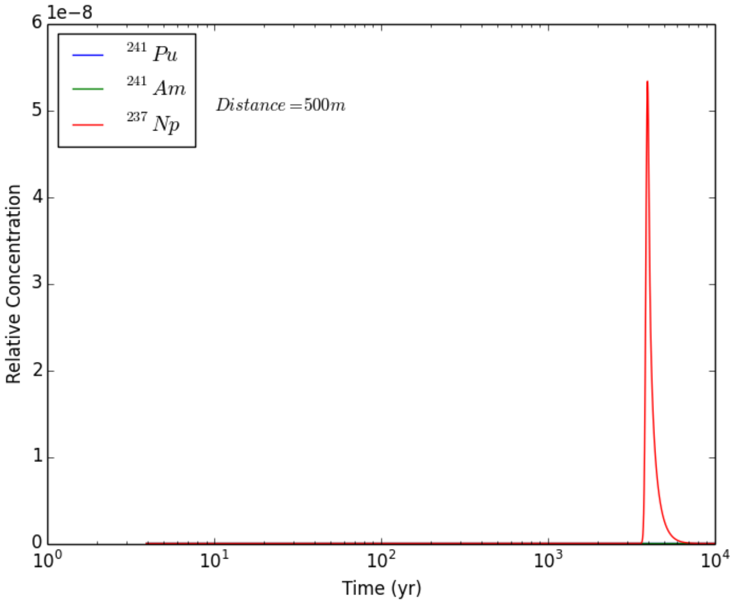

Figure 3.11: Temporal Profile of Radionuclides in the Decay Chain at 500 m

Verification and validation

The numerical results are compared with analytical solution published elsewhere in [Lester et al., 1974; Burkholder et al., 1980; Higashi et al., 1980] and good agreement between them is established.

3.6 Summary

In this chapter, a interfaced algorithm for multi-component and long term reactive transport is formulated by interfacing the LBM based solute transport solver developed in the previous chapter with an commercial geochemical software, PHREEQC.

On the onset of this chapter, we have discussed about two approaches for modeling multi-component reactive transport at continuum scale, which are (i) based on empirical model of sorption and (ii) Geochemical reaction based model. A brief overview of various isotherms, including linear isotherm, Langmuir isotherm, Freundlich are given. Special emphasis is given on the formulation of geochemical reaction based model, where we have shown how to incorporate various homogeneous and heterogeneous reactions into the solute transport model equation. Concept of primary and secondary species and their use to reduce the number of equations to be solved is discussed.

We have given lattice Boltzmann schemes for following four type of formulations of reactive transport: (1) sorption isotherm based single component reactive transport, (ii) geochemical reaction based single component reactive transport, (iii) sorption isotherm based multi-component reactive transport, (iv) geochemical reaction based multi-component reactive transport. A new lattice Boltzmann scheme for sorption isotherm based multi-component reactive transport is proposed using the concept of diffusion velocity lattice Boltzmann. For simulation of geochemical reaction based multi-component reactive transport, we have interfaced our in-house developed LBM based solute transport solver with commercial geochemical software PHREEQC. Though, the similar coupling scheme was already developed and used for pore scale reactive transport, we further enhanced its scope by simulating continuum scale reactive transport. The developed schemes are validated and verified by solving three standard benchmark problems.

Chapter 4

Modeling Uncertainty Analysis in Solute Transport with Imprecise Model Parameters

4.1 Introduction

This chapter is intended to develop robust numerical schemes for modeling uncertainty associated with solute transport model output when the parameters of the governing equation are imprecise. In chapters 2 and 3, parameters of ADE such as groundwater velocity and dispersion coefficient were taken as crisp parameters, i.e., single representative values were assigned for each variable. But in reality, the measured values of these model parameters are imprecise either due to lack of measurements (few samples) or low precision measuring instruments used for experiment. Imprecise parameters are best represented by fuzzy numbers and corresponding partial differential equation (PDE) is called fuzzy PDE. In this study, groundwater velocity and dispersion coefficient are taken as fuzzy variables and thus the solute transport equation (ADE) is a fuzzy ADE. The imprecise parameters are represented by triangular fuzzy numbers (TFNs), because TFN encodes only most likely value (mean value) and the spread (standard deviation). Aggregation of all the fuzzy numbers for the estimation of uncertainty is carried out using fuzzy vertex method (FVM). LBM and DQM based schemes are developed to solve the fuzzy ADE numerically and due to this the present numerical approaches are termed as fuzzy lattice Boltzmann and fuzzy differential quadrature method, respectively. Uncertainty quantification of the solute concentration as solution of the governing fuzzy partial differential equation is carried out and epistemic uncertainty of the solute concentration thus computed is expressed in terms of lower and upper bounds. The structure of the chapter is as follows. Basics of fuzzy set theory and fuzzy logic, which are required for quantifying uncertainty involved with the solute transport model, are reviewed in section 4.2. The mathematical model of solute transport in presence of imprecise parameters is developed in section 4.3. In section 4.4, numerical framework for solution of the fuzzy solute transport model using LBM is carried out. Similar formulation with DQM is carried out in section 4.5. Finally the developed techniques are applied to various engineering problems in section 4.6.

4.2 Basics of Fuzzy Set Theory and Fuzzy Logic

In this section some essential concepts and definitions of fuzzy set theory and fuzzy logic, which are required for uncertainty analysis of solute transport process with imprecise model parameters, are provided in brief [Pal et al., 2015].

4.2.1 Fuzzy Sets

The concept of fuzzy set was introduced by Zadeh in 1965 [Zadeh, 1965]. The basic difference between an ordinary set and a fuzzy set is that members of a fuzzy set have a partial degree of membership in the range from 0 (no membership) to 1 (full membership) whereas, membership value of an element of ordinary set is either 0 or 1. A Fuzzy set can be defined mathematically by assigning a value, representing its grade of membership in the fuzzy set, to each possible individual in the universe of discourse, and hence it can be represented as a set of pairs of numbers as

$$A = \{(x, \mu(x)) \mid, x \in R, \mu(x) \in [0,1]\} \tag{4.1}$$

where μ(x) represents the membership grades of the crisp value, x, R is the universal set of real numbers . The fuzzy set A is normal if there exit at least one crisp value (x) for which $\mu_A(x) = 1$. A fuzzy set is said to be convex if for every real number a, b, c with $a < c < b$, $\mu_A(c) \geq min(\mu_A(a), \mu_A(b))$.

4.2.2 Fuzzy Numbers

Fuzzy numbers are special cases of fuzzy sets with a normal, fuzzy convex and continuous membership functions with bounded support. Generally two types of fuzzy membership functions (triangular and trapezoidal) are used to illustrate uncertainties associated with the model parameters.

Triangular Fuzzy Number

A triangular fuzzy number is a fuzzy subset $A \subset R$ characterized by a membership function $\mu_A : R \to [0,1]$ and defined by

$$\mu(x) = \begin{cases} \frac{x_L - a}{b-a}, & a \leq x_L \leq b \\ \frac{c - x_R}{c-b}, & b \leq x_R \leq c \\ 0, & otherwise \end{cases} \tag{4.2}$$

where a,b, and c are real numbers called lower, most probable, and upper bound of the fuzzy number, x_L and x_R are the two variables for the left and right sides, respectively. From the above Eq. (4.2) it can observed that a triangular fuzzy number can be defined if the values of a, b, and c are known. Hence, a triangular fuzzy number is denoted as $\widetilde{A} = [a, b, c]$. Schematic view of triangular fuzzy number is shown in Figure 4.1.

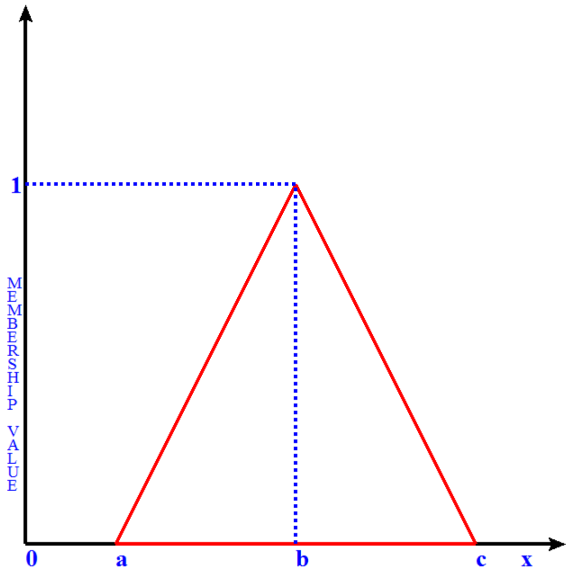

Figure 4.1: Fuzzy variable with triangular membership function

Trapezoidal Fuzzy Number

A trapezoidal fuzzy number is a fuzzy subset $A \subset R$ characterized by a membership function $\mu_A : R \rightarrow [0, 1]$ and defined by

$$\mu\left(x\right) = \begin{cases} \frac{x-a}{b-a}, & a \leq x \leq b \\ \frac{c-x}{d-c}, & c \leq x \leq d \\ 1, & b \leq x \leq c \\ 0, & otherwise \end{cases} \tag{4.3}$$

where a,b, c and d are real numbers with $a \leq b \leq c \leq d$. From the above Eq. (4.3) it can observed that a trapezoidal fuzzy number can be defined if the values of a, b, c, and d are known. Hence, a trapezoidal fuzzy number is denoted as $\widetilde{A} = [a, b, c, d]$. Schematic view of trapezoidal fuzzy number is shown in Figure 4.2

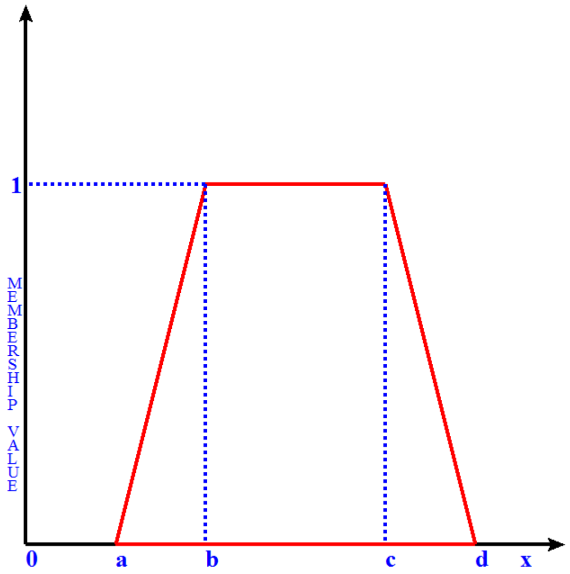

Figure 4.2: Fuzzy variable with trapezoidal membership function

4.2.3 α-cut of a Fuzzy Set

The α-cut of a fuzzy set is the (crisp) set of all elements that have a membership value greater than or equal to α. The α-cut of a fuzzy set, $A = \{x, \mu(x)\}$, is written as $A_\alpha = \{x \mid \mu_A(x) \geq \alpha\}$. It allows us to describe a fuzzy set as a composition of crisp sets. α-cut of a triangular fuzzy number, $\widetilde{A} = [a, b, c]$ is written as

$$A_\alpha = [x_L^\alpha, x_R^\alpha] = [a + (b - a)\,\alpha, c - (c - b)\,\alpha] \tag{4.4}$$

α-cut of a trapezoidal fuzzy number, $\widetilde{A} = [a, b, c, d]$ is written as

$$A_\alpha = [x_L^\alpha, x_R^\alpha] = [a + (b - a)\,\alpha, d - (d - c)\,\alpha] \tag{4.5}$$

4.3 Development of Fuzzy Solute Transport Model

From the discussion in Chapter 2, we rewrite the simplified form of solute transport equation (ADE)

$$\frac{\partial C}{\partial t} = D_j \frac{\partial^2 C}{\partial x_j^2} - u_j \frac{\partial C}{\partial x_j} \tag{4.6}$$

Measurement values of the model parameters (dispersion coefficient and groundwater velocity) are expressed around the most likely value and hence the fuzziness of these measures is expressed in the form of a triangular fuzzy number to maintain the measurement uncertainty. Considering the parameters of the Eq. (4.6) are imprecise, we can written the above equation as

$$\frac{\partial \widetilde{C}}{\partial t} = \widetilde{D_j} \frac{\partial^2 \widetilde{C}}{\partial x_j^2} - \widetilde{u_j} \frac{\partial \widetilde{C}}{\partial x_j} \tag{4.7}$$

where $\widetilde{D_j}$ and $\widetilde{u_j}$ are dispersion coefficient and groundwater velocity, respectively. The tilde, $\widetilde{}$, sign signifies the variable as fuzzy variable and distinguishes them from their classical (crisp) counterpart. The above equation is called fuzzy advection dispersion equation. In order to solve the above equation, we need to represent it using α-cut formulation. The α-cut representation of Eq. (4.7) can be written as

$$\frac{\partial C_\alpha}{\partial t} = D_{j\alpha} \frac{\partial^2 C_\alpha}{\partial x_j^2} - u_{j\alpha} \frac{\partial C_\alpha}{\partial x_j} \tag{4.8}$$

where $D_{j\alpha}$ and $u_{j\alpha}$ are the values of dispersion coefficient and groundwater velocity at membership value α and C_α is the corresponding solute concentration.

4.4 Development of Fuzzy Lattice Boltzmann Scheme

Details of LBM based schemes for solute and reactive transport have been described in previous chapters. In this section, LBM based scheme is developed to solve fuzzy solute transport equation (4.7) [Pal et al., 2017]. We rewrite SRT LBE

$$f_i\left(\overrightarrow{r} + \overrightarrow{e_i}\Delta t, t + \Delta t\right) = f_i\left(\overrightarrow{r}, t\right) + \Omega_i^{BGK}\left(\overrightarrow{r}, t\right) \tag{4.9}$$

$$\Omega_i^{BGK}\left(\overrightarrow{r}, t\right) = \frac{1}{\tau}\left[f_i^{eq}\left(\overrightarrow{r}, t\right) - f_i\left(\overrightarrow{r}, t\right)\right] \tag{4.10}$$

where $f_i\left(\overrightarrow{r}, t\right)$ is particle distribution function at spatio-temporal coordinate $\left(\overrightarrow{r}, t\right)$ along i^{th} direction, $\overrightarrow{e_i}$ represents particle velocity along i^{th} direction, $\Omega_i^{BGK}\left(\overrightarrow{r}, t\right)$ is BGK collision operator along i^{th} direction at same spatio-temporal coordinate, Δt is time step, τ is relaxation coefficient, and $f_i^{eq}\left(\overrightarrow{r}, t\right)$ is particle equilibrium distribution function (EDF) along i^{th} direction. Since macroscopic particle density is the zero order velocity moment of distribution function, concentration of solute at a given α-cut can be written in terms of corresponding discrete particle distribution function as

$$C_\alpha\left(\overrightarrow{r}, t\right) = \sum_i f_{i\alpha}\left(\overrightarrow{r}, t\right) \tag{4.11}$$

Therefore, the lattice Boltzmann equation for the evolution of $f_{i\alpha}\left(\overrightarrow{r}, t\right)$ can be written as

$$f_{i\alpha}\left(\overrightarrow{r} + \overrightarrow{e_i}\Delta t, t + \Delta t\right) = f_{i\alpha}\left(\overrightarrow{r}, t\right) + \Omega_{i\alpha}^{BGK}\left(\overrightarrow{r}, t\right) \tag{4.12}$$

$$\Omega_{i\alpha}^{BGK}\left(\overrightarrow{r}, t\right) = \frac{1}{\tau}\left[f_{i\alpha}^{eq}\left(\overrightarrow{r}, t\right) - f_{i\alpha}\left(\overrightarrow{r}, t\right)\right] \tag{4.13}$$

The above equations can be treated as α-cut representation of the SRT LBE. The EDF plays important role for solving any physical problem using LBM. Since Eq. (4.8) is an ADE, EDF for the same (4.8) can be written as

$$f_{i\alpha}^{eq}\left(\overrightarrow{r}, t\right) = w_i C_\alpha\left(\overrightarrow{r}, t\right)\left(1 - \frac{\overrightarrow{e_i}.\overrightarrow{u_\alpha}}{e_s^2}\right) \tag{4.14}$$

where w_i are the weights for particle's distribution function along i^{th} direction, $\overrightarrow{u_\alpha} = (u_x, u_y, u_z)$, and e_s is "pseudo sound speed" [Chen et al., 1998]. The EDF (4.14) and weight factors satisfy the following properties

$$\sum_i w_i = 1 \tag{4.15}$$

$$\sum_i f_{i\alpha}^{eq}\left(\overrightarrow{r}, t\right) = C_\alpha\left(\overrightarrow{r}, t\right) \tag{4.16}$$

$$\sum_i e_{ix} f_{i\alpha}^{eq}\left(\overrightarrow{r}, t\right) = u_{x\alpha} C_\alpha\left(\overrightarrow{r}, t\right) \tag{4.17}$$

$$\sum_i e_{ix} e_{iy} f_{i\alpha}^{eq}\left(\overrightarrow{r}, t\right) = e_s^2 C_\alpha\left(\overrightarrow{r}, t\right) \delta_{x,y} \tag{4.18}$$

where $\delta_{x,y}$ is the Dirac delta function, which is equal to 1 when $x = y$ and equal to 0 when $x \neq y$. In the following part of this section we will derive the ADE governing solute transport process (4.8) from LBE (4.12) using multi-scale Chapman-Enskog expansion technique. For this, we assume that Δt is a small parameter and equal to ε.

$$\Delta t = \varepsilon \tag{4.19}$$

Substitution of the above equation into Eq. (4.12) leads to

$$f_{i\alpha}\left(\overrightarrow{r} + \overrightarrow{e_i}\varepsilon, t + \varepsilon\right) = f_{i\alpha}\left(\overrightarrow{r}, t\right) + \frac{1}{\tau}\left[f_{i\alpha}^{eq}\left(\overrightarrow{r}, t\right) - f_{i\alpha}\left(\overrightarrow{r}, t\right)\right] \tag{4.20}$$

Using Chapman-Enskog expansion technique, particle distribution function can be expanded as

$$f_{i\alpha} = f_{i\alpha}^{(0)} + \sum_{n=1}^{\infty} \varepsilon^n f_{i\alpha}^{(n)} = f_{i\alpha}^{(0)} + \varepsilon f_{i\alpha}^{(1)} + \varepsilon^2 f_{i\alpha}^{(2)} + \vartheta\left(\varepsilon^3\right) \tag{4.21}$$

Taylor series expansion of the left-hand side of the Eq. (4.20) with respect to time and space around point $(\overrightarrow{r}, t)$ can be written as

$$\sum_{n=1}^{\infty} \frac{\varepsilon^n}{n!} \left(\frac{\partial}{\partial t} + e_{ij} \frac{\partial}{\partial x_j} \right)^n f_{i\alpha} (\overrightarrow{r}, t) = \frac{1}{\tau} \left[f_{i\alpha}^{eq} (\overrightarrow{r}, t) - f_{i\alpha} (\overrightarrow{r}, t) \right] \tag{4.22}$$

Substitution of Eq. (4.21) into Eq. (4.22) leads to

$$\begin{aligned} &\sum_{n=1}^{\infty} \frac{\varepsilon^n}{n!} \left(\frac{\partial}{\partial t} + e_{ij} \frac{\partial}{\partial x_j} \right)^n \left(f_{i\alpha}^{(0)} + \varepsilon f_{i\alpha}^{(1)} + \varepsilon^2 f_{i\alpha}^{(2)} \right) \\ &\qquad = \frac{1}{\tau} \left[f_{i\alpha}^{eq} - \left(f_{i\alpha}^{(0)} + \varepsilon f_{i\alpha}^{(1)} + \varepsilon^2 f_{i\alpha}^{(2)} \right) \right] \end{aligned} \tag{4.23}$$

Since for ADE we require only up to second order terms of the expanded distribution function (4.21), higher order terms are neglected. Grouping terms of the same order in ε yields the following successive approximations

$$\vartheta \left(\varepsilon^0 \right) : f_{i\alpha}^{eq} = f_{i\alpha}^{(0)} \tag{4.24}$$

$$\vartheta \left(\varepsilon^1 \right) : \left(\frac{\partial}{\partial t} + e_{ij} \frac{\partial}{\partial x_j} \right) f_{i\alpha}^{(0)} = -\frac{1}{\tau} f_{i\alpha}^{(1)} \tag{4.25}$$

$$\vartheta \left(\varepsilon^2 \right) : \left(\frac{\partial}{\partial t} + e_{ij} \frac{\partial}{\partial x_j} \right) f_{i\alpha}^{(1)} + \frac{1}{2} \left(\frac{\partial}{\partial t} + e_{ij} \frac{\partial}{\partial x_j} \right)^2 f_{i\alpha}^{(0)} = -\frac{1}{\tau} f_{i\alpha}^{(2)} \tag{4.26}$$

Substituting Eq. (4.25) into the above Eq. (4.26), we get

$$\left(1 - \frac{1}{2\tau} \right) \left(\frac{\partial}{\partial t} + e_{ij} \frac{\partial}{\partial x_j} \right) f_{i\alpha}^{(1)} = -\frac{1}{\tau} f_{i\alpha}^{(2)} \tag{4.27}$$

Eq. (4.25)+$\varepsilon\times$ Eq. (4.27) leads to

$$\begin{aligned} &\left(\frac{\partial}{\partial t} + e_{ij} \frac{\partial}{\partial x_j} \right) f_{i\alpha}^{(0)} + \varepsilon \left(1 - \frac{1}{2\tau} \right) \left(\frac{\partial}{\partial t} + e_{ij} \frac{\partial}{\partial x_j} \right) f_{i\alpha}^{(1)} \\ &\qquad = -\frac{1}{\tau} \left(f_{i\alpha}^{(1)} + \varepsilon f_{i\alpha}^{(2)} \right) \end{aligned} \tag{4.28}$$

Using the properties of distribution function as given in Eq. (4.16) and (4.17), we can impose following constraints on fluctuating parts of the distribution function

$$\sum_i f_{i\alpha}^{(k)}\left(\overrightarrow{r},t\right)=0, \qquad k=1,2,3,... \tag{4.29}$$

$$\frac{\partial}{\partial t}\sum_i f_{i\alpha}^{(k)}\left(\overrightarrow{r},t\right)=0, \qquad k=1,2,3,... \tag{4.30}$$

Summing over i and using Eq. (4.29) and (4.30), Eq. (4.28) can be written as

$$\frac{\partial}{\partial t}\sum_i f_{i\alpha}^{(0)}+\frac{\partial}{\partial x_j}\sum_i e_{ij}f_{i\alpha}^{(0)}+\varepsilon\left(1-\frac{1}{2\tau}\right)\frac{\partial}{\partial x_j}\sum_i e_{ij}f_{i\alpha}^{(1)}=0 \tag{4.31}$$

Substituting the value of $f_{i\alpha}^{(1)}$ from Eq. (4.25) into the above equation, we get

$$\begin{gathered}\frac{\partial}{\partial t}\sum_i f_{i\alpha}^{(0)}+\frac{\partial}{\partial x_j}\sum_i e_{ij}f_{i\alpha}^{(0)}+-\tau\varepsilon\left(1-\frac{1}{2\tau}\right)\frac{\partial}{\partial x_j}\sum_i e_{ij}\frac{\partial}{\partial t}f_{i\alpha}^{(0)}\\ -\tau\varepsilon\left(1-\frac{1}{2\tau}\right)\frac{\partial}{\partial x_j}\sum_i e_{ij}e_{ik}\frac{\partial}{\partial x_k}f_{i\alpha}^{(0)}=0\end{gathered} \tag{4.32}$$

The term containing time derivative of EDF is smaller compared to the other three terms and hence, it can be omitted and can be treated as error term. Using the properties of EDF as given in Eqs. (4.16), (4.17), and (4.18), Eq. (4.32) can be written as

$$\frac{\partial C_\alpha}{\partial t}+\frac{\partial\left(u_{j\alpha}C_\alpha\right)}{\partial x_j}-\varepsilon\left(\tau-\frac{1}{2}\right)\frac{\partial}{\partial x_j}\left(e_s^2\frac{\partial C_\alpha}{\partial x_j}\right)=0 \tag{4.33}$$

The above equation can be rearranged as

$$\frac{\partial C_\alpha}{\partial t}=\frac{\partial}{\partial x_j}\left(D_\alpha\frac{\partial C_\alpha}{\partial x_j}\right)-\frac{\partial\left(u_{j\alpha}C_\alpha\right)}{\partial x_j} \tag{4.34}$$

where

$$D_\alpha = e_s^2 \varepsilon \left(\tau - \frac{1}{2}\right) \tag{4.35}$$

From Eq. (4.19) we have, $\varepsilon = \Delta t$. Therefore, Eq. (4.35) can be written as

$$D_\alpha = e_s^2 \Delta t \left(\tau - \frac{1}{2}\right) \tag{4.36}$$

Eq. (4.34) is the α-cut representation of the fuzzy ADE as given in Eq. (4.7). Equation (4.36) correlates macroscopic parameter dispersion coefficient with microscopic parameter relaxation coefficient. From Eq. (4.36) it is observed that dispersion coefficient is a function of relaxation coefficient; therefore, in order to solve LBEs (4.12) for various α-cut values of dispersion coefficient, we need to use τ_α instead of τ, where τ_α is the relaxation coefficient corresponding to particular α-cut value of dispersion coefficient. Since LB solutions are more stable in lattice unit compared to physical unit, we have solved LBE in lattice unit. In lattice unit Eq. (4.36) can be written as

$$D_\alpha^* = e_s^2 \Delta t^* \left(\tau - \frac{1}{2}\right) \tag{4.37}$$

where D_α^* is the lattice dispersion coefficient. For unit lattice time step $\Delta t^* = 1$ and unit lattice spatial step $\Delta x^* = 1$, lattice velocity $e = \Delta x^*/\Delta t^* = 1$, and $e_s = e/\sqrt{3}$ (valid for D1Q3, D2Q5, D2Q9, and similar lattices [Sukop et al., 2006; Mohamad, 2011]. Substituting these values in Eq. (4.37) we obtain the value of lattice dispersion coefficient for D1Q3 lattice as

$$D_\alpha^* = \frac{1}{3}\left(\tau - \frac{1}{2}\right) \tag{4.38}$$

The relation between lattice diffusion coefficient and physical diffusion coefficient is (Eq. 2.64)

$$D_\alpha^* = \frac{D_\alpha}{\frac{(\Delta x)^2}{\Delta t}} \tag{4.39}$$

Using Eqs. (4.38) and (4.39), we obtain the expression for physical time step as

$$\Delta t = \frac{(\Delta x)^2}{3D_\alpha}\left(\tau - \frac{1}{2}\right) \tag{4.40}$$

For $\tau = 1$, Eq. (4.40) can be written as

$$\Delta t = \frac{(\Delta x)^2}{6D_\alpha} \tag{4.41}$$

Eq. (4.41) shows that corresponding to each α-cut value of diffusion coefficient, we have different time step value (Δt) and therefore, the above equation can be written as

$$\Delta t_\alpha = \frac{(\Delta x)^2}{6D_\alpha} \tag{4.42}$$

In fuzzy logic, corresponding to each α-cut value (except α-cut = 1), we have four combinations of input parameters (dispersion coefficient and groundwater velocity), such as, $[D_{Low}, u_{Low}]_\alpha$, $[D_{Low}, u_{High}]_\alpha$, $[D_{High}, u_{Low}]_\alpha$,$[D_{High}, u_{High}]_\alpha$. Our task in Fuzzy LBM is to solve the LBE (4.12) using each combination of input parameters. Change in velocity alters the equilibrium distribution function through Eq. (4.14) and therefore, effect of change in velocity is directly incorporated into the LB equation through change in equilibrium distribution function. The physical dispersion coefficient is not directly involved with LBE but, its effect can be incorporated into LB equation in the following way; change in dispersion coefficient alters the physical time step value through Eq. (4.42) and physical time step value decides the number of iteration to be performed for a given simulation time.

4.5 Development of Fuzzy Differential Quadrature Scheme

Basic working principle of DQM and DQM based numerical scheme for solute transport have already been described in the first and second chapter, respectively. In this section, DQ scheme for fuzzy solute transport equation is formulated [Datta et al., 2017]. To begin with we first rewrite the α-cut representation of the fuzzy ADE, as presented in section 4.3.

$$\frac{\partial C_\alpha}{\partial t} = D_{j\alpha}\frac{\partial^2 C_\alpha}{\partial x_j^2} - u_{j\alpha}\frac{\partial C_\alpha}{\partial x_j} \tag{4.43}$$

Using DQM we can write the first and second order derivatives of C_α with respect to three Cartesian co-ordinate directions as

$$\begin{aligned}
\frac{\partial C_\alpha}{\partial x}\,|_{x=x_i,y=y_j,z=z_k} &= \sum_{m=1}^{N_x} X_{im}^{(1)} C_{mjk\alpha}\\
\frac{\partial C_\alpha}{\partial y}\,|_{x=x_i,y=y_j,z=z_k} &= \sum_{m=1}^{N_y} Y_{jm}^{(1)} C_{imk\alpha}\\
\frac{\partial C_\alpha}{\partial z}\,|_{x=x_i,y=y_j,z=z_k} &= \sum_{m=1}^{N_z} Z_{km}^{(1)} C_{ijm\alpha}\\
\frac{\partial^2 C_\alpha}{\partial x^2}\,|_{x=x_i,y=y_j,z=z_k} &= \sum_{m=1}^{N_x} X_{im}^{(2)} C_{mjk\alpha}\\
\frac{\partial^2 C_\alpha}{\partial y^2}\,|_{x=x_i,y=y_j,z=z_k} &= \sum_{m=1}^{N_y} Y_{jm}^{(2)} C_{imk\alpha}\\
\frac{\partial^2 C_\alpha}{\partial z^2}\,|_{x=x_i,y=y_j,z=z_k} &= \sum_{m=1}^{N_z} Z_{km}^{(2)} C_{ijm\alpha}
\end{aligned}$$

where x_i, y_jandz_k are the discrete nodes in the domain at which function values are known, C_{ijk} are the concentrations values at these nodes at time t, N_x, N_y, N_z are the total number of grid points along x, y and z directions, respectively. $X^{(2)}, Y^{(2)}$ and $Z^{(2)}$ are the weight matrices for the second order derivatives along x, y and z directions, respectively and $X^{(1)}, Y^{(1)}$ and $Z^{(1)}$ are the weight matrices for the first order derivatives. Now substituting the above formulations into Eq. (4.43) and taking finite difference discretization of the temporal derivative we get

$$\begin{aligned} C_{ijk\alpha}^{s+1} = C_{ijk\alpha}^{s} + \Delta t \Bigg(& D_{x\alpha} \sum_{m=1}^{N_x} X_{im}^{(2)} C_{mjk\alpha}^{s} + D_{y\alpha} \sum_{m=1}^{N_y} Y_{jm}^{(2)} C_{imk\alpha}^{s} \\ & + D_{z\alpha} \sum_{m=1}^{N_z} Z_{km}^{(2)} C_{ijm\alpha}^{s} - u_{x\alpha} \sum_{m=1}^{N_x} X_{im}^{(1)} C_{mjk\alpha}^{s} \\ & - u_{y\alpha} \sum_{m=1}^{N_y} Y_{jm}^{(1)} C_{imk\alpha}^{s} - u_{z\alpha} \sum_{m=1}^{N_z} Z_{km}^{(1)} C_{ijm\alpha}^{s} \Bigg) \end{aligned} \tag{4.44}$$

Equation (4.44) calculates solute concentration at each node at a particular α-cut value. Membership function of solute concentration can be calculated by solving the above equation for various α-cut values.

4.6 Numerical Problem Solved

In this section various solute transport problems with imprecise model parameters are solved using the developed fuzzy LB and fuzzy DQ methods. The results are presented in terms of membership function of solute concentration.

4.6.1 One-Dimensional solute transport with constant source using Fuzzy LBM

Problem statement

This problem represent one-dimensional transport of solute in a saturated porous media. The model computes the concentration of solutes at any spatio-temporal location from the point of release of the chemicals. The release rate is controlled in such a way that the source concentration at the place of discharge can be taken as constant. Measured parameters associated with this model are groundwater flow and dispersion coefficient and these are considered as fuzzy numbers due to insufficiency in their measured values. Both these parameters are represented here as triangular fuzzy numbers because imprecision result is around the most likely value.

This solute transport process is modeled as a one-dimensional fuzzy solute transport equation. The governing equation can be written using Eq. (4.7) as

$$\frac{\partial \widetilde{C}}{\partial t} = \widetilde{D_x}\frac{\partial^2 \widetilde{C}}{\partial x^2} - \widetilde{u_x}\frac{\partial \widetilde{C}}{\partial x} \tag{4.45}$$

where $\widetilde{D_x}$ and $\widetilde{u_x}$ are the fuzzy variables and represent x directional dispersion coefficient and groundwater velocity, respectively. Initial and boundary conditions of the solute transport problem are

$$\begin{aligned} &C\left(x, t=0\right) = 0 \\ &C\left(x=0, t\right) = C_0 \\ &C\left(x=\infty, t\right) = 0 \end{aligned} \tag{4.46}$$

Fuzzy lattice Boltzmann solution

Fuzzy LBM based simulation of the problem is carried out using D1Q3 lattice (Figure 2.2). Lattice length and time step values in lattice units are fixed at unit value, i.e., Δx =1 lbu, and Δt =1 lbu. Corresponding lattice length in physical unit is taken as, Δx =1 m and time step, which depends upon diffusion coefficient, D_x, is calculated for each α-cut using Eq. (4.42). The concentration of the constant source is taken at 1 $mol.m^{-3}$. The chemicals are discharged at x = 0 m in the domain having domain length L = 1000 m. The fuzzy input parameters used in the simulation are constructed using experts opinion in terms of mean value and corresponding error bar. The numerical values of lower bound, most likely and upper bound of dispersion coefficient and groundwater velocity are given in Table 4.1. The fuzzy LBM simulations are carried out at 11 different α-cuts ranging from 0 to 1 with an interval of 0.1. Membership values of the model parameters at these α-cuts are given in tabular from in Table 4.2. Membership functions of the model parameters are shown in Figures 4.3 and 4.4. Uncertainty in solute concentration is expressed in terms of a closed interval bounded by lower and upper value of solute concentration.

Table 4.1: Input parameters used in fuzzy LBM simulation for constant source

Parameters	Lower Bound	Most Likely	Upper Bound
Dispersion coefficient (m)	1.43×10^{-5}	3.08×10^{-5}	6.58×10^{-5}
Velocity of flow (m/day)	4.23×10^{-6}	6.18×10^{-6}	7.82×10^{-6}

Table 4.2: Membership values of D_x and u_x at various α-cut values

α-cut value	D$_x$ $\left(m^2s^{-1}\right)\times10^{-5}$		u$_x$ $\left(ms^{-1}\right)\times10^{-6}$	
	Lower	Upper	lower	Upper
0	1.430	6.580	4.230	7.820
0.1	1.595	6.230	4.425	7.656
0.2	1.760	5.880	4.620	7.492
0.3	1.925	5.530	4.815	7.328
0.4	2.090	5.180	5.010	7.164
0.5	2.255	4.830	5.205	7.000
0.6	2.420	4.480	5.40	6.836
0.7	2.585	4.130	5.595	6.672
0.8	2.750	3.780	5.790	6.508
0.9	2.915	3.430	5.985	6.344
1.0	3.080	3.080	6.180	6.180

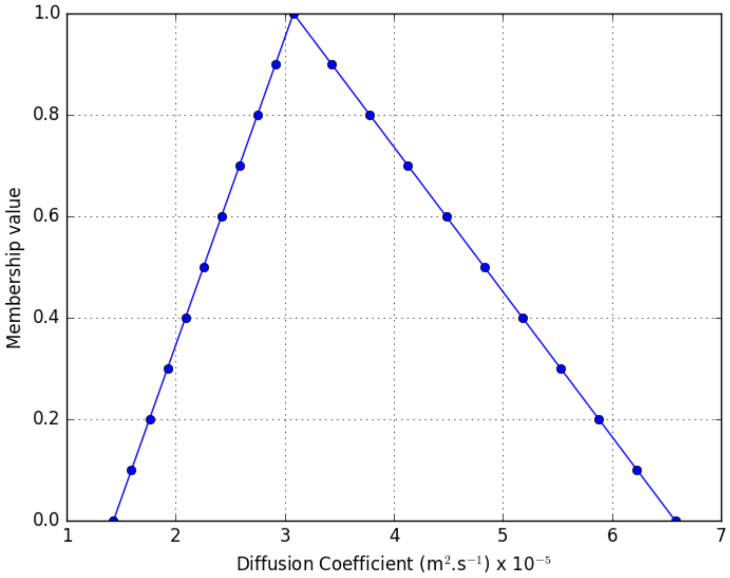

Figure 4.3: Triangular membership function of diffusion coefficient

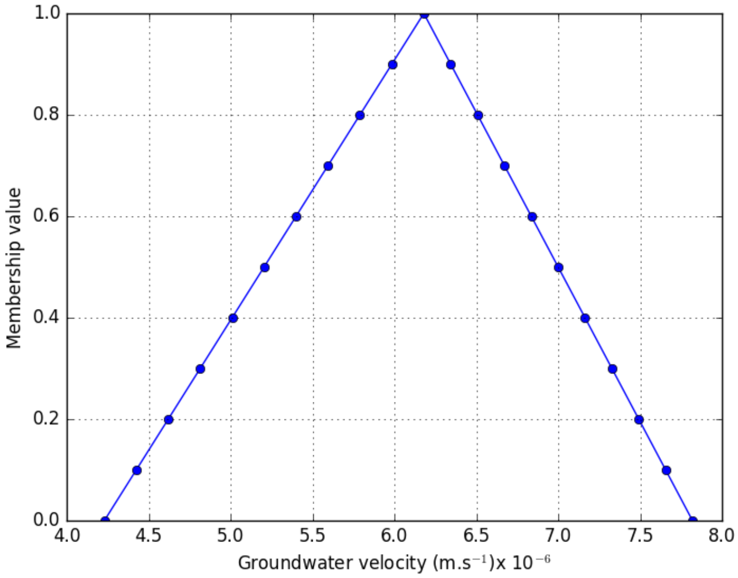

Figure 4.4: Triangular membership function of groundwater velocity

Validation and verification

Validation and verification of the fuzzy LBM scheme is carried out by comparing the results of fuzzy LBM with closed form analytical solution. The Eq. (4.45) together with the initial and boundary conditions (4.46) has a closed form analytical solution which can be written as [Dou et al., 1995]

$$\widetilde{C} = \frac{C_0}{2} \times \left[erfc\left(\frac{x - \widetilde{u_x}t}{2\sqrt{\widetilde{D_x}t}} \right) + exp\left(\frac{\widetilde{u_x}x}{\widetilde{D_x}} \right) erfc\left(\frac{x + \widetilde{u_x}t}{2\sqrt{\widetilde{D_x}t}} \right) \right] \tag{4.47}$$

The numerical calculation of the upper and lower bound of the solute concentration for a specific time and at each length of the domain results the fuzziness of the solute concentration. LB solutions for most probable values of input parameters at time t = 365 $days$, 600 $days$, and 1000 $days$ are compared with corresponding analytical results. The comparison of numerical and analytical solutions is shown graphically in Figure 4.5.

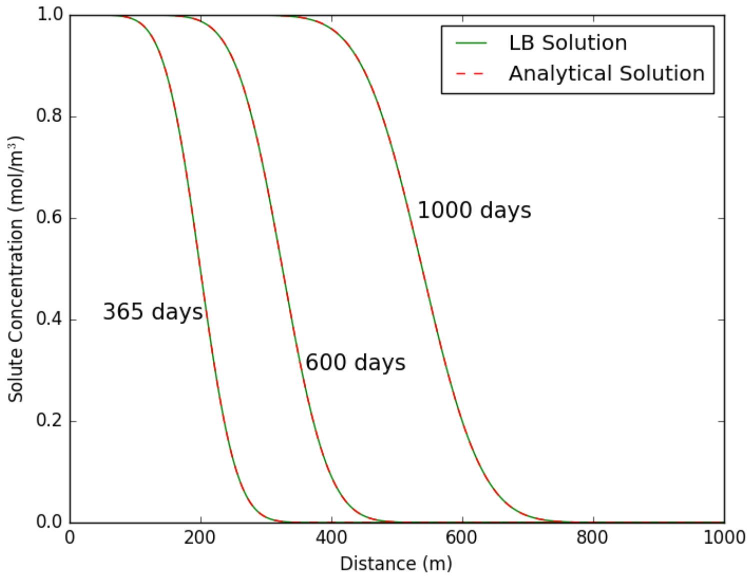

Figure 4.5: Spatial concentration profile of solute with most probable value of input parameters: comparison of LB and Analytical solution

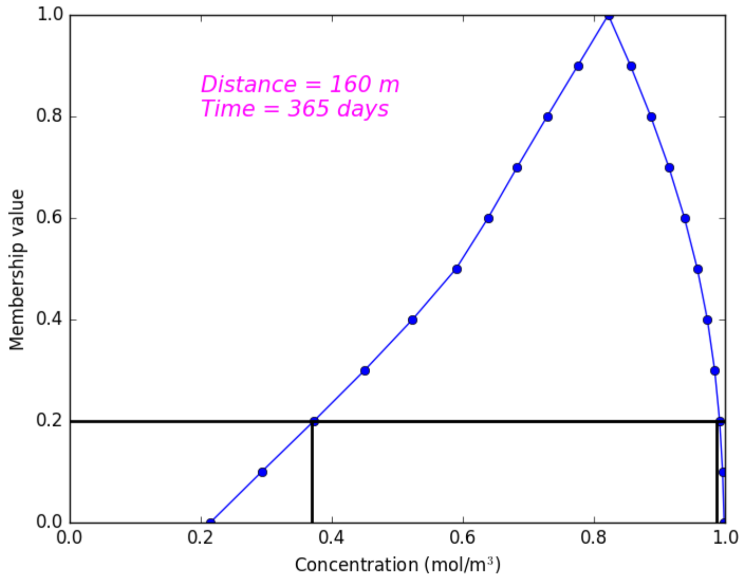

Figure 4.6: Membership function of of solute concentration at length 160 m

Results and discussions

The fuzziness of the solute concentration at lengths, x = 160 m, 200 m, and 230 m for specific time (t=365 $days$) are represented in terms of the membership function of solute concentration and the results are shown in Figures 4.6, 4.7, and 4.8. Spatial profiles of solute concentration using four different combinations of fuzzy input parameters at α-cut of 0.4 and 0.7 for the total time of simulation (t = 365 $days$) are computed. Lower and upper concentration of solute at each spatial point for the same α-cut values and total simulation time are extracted from the four different spatial profiles. Spatial profiles of lower and upper bound and most probable value of solute concentration are shown in Figures 4.9 and 4.10, for α-cut value of 0.4 and 0.7, respectively. It can be observed from the Figures 4.9 and 4.10 that transport of solute results an uncertainty (due to the fuzziness of the model parameters) in solute concentration. The uncertainty increases with decrease of α-cut value which is an obvious fact because lower the α-cut value higher is the fuzziness in the input parameters. LB based spatial profiles are compared with analytical solution and good agreement between the two results is established.

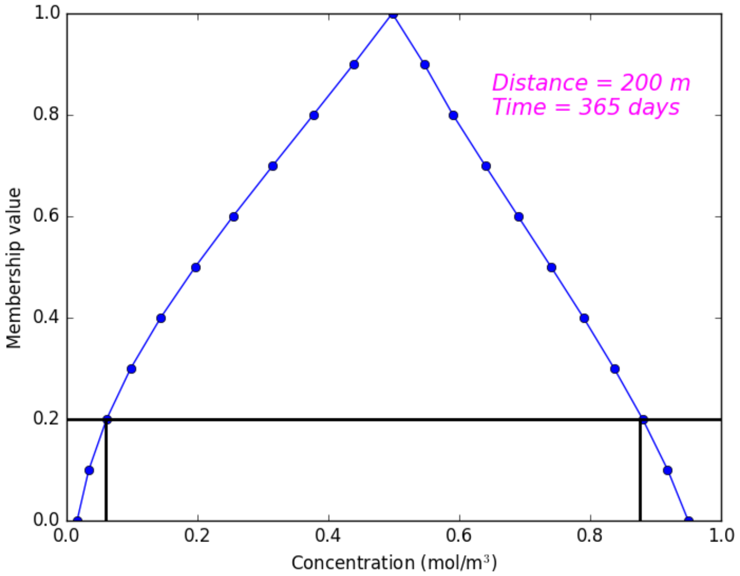

Figure 4.7: Membership function of of solute concentration at length 200 m

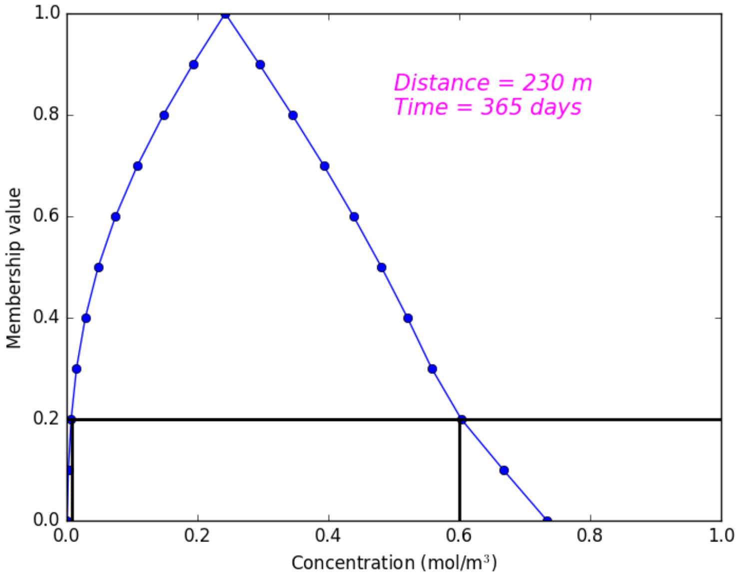

Figure 4.8: Membership function of of solute concentration at length 230 m

Uncertainty of solute concentration at 160 m downstream and after 365 $days$ at any α-cut level, say, α = 0.2 can be quantified from Figure 4.6 as [0.370, 0.987] $mol.m^{-3}$ and the same is represented as an interval bounded within two vertical lines. In a similar way, Figure 4.7 can be used to quantify the uncertainty bounds of solute concentration at 200 m downstream and at

365 $days$ for a specific α-cut of 0.2 as [0.060, 0.875] $mol.m^{-3}$ and Figure 4.8 can be used to quantify the uncertainty bounds of solute concentration at 230 m downstream and at 365 $days$ for a specific α-cut of 0.2 as [0.080, 0.600] $mol.m^{-3}$

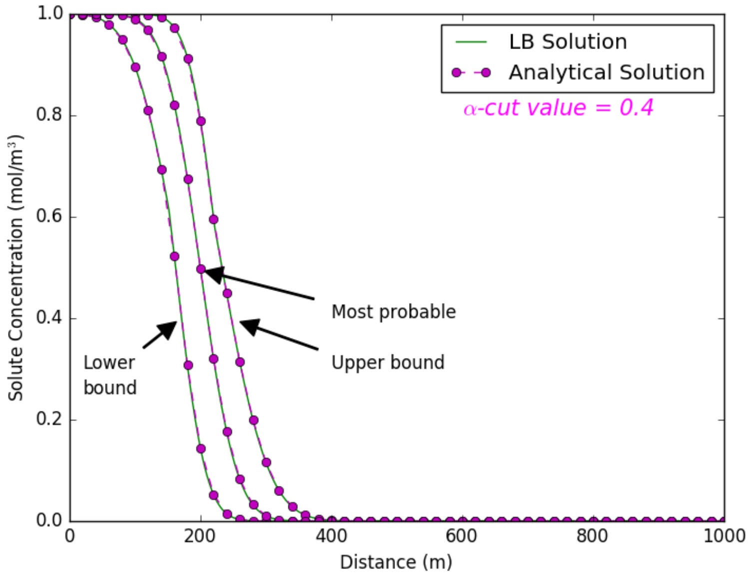

Figure 4.9: Lower bound, upper bound, and most probable value of spatial profile of solute concentration at α-cut=0.4

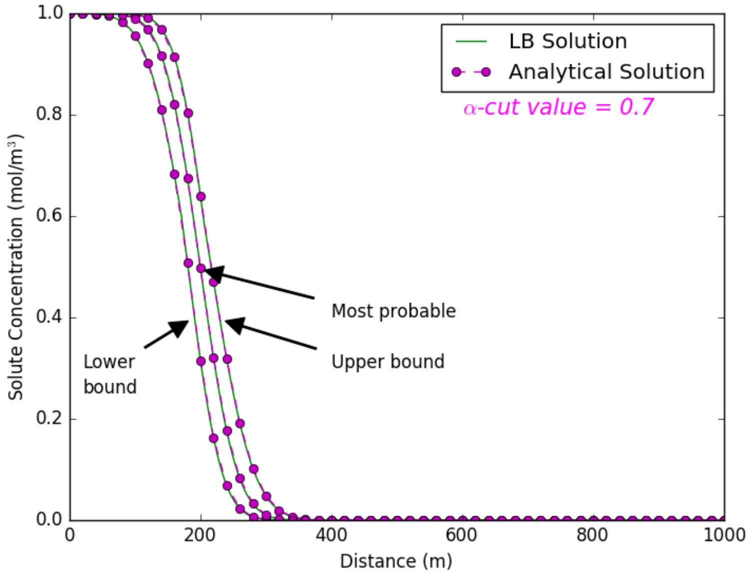

Figure 4.10: Lower bound, upper bound, and most probable value of spatial profile of solute concentration at α-cut=0.7

4.6.2 One-Dimensional Solute Transport with instantaneous point source using Fuzzy LBM

Problem statement

The deterministic form of this solute transport problem is similar to one of the problems solved in second chapter. The measured parameters associated with this model are groundwater flow and dispersion coefficient and these are considered as fuzzy numbers due to insufficiency in their measured values. Both these parameters are represented here as triangular fuzzy number because imprecision result is around the most likely value. The mathematical equation governing the solute transport process can be written in one-dimensional form as (4.8)

$$\frac{\partial \widetilde{C}}{\partial t} = \widetilde{D_x} \frac{\partial^2 \widetilde{C}}{\partial x^2} - \widetilde{u_x} \frac{\partial \widetilde{C}}{\partial x} \tag{4.48}$$

where D_x and u_x are x directional dispersion coefficient and groundwater velocity, respectively. Initial condition of the solute transport problem is

$$C(x, t = 0) = C_0 \delta(x) \tag{4.49}$$

where δ is the Kronecker delta function, C_0 is concentration of point source. Since the domain length is very large, it is reasonable to consider following Dirichlet boundary conditions.

$$C(x = \pm\infty, t) = 0 \tag{4.50}$$

Fuzzy lattice Boltzmann solution

Fuzzy LBM based simulation of the problem is carried out using D2Q5 lattice (2.4). Lattice length and time step values in lattice units are fixed at unit value, i.e., Δx =1 lbu, and Δt =1 lbu. Corresponding spatial step lengths is taken as, Δx =1 m and time step, which depends upon diffusion coefficient, D_x, is calculated for each α-cut using Eq. (4.42). The effluent having initial concentration of 1kg/m is discharged as a point source at x = 10 m in a channel with length L = 400 m. The fuzzy input parameters used in the simulation are constructed using experts opinion in terms of mean value and corresponding error bar. The numerical values of lower bound, most likely and upper bound of dispersion coefficient and groundwater velocity are given in Table 4.3. The fuzzy LBM simulations are carried out at 11 different α-cuts ranging from 0 to 1 with an interval of 0.1. Membership values of the model parameters at these α-cuts are given in tabular from in Table 4.4 and in graphical form in Figures 4.11 and 4.12. Uncertainty in solute concentration is expressed in terms of a closed interval bounded by lower and upper value of solute concentration.

Table 4.3: Input parameters used in fuzzy LBM simulation for instantaneous point source

Parameters	Lower Bound	Most Likely	Upper Bound
Dispersion coefficient (m)	0.010	0.014	0.017
Velocity of flow (m/day)	0.01	0.012	0.014

Table 4.4: Membership values of D_x and u_x at various α-cut values

α-cut value	D$_x$ $\left(m^2s^{-1}\right)$		u$_x$ $\left(ms^{-1}\right)$	
	Lower	Upper	lower	Upper
0	0.0100	0.0170	0.0100	0.0140
0.1	0.0104	0.0167	0.0102	0.0138
0.2	0.0108	0.0164	0.0104	0.0136
0.3	0.0112	0.0161	0.0106	0.0134
0.4	0.0116	0.0158	0.0108	0.0132
0.5	0.0120	0.0155	0.0110	0.0130
0.6	0.0124	0.0152	0.0112	0.0128
0.7	0.0128	0.0149	0.0114	0.0126
0.8	0.0132	0.0146	0.0116	0.0124
0.9	0.0136	0.0143	0.0118	0.0122
1.0	0.0140	0.0140	0.0120	0.0120

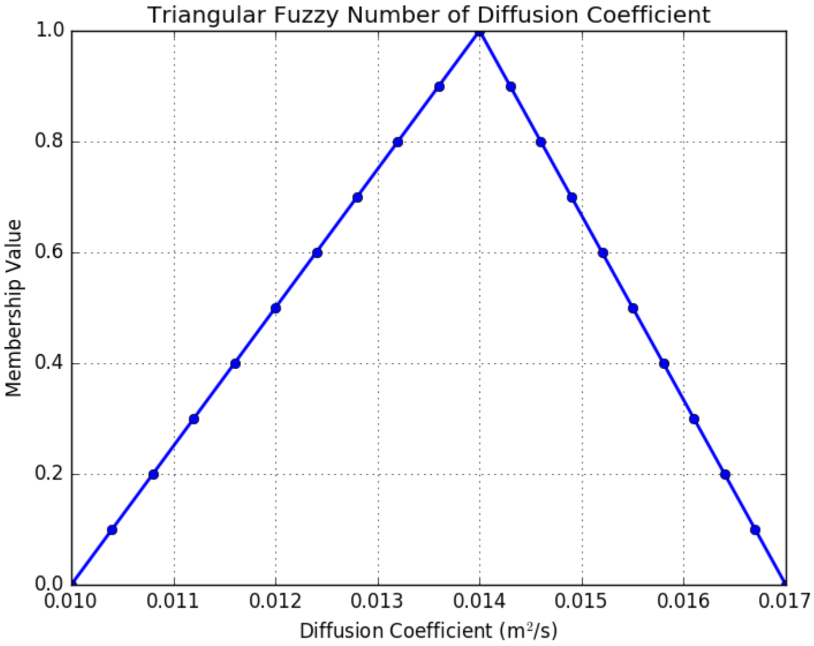

Figure 4.11: Triangular membership function of diffusion coefficient

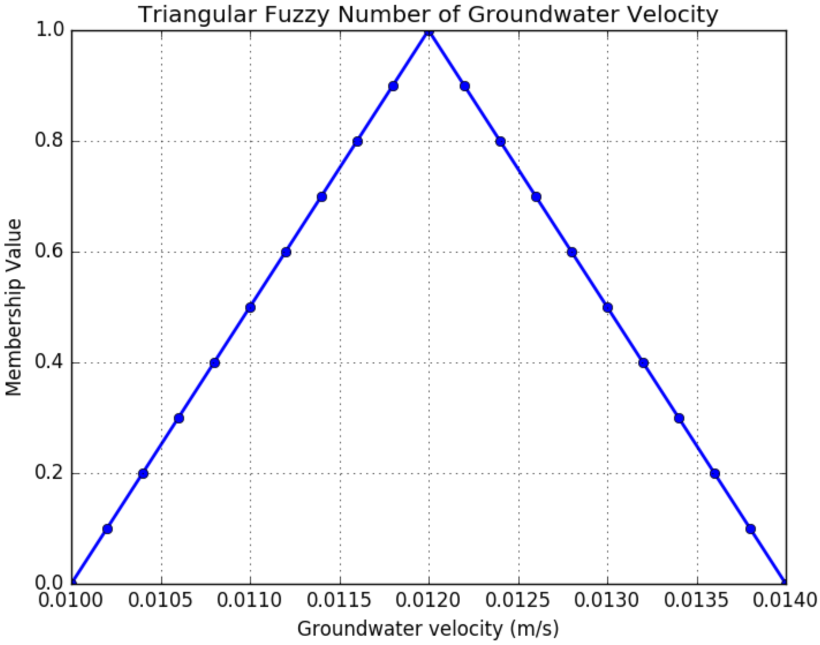

Figure 4.12: Triangular membership function of groundwater velocity

Results and discussions

Our LBM based scheme has already been verified in Chapter 2 for crisp values of input parameters of the same problem. The fuzziness of the solute concentration at lengths, x = 125 m, 140 m, and 150 m for specific time (t=10000 s) are represented in terms of the membership function of solute concentration and the results are shown in Figures 4.13, 4.14, and 4.15. Spatial profiles of solute concentration using four different combinations of fuzzy input parameters at α-cut of 0.5 and 0.8 for the total time of simulation (t = 10000 s) are computed and graphically shown in Figures 4.16 and 4.17, respectively. Lower and upper concentration of solute at each spatial point for the same α-cut values and total simulation time are extracted from the four different spatial profiles. Spatial profiles of lower and upper bound of solute concentration are shown in Figures 4.18 and 4.19, for α-cut value of 0.5 and 0.8, respectively. It can be observed from the Figures 4.18 and 4.19 that transport of solute results an uncertainty (due to the fuzziness of the model parameters) in solute concentration. The uncertainty increases with decrease of α-cut value which is an obvious fact because lower the α-cut value higher is the fuzziness in the input parameters. Comparison between analytical model and Fuzzy-Lbm model based uncertainty is shown graphically in Figure 4.20 and a good agreement between the two results is established.

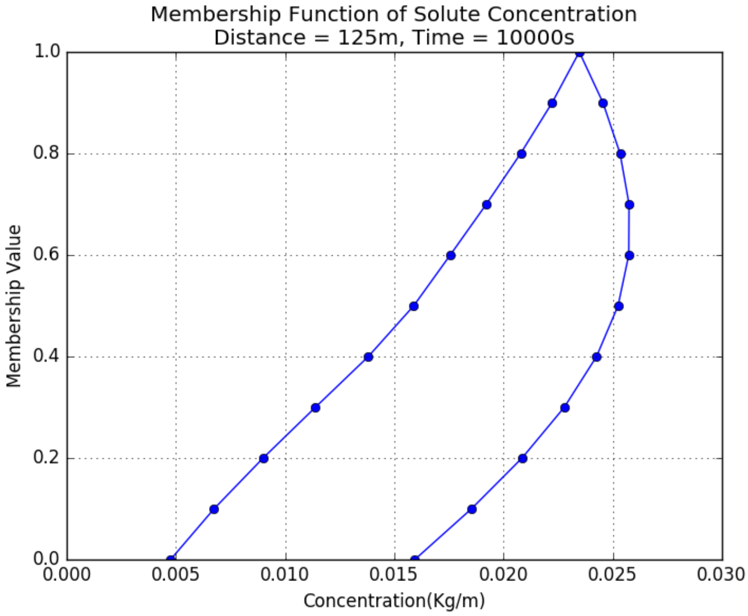

Figure 4.13: Membership function of of solute concentration at length 125 m

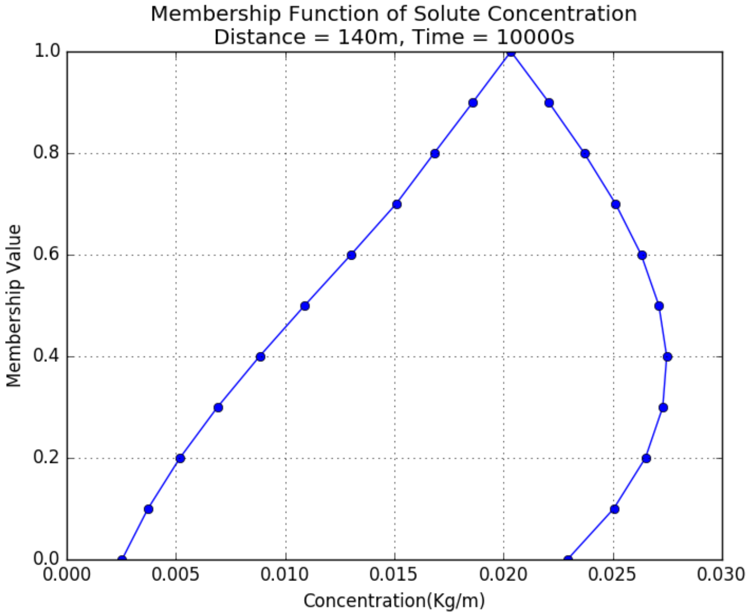

Figure 4.14: Membership function of solute concentration at length 140 m

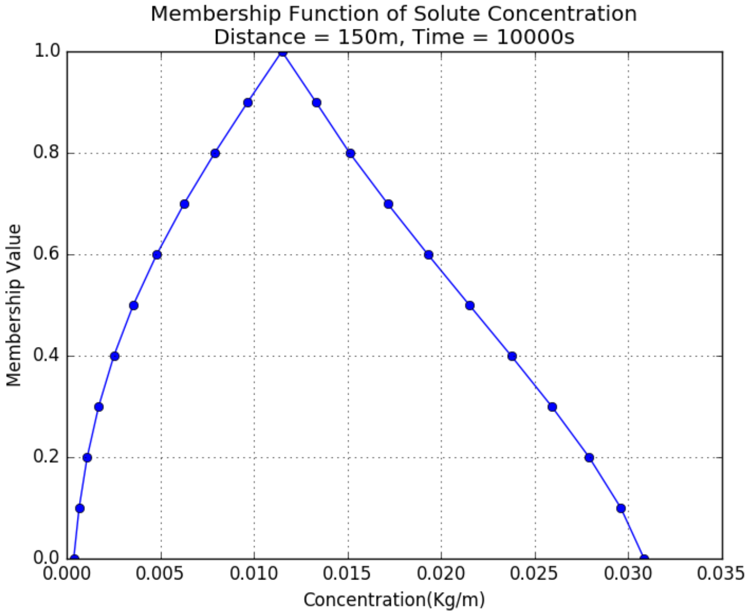

Figure 4.15: Membership function of of solute concentration at length 150 m

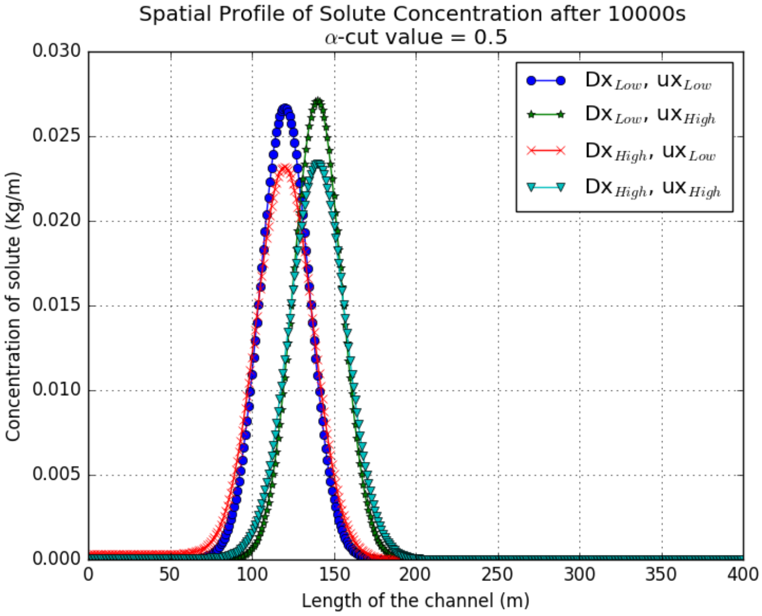

Figure 4.16: Spatial profile of solute with different combination of inputs at α-cut=0.5

Uncertainty of solute concentration at 160 m downstream and after 365 $days$ at any α cut level, say, α = 0.2 can be quantified from Figure 4.6 as [0.370, 0.987] $mol.m^{-3}$ and the same is represented as an interval bounded within two vertical lines. In a similar way, Figure 4.7 can be used to quantify the uncertainty bounds of solute concentration at 200 m downstream and at 365 $days$ for a specific α-cut of 0.2 as [0.060, 0.875] $mol.m^{-3}$ and Figure 4.8 can be used to quantify the uncertainty bounds of solute concentration at 230 m downstream and at 365 $days$ for a specific α-cut of 0.2 as [0.080, 0.600] $mol.m^{-3}$

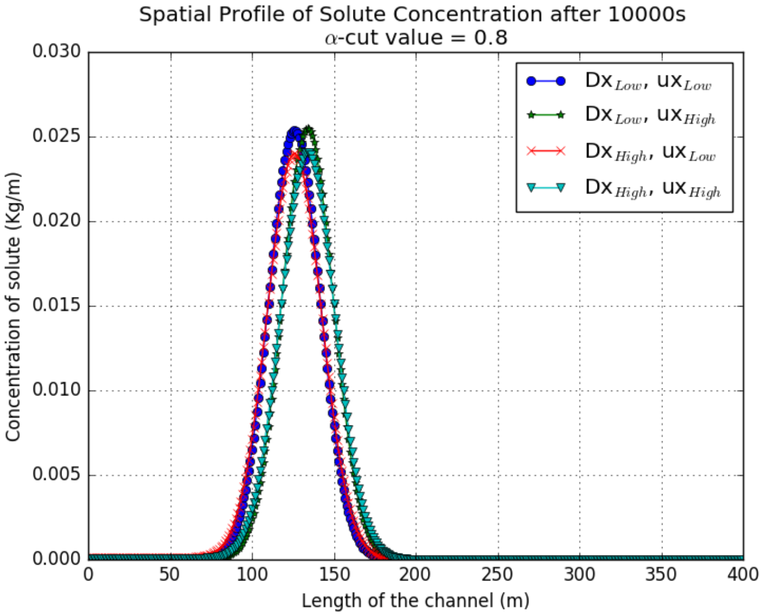

Figure 4.17: Spatial profile of solute with different combination of inputs at α-cut=0.8

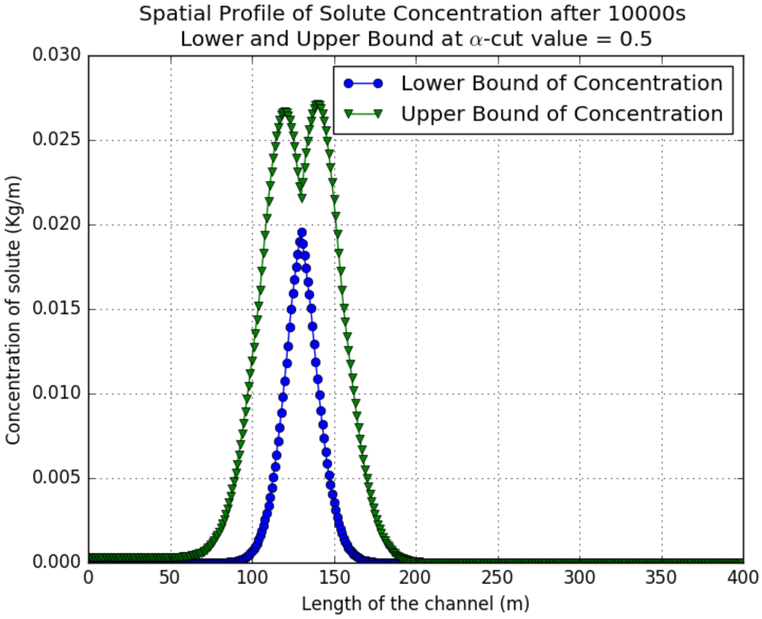

Figure 4.18: Lower and upper bound of spatial profiles at α-cut=0.5

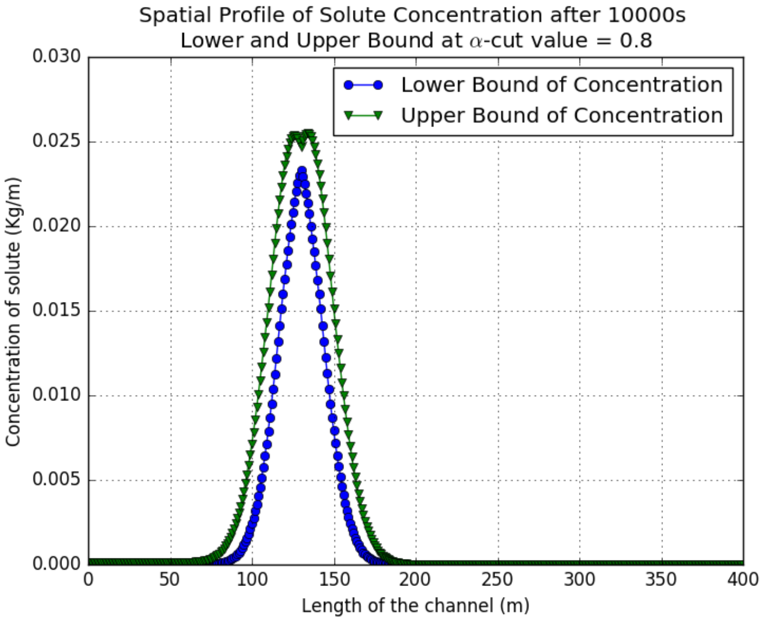

Figure 4.19: Lower and upper bound of spatial profiles at α-cut=0.8

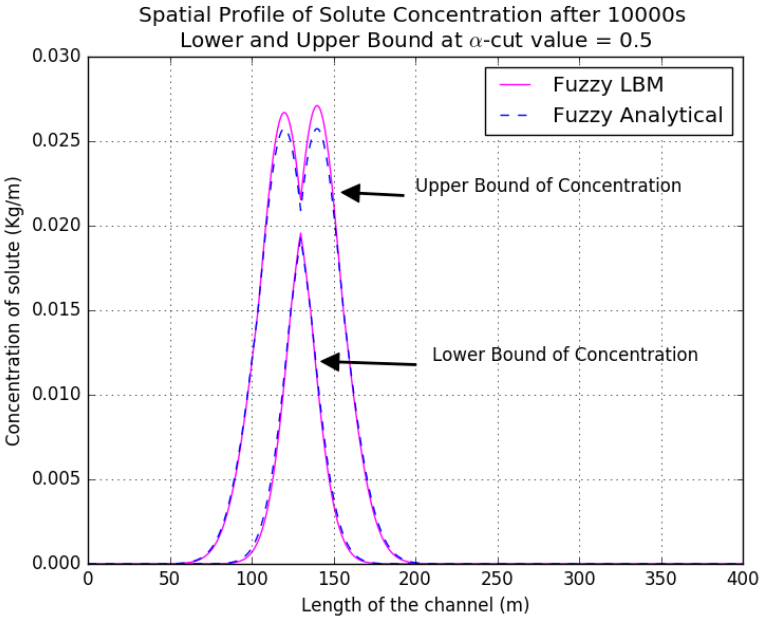

Figure 4.20: Comparison between fuzzy LBM and fuzzy analytical based uncertainty at α-cut=0.5

4.6.3 Two dimension solute transport using Fuzzy DQ Method

Problem statement

This problem considers a continuous line source at $x = 0$ and $y = 0$ in a uniform flow field for an infinite aquifer. The line source releases a nonreactive solute at a rate of C_0 ($mg.L^{-2}$). The two dimensional model computes the concentration of a dissolved chemical species (contaminant) in the aquifer at any time and at any specified distance from the point of release of the chemical. Measured parameters associated with the present model are x-directional groundwater velocity (u_x, longitudinal dispersivity (ϵ_L), and transverse dispersivity (ϵ_T) and these parameters are considered as fuzzy numbers due to the insufficiency (inadequate repetition of experiments) in their measured values. Similar to the one dimensional problems all the three fuzzy parameters are represented here as triangular fuzzy number. The governing equation of two-dimension solute transport in saturated porous media is a two-dimensional ADE, which can written as

$$\frac{\partial \widetilde{C}}{\partial t} = \widetilde{D_L}\frac{\partial^2 \widetilde{C}}{\partial x^2} + \widetilde{D_T}\frac{\partial^2 \widetilde{C}}{\partial y^2} - \widetilde{u_x}\frac{\partial \widetilde{C}}{\partial x} \tag{4.51}$$

where D_L and D_T are longitudinal and transverse dispersion coefficient($m^2.day^{-1}$), respectively. The longitudinal and transverse dispersion coefficients by definition are given by $D_L = \epsilon_L u_x$ and $D_T = \epsilon_T u_x$, respectively. The tilde sign,$\widetilde{}$ signifies that corresponding quantity is a fuzzy variable. Initial condition of the solute transport problem can be written as

$$C(x, y, t = 0) = 0, \quad \text{for } x \geq 0 \text{ and } y \geq 0 \tag{4.52}$$

Boundary conditions of the solute transport problem are

$$\begin{aligned} &C(x = 0, y = 0, t) = C_0 \\ &C(x = \infty, y, t) = 0 \\ &C(x, y = \pm\infty, t) = 0 \end{aligned} \tag{4.53}$$

Fuzzy differential quadrature solution

To solve the Eq. (4.51), we first write down its α-cut representation as

$$\frac{\partial C_\alpha}{\partial t} = D_{L\alpha}\frac{\partial^2 C_\alpha}{\partial x^2} + D_{T\alpha}\frac{\partial^2 C_\alpha}{\partial y^2} - u_{x\alpha}\frac{\partial C_\alpha}{\partial x} \tag{4.54}$$

Using DQM we can write the first and second order derivatives of C_α with respect to x and y coordinates as

$$\begin{aligned}
\frac{\partial C_\alpha}{\partial x}\,|_{x=x_i} &= \sum_{m=1}^{N_x} X_{im}^{(1)} C_{mj\alpha} \\
\frac{\partial C_\alpha}{\partial y}\,|_{y=y_j} &= \sum_{m=1}^{N_y} Y_{jm}^{(1)} C_{im\alpha} \\
\frac{\partial^2 C_\alpha}{\partial x^2}\,|_{x=x_i} &= \sum_{m=1}^{N_x} X_{im}^{(2)} C_{mj\alpha} \\
\frac{\partial^2 C_\alpha}{\partial y^2}\,|_{y=y_j} &= \sum_{m=1}^{N_y} Y_{jm}^{(2)} C_{im\alpha}
\end{aligned} \tag{4.55}$$

where $x_i,$ and y_j are the discrete nodes in the domain at which function values are known, C_{ij} are the concentrations values at these nodes at time t, N_x and N_y are the total number of grid points along x and y directions, respectively. $X^{(2)}$ and $Y^{(2)}$ are the weighting matrix for the second order derivative along x and y directions, respectively, $X^{(1)}$ and $Y^{(1)}$ are the corresponding weight matrices for the first order derivatives. Now substituting the above formulations into Eq. (4.54) and taking finite difference discretization of the temporal derivatives we get

$$C_{ij\alpha}^{s+1} = C_{ij\alpha}^{s} + \Delta t\left(D_{L\alpha}\sum_{m=1}^{N_x} X_{im}^{(2)} C_{mj\alpha}^{s} + D_{T\alpha}\sum_{m=1}^{N_y} Y_{jm}^{(2)} C_{im\alpha}^{s} - u_{x\alpha}\sum_{m=1}^{N_x} X_{im}^{(1)} C_{mj\alpha}^{s}\right) \tag{4.56}$$

where Δt is the time step. Input parameters used in the simulation are longitudinal dispersivity, transverse dispersivity and groundwater velocity. The input values of all the fuzzy parameters (imprecise or uncertain) used for uncertainty analysis are quoted from [Dou et al., 1997] as

Table 4.5: Input Fuzzy parameters for 2D Problem

Parameters	Lower Bound	Most Likely	Upper Bound
Longitudinal dispersivity, ϵ_L (m)	100	200	300
Transverse dispersivity, ϵ_T (m)	20	40	60
Velocity of flow (m/day)	0.3	0.6	1.0

benchmark. List of input fuzzy parameters is as shown in Table 4.5.

From the membership functions of the fuzzy input parameters (u_x, ϵ_L, and ϵ_T) membership function of the longitudinal and transverse diffusion coefficients (D_L and D_T) are constructed using fuzzy vertex method) on the product of longitudinal and transverse dispersivity and velocity of flow. Equal number of spatial grid point along x and y directions are considered. Spatial domain length along x (1500 m) and y(900 m) direction, number of spatial grid points (11), total time of simulation (1000 $days$) and number of temporal grid points (1000) are used for numerical simulation of fuzzy concentration of the solute. Solute concentration at x = 0 m, y = 0 m for any time $t > 0$ is taken as $C_0 = 1\ mg.l^{-1}$. Solute concentration plume at time t = 1000 $days$ are calculated at different α-cut level. Upper and lower bound of the solute plume at α-cut =0.0 are shown in Figures 4.21 and 4.22, respectively. These two contaminant plumes are of different shapes. The upper bound plume has migrated a much larger extent than the lower bound plume.

Validation and verification

Validation and verification of the fuzzy DQM scheme is carried out by comparing the results of fuzzy DQM with closed form analytical solution. The steady state analytical solution of the model described can be written as [Sayre, 1973]

$$C(x,y) = \frac{C_0}{4\pi t\sqrt{D_L D_T}} \times exp\left(\frac{ux}{2D_L}\right) K_0 \left[\frac{u}{\sqrt{4D_L}}\sqrt{\frac{x^2}{D_L} + \frac{y^2}{D_T}}\right] \tag{4.57}$$

where $K_0\,[\,]$ is the zero order modified Bessel function of the second kind.

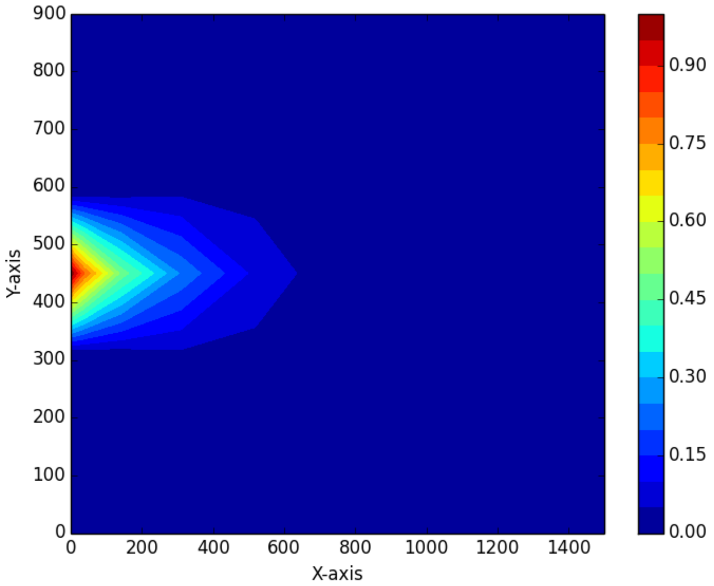

Figure 4.21: Lower bound (α-cut=0.0) of solute plume after 1000 days

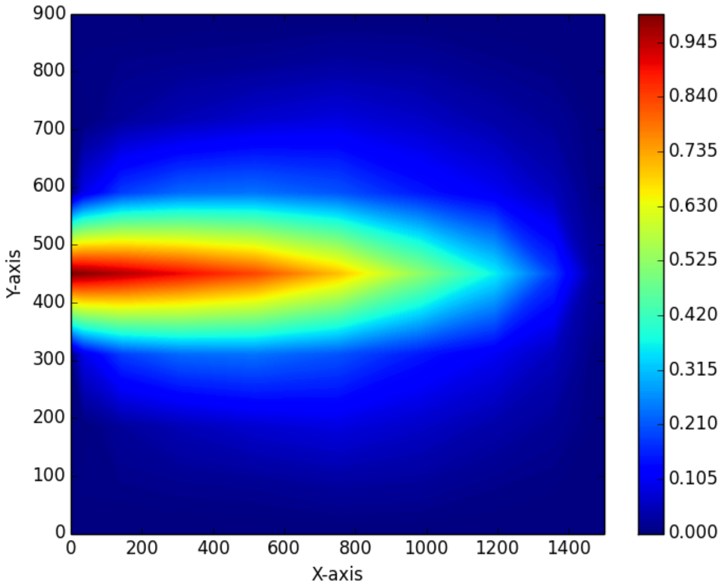

Figure 4.22: Upper bound (α-cut=0.0) of solute plume after 1000 days

4.7 Summary

In this chapter, we have enhanced the scope of LBM and DQM by developing two new numerical schemes for solving solute transport equation in presence of imprecise parameters. The developed schemes have been utilized for modeling uncertainty analysis of solute transport process.

On the onset of this chapter, we have reviewed the basics of fuzzy set theory and fuzzy logic, which are required for epistemic uncertainty analysis using fuzzy logic. Then we have mathematically modeled the solute transport process in presence of imprecise model parameters, such as groundwater velocity and dispersion coefficient. We have developed two new numerical schemes, called fuzzy lattice Boltzmann method and fuzzy differential quadrature method for the fuzzy solute transport model. The developed schemes have been verified and validated by modeling uncertainty analysis of two standard one-dimensional and one two-dimensional benchmark problems. Using the developed schemes membership functions of solute concentrations are constructed using fuzzy vertex method.

Chapter 5

Summary and Conclusions

In this final chapter, the work carried out on the study is summarized and based on the results obtained conclusions of this study is drawn. This chapter also covers the outline of future work proposal that can be taken up in continuation of this research work.

5.1 Summary of this thesis work

In this thesis numerical simulation of solute transport and multi-component reactive transport in presence of both precise and imprecise model parameters have been carried out using two relatively new and advanced numerical techniques called LBM and DQM. The work carried out in this thesis is divided into three parts: (i) Development of LBM and DQM based computer algorithms for solute transport, which is mathematically governed by ADE, (ii) Development of an interfaced algorithm that can assist to utilize the capabilities of commercial geochemical software (PHREEQC) in LBM based solute transport solver for multi-component and long term reactive transport, which is mathematically modeled as ADRE, and (iii) Modeling uncertainty in solute transport model output when the parameter of ADE are imprecise. The work carried out in this thesis are summarized in the following paragraph.

In the first chapter, highlighted the importance of nuclear energy as an indispensable option for long term energy security in under-developing countries, especially in India. India's vast thorium resources and well developed nuclear technology together with requirement for clean energy sources are supposed to boost up nuclear energy share in the country's total energy production. One of the biggest challenge that the nuclear industry facing today is long term management of long lived fission products and actinides generated in the nuclear fuel cycle. Among the various options available for isolating these radionuclides from the environment for a long period of time, scientific community has more consensus on disposal of them in DGR. In India HLLW are generated during the reprocessing of spent fuels in reprocessing plants. These HLLW are vitrified into borosilicate glass in SS canisters, which are at present under cooling and surveillance in interim storage facilities. Research and development works towards setting up of DGR is an ongoing activity in India. For obtaining licenses from regularity authorities for the construction of DGR, waste management authorities need to assess the radiological safety of the DGR and quantify risk associated with this activity on waste disposal. Biggest challenge of this safety assessment is due to involvement of very long time period and spatial heterogeneity of the host rock. This safety assessment work need to predict the time evolution of various components of the multi-barrier DGR system and spatio-temporal spreading of the leached out radionuclides. In this aspect multi-component reactive transport models are indispensable tools. These reactive transport models are capable to simulate the migration of radionuclides in presence of various physico-chemical processes, such as advection, dispersion, geochemical interactions. Simulation of these kind of reactive transport demands for huge computational resources in terms of computer memory and speed of computation because the dissolved radionuclides stay in the liquid phase in a multi-species form and these species are involved with various homogeneous and heterogeneous geochemical interactions. Though traditional numerical techniques (FDM, FEM, FVM) are successfully used for this purpose, communication overload in their parallel algorithm has always attracted researchers for development of new numerical scheme that can harness the modern day parallel computational resources. LBM being a parallel algorithm has already been used for this purpose. Another numerical technique called DQM has some important characteristics, such as requirement of very few grid points to numerically solve a PDE. In this thesis LBM and DQM are used as numerical frameworks. In brief, we have highlighted the need for fast algorithms for simulation of multi-component reactive transport in parallel context and provided an exhaustive survey of literatures on the similar field. Research gap areas and strategy of the present work are also highlighted in the first chapter.

In the second chapter, numerical framework for solute transport using LBM and DQM are formulated. Though TRT and MRT schemes of LBM provide more stable solution, we have used SRT scheme of LBM because it's algorithm is simpler than the other two. For the sake of completeness of this thesis work, we have first derived LBE from the the continuous Boltzmann equation, derived equilibrium distribution function for ADE from Maxwell-Boltzmann distribution function, discussed on various lattices generally used in LBM. The ADE is then derived from LBE using Chapman-Enskog multi-scale analysis technique. By doing this derivation, relation between lattice Boltzmann diffusion coefficient and relaxation parameter is established. Mathematical preliminaries required for DQM are provided. The developed LBM and DQM based solvers for ADE are then validated by solving benchmark problems and LBM based solute transport solver is then further utilized in the third chapter for development of multi-component reactive transport.

In the third chapter, mathematical formulation of multi-component reactive transport and numerical schemes based on LBM are formulated. In the mathematical formulation, two type of approaches such as sorption isotherm based and geochemical reaction based to model the reaction terms are elaborated. Various isotherms, such as linear, Freundlich and Langmuir, are discussed and multi-component reactive transport model equations are formulated using linear isotherm also known as Kd approach. Limitation of these isotherm based models and need for consideration of geochemical reaction models are highlighted. Since dissolved radionuclides generally stay in liquid phase in various species form and these species take part in different geochemical reactions, general equation for reactive transport is formulated considering all the species. To reduce the number of species for which the reactive transport equation need to be solved, the multi-species reactive transport equations are then written in terms of total concentration of primary species. The resulting equation is called multi-component reactive transport equation, which is also known as ADREs when transport due to charge imbalance is neglected. In order to solve these equations we have adopted SIA. In this approach, transport and reaction terms are treated separately. We have interfaced the LBM based multi-component transport solver, developed in the previous chapter, with geochemical software, PHREEQC. Both the two version of PHREEQC known as IPhreeqc and PhreeqcRM, which were developed in order to be used as commercial modules for a client program, have been successfully interfaced with our LBM based solver for multi-component ADE. The coupling algorithm is then tested by solving benchmark problems.

In the fourth chapter, LBM and DQM based numerical schemes are developed to solve solute transport equation with imprecise model parameters. Uncertainty analysis of solute transport model output is important for modeling safety analysis of DGR. In chapter two and three, the models parameter of ADE were taken as crisp values, which represent a homogeneous media. But, in nature the rock mass through which migration of radionuclides takes place are highly heterogeneous. To deal with spatial heterogeneity stochastic solute transport models are generally used, where the solute transport model parameters are taken as random parameters. The randomness of the model parameters are represented by a probability distribution function and the corresponding solute transport model output is represented by statistical parameter, such as mean and standard deviation, which is treated as a spread in the model output. This kind of uncertainty analysis is known as aleatory uncertainty analysis. The success of aleatory uncertainty analysis totally depends on how accurately we can represent the experimental data with a distribution function. This task of representing experimental data with some distribution requires huge data volume, but in practice we generally ends up with very few numbers of data because experimental cost for generation of data at field is very big. This type of small data set is called imprecise data set and corresponding uncertainty in the model output is called epistemic uncertainty. Fuzzy set theory is used to quantify epistemic uncertainty. The solute transport model parameters, dispersion coefficient and groundwater velocity, are experimentally measured at field and generally possess epistemic behavior. We have represented these imprecise model parameters by triangular fuzzy numbers because, most likely value (measured mean) of these parameters are circumvented by the corresponding boundaries (left and right bounds) as mean ± error. Numerical uncertainty analysis is a time consuming task because, the model simulator need to be run several times. There are very few studies on uncertainty estimation using numerical techniques. Dou et al. used FDM for solving fuzzy ADE [Dou et al., 1997]. In this study we have developed LBM and DQM based numerical scheme using fuzzy vertex method to solve the ADE with triangular input parameters. The predicted solute concentration is presented as intervals at various α-cuts. The stability of the newly developed methodology of uncertainty modeling was assessed by comparing the numerical solution with possible analytical solution.

5.2 Conclusions of this study

The study carried out in this thesis has shown that LBM based numerical solution of solute transport equation gives accurate results as comparison with analytical solutions. The scheme is unconditionally stable when the simulation is carried out using lattice units and the conversion between the lattice unit and physical unit is very straightforward. The comparative study between LBM and explicit FDM shows that LBM based solutions are more accurate than explicit FDM based results for the same time step value. This result can be interpreted in other way as for the same accuracy LBM based calculations are more faster than explicit FDM based calculations. More faster calculation is achieved by utilizing its parallelization capabilities. The developed parallel LBM solvers for solute transport were run in supercomputing facility with 64 processors. The developed interfaced algorithm is capable of simulating kinetically controlled reactions in a repository environment. The scope of the interfaced numerical scheme for solving multi-component reactive transport is enhanced by utilizing the modeling capabilities of PHREEQC software within LBM framework. Therefore, it can be utilized to simulate complicated geochemical reactions that are expected to occur in DGR. DQM based solution of ADE shows that accurate results can be obtained with very few number of non-linear grid points (in this study 11 grid points). The developed LBM and DQM based numerical schemes for solving fuzzy solute transport model are named as fuzzy lattice Boltzmann method (FLBM) and fuzzy differential quadrature method (FDQM). In these schemes, LBM and DQM are basically amalgamated with fuzzy vertex theory of incorporating fuzziness of the fuzzy parameters in the model of interest for uncertainty analysis. Using the FLBM and FDQM schemes the membership function of the solute concentration at a particular spatio-temporal coordinate is constructed. This kind of calculation facilitates the decision makers to specify the uncertainty band of the solute concentration. The calculated lower and upper bounds of spatial and temporal profiles of solute concentration at any specific α-cut are compared with the corresponding analytical solution of the solute concentration at the same α-cut level and good agreement between the two results is established. Since FDQM requires very small number of grid points (in this study 11 grid points) for numerical simulation to be carried out, it requires much less computational time and memory for storage. This property of DQM makes it computationally efficient technique. Therefore, DQM can readily be used as numerical tool for computationally intensive calculations, such as regression analysis, correlation analysis, uncertainty analysis.

Finally, it is worth to mention here that although this development work for fast algorithms for multi-component and long term reactive transport is a small step towards simulating the complex processes that are expected to occur in DGR, nonetheless the developed FLBM and FDQM schemes scoped two new technique of uncertainty analysis of fluid dynamic system.

5.3 Outline of future work proposal

In the following, we draw the outline of future work proposal that can be taken up in continuation to the thesis investigations.

- Update in geometry due to dissolution/precipitation reactions is not considered in this study. This study will help to simulate dynamic change in hydrogeological parameters, such as porosity, permeability.
- The developed solute transport and multi-component reactive transport solvers are based on SRT scheme of LBM. Similar development with TRT and MRT LBM schemes will have more scope for simulating anisotropic dispersion and will be more stable than the current scheme. Therefore, future efforts can be attempted towards these developmental aspects.
- The various schemes developed in this thesis are validated by comparing their solutions

with closed form analytical solutions, which are generally available for simple problems. Therefore, efforts need to be given for solving problems with complex geochemical interactions and validation of the results by simulating the same problem with commercial FEM based softwares.

- DQM has not been used in this thesis for multi-component reactive transport simulation. Since DQM requires much less computational time and memory for storage, it will be an efficient solver for multi-component reactive transport if the coupling between DQM based solute transport and commercial geochemical software is established.
- Uncertainty modeling of multi-component reactive transport with imprecise parameters involved with the reaction term, such as reactive surface area and K_d values will have more impact on the design of various component of DGR.
- Finally, setting up of laboratory or field scale based experiments on multi-component reactive transport and simulation of the same with the developed schemes will have more weight on validation.

Appendix I

Development of supporting graphical user interface tool

All the simulation works carried out in this thesis are done using our in-house developed graphical user interface tool (GUI). The tool is developed during this research period using a mixed computer programming language language (Python and Fortran). It is well known that computation speed is faster in Fortran language than in Python. The development of F2Py module in Python has made it easier to develop client program in Python that can easily interact with server programs developed in other programming language [Peterson, 2009]. The Fortran files for solute transport modules for different type of problems (solute transport, reactive transport using LBM and uncertainty modeling using fuzzy LBM) solved in this research are compiled using F2Py tool and the generated object files are linked with one Python program that create the GUI framework. The screen-shots of the developed GUI after the simulation run for uncertainty analysis are shown in Figures 5.1 and 5.2. At present the tool can simulate one-dimensional and two-dimension problems using D1Q2, D1Q3, D2Q4 and D2Q5 lattices. The python script file is further converted to a portable source file that can run in different platforms without any Python source file installation.

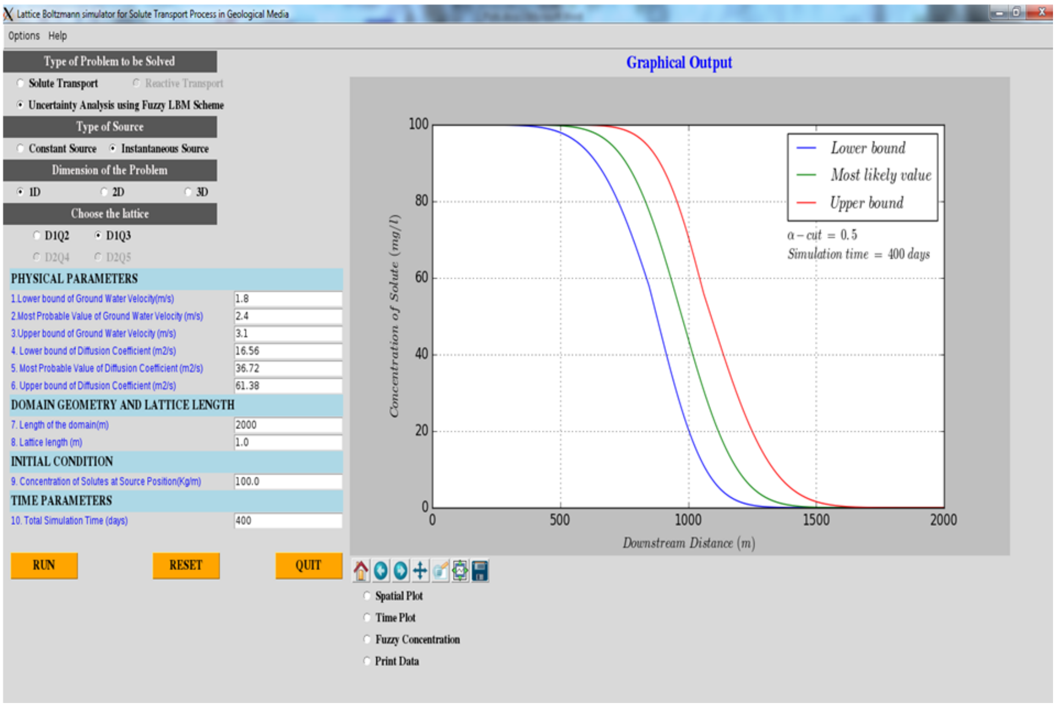

Type of Problem to be Solved
○ Solute Transport ○ Reactive Transport
● Uncertainty Analysis using Fuzzy LBM Scheme

Type of Source
○ Constant Source ● Instantaneous Source

Dimension of the Problem
● 1D ○ 2D ○ 3D

Choose the lattice
○ D1Q2 ● D1Q3
○ D2Q4 ○ D2Q5

PHYSICAL PARAMETERS
1.Lower bound of Ground Water Velocity(m/s): 1.8
2.Most Probable Value of Ground Water Velocity (m/s): 2.4
3.Upper bound of Ground Water Velocity (m/s): 3.1
4. Lower bound of Diffusion Coefficient (m2/s): 16.56
5. Most Probable Value of Diffusion Coefficient (m2/s): 36.72
6. Upper bound of Diffusion Coefficient (m2/s): 61.38

DOMAIN GEOMETRY AND LATTICE LENGTH
7. Length of the domain(m): 2000
8. Lattice length (m): 1.0

INITIAL CONDITION
9. Concentration of Solutes at Source Position(Kg/m): 100.0

TIME PARAMETERS
10. Total Simulation Time (days): 400

○ Spatial Plot
○ Time Plot
○ Fuzzy Concentration
○ Print Data

Figure 5.1: Screen-shot of the GUI showing fuzzy spatial profile of solute concentration using D1Q3 lattice

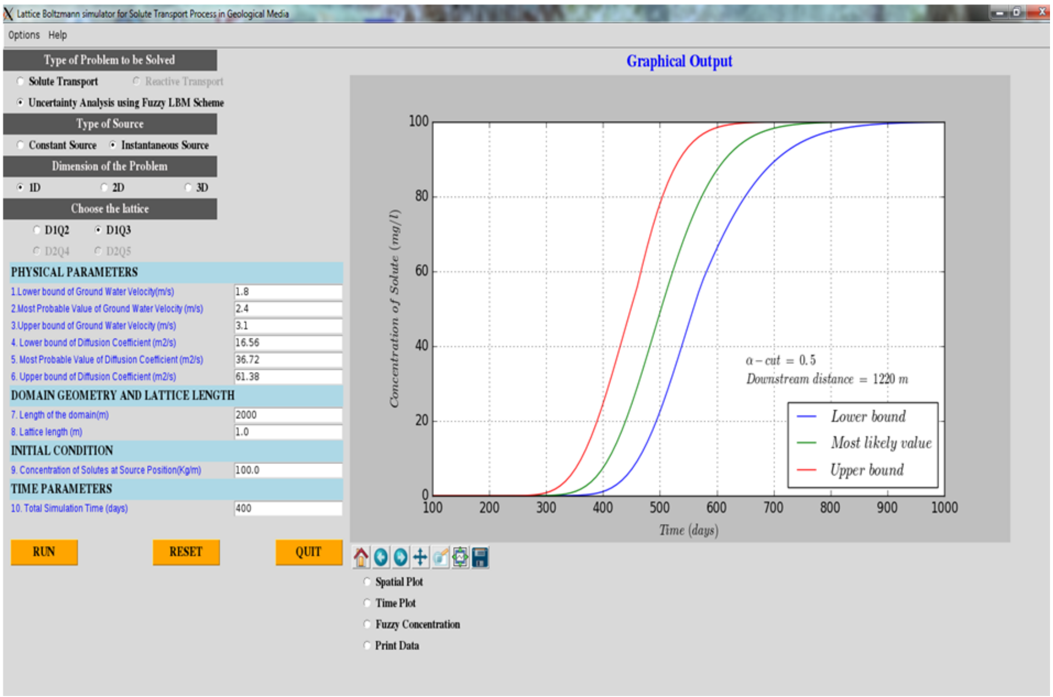

Type of Problem to be Solved
○ Solute Transport ○ Reactive Transport
● Uncertainty Analysis using Fuzzy LBM Scheme

Type of Source
○ Constant Source ● Instantaneous Source

Dimension of the Problem
● 1D ○ 2D ○ 3D

Choose the lattice
○ D1Q2 ● D1Q3
○ D2Q4 ○ D2Q5

PHYSICAL PARAMETERS
1.Lower bound of Ground Water Velocity(m/s): 1.8
2.Most Probable Value of Ground Water Velocity (m/s): 2.4
3.Upper bound of Ground Water Velocity (m/s): 3.1
4. Lower bound of Diffusion Coefficient (m2/s): 16.56
5. Most Probable Value of Diffusion Coefficient (m2/s): 36.72
6. Upper bound of Diffusion Coefficient (m2/s): 61.38

DOMAIN GEOMETRY AND LATTICE LENGTH
7. Length of the domain(m): 2000
8. Lattice length (m): 1.0

INITIAL CONDITION
9. Concentration of Solutes at Source Position(Kg/m): 100.0

TIME PARAMETERS
10. Total Simulation Time (days): 400

○ Spatial Plot
○ Time Plot
○ Fuzzy Concentration
○ Print Data

Figure 5.2: Screen-shot of the GUI showing fuzzy temporal profile of solute concentration using D1Q3 lattice

Appendix II

Development of parallel lattice Boltzmann program

The parallelization capability of lattice Boltzmann algorithm method is explored by converting in-house developed serial programs for solute transport written in Fortran programming language into parallel versions using domain decomposition technique [Wang et al., 2005]. Parallel programs are run on both shared memory and distributed memory platform. Using Intel G1 quad-core processor 2 times reduction in computing time for a given benchmark problem (benchmark problem given in Section 2.4.1 is parallelized in this study) is obtained for OpenMP based parallel program. The MPI based parallel version of the program is tested in Anupam supercomputing facility using 64 processors and up to 10 times reduction in computing time is achieved. Parallel implementation of the reactive transport code using PhreeqcRM module of PHREEQC is an ongoing activity.

Bibliography

Albuquerque, P., Alemani, D., Chopard, B., Leone, P. (2004, June) *Coupling a lattice Boltzmann and a finite difference scheme*, In International Conference on Computational Science (pp. 540-547). Springer, Berlin, Heidelberg.

Arumugham, V. (1994) *Site Characterization for Location of Radioactive Waste Repository-a Case Study*, Ph.D thesis, Indian Institute of Technology, Bombay, India.

Aswin V.S., Awasthi A., Anu C. (2015) *A Comparative Study of Numerical Schemes for Convection-diffusion Equation*, Procedia Engineering, 127, 621-627.

Ayyub, B.M., Klir, J.G. (2006) *Uncertainty Modelling and Analysis in Engineering and the Sciences*, first ed., Chapman and Hall/CRC Press, Boca Ratan.

Bajpai, R.K., Narayan, P.K. (2008) *Role of earth sciences in deep geological disposal of radioactive wastes*, Journal of Applied geochemistry, 10(2A), 481-499.

Banerjee S., Gupta H. C. (2017) *The evolution of the Indian nuclear power programme*, Prog. Nucl. Energy, 101, 4-18.

Baraldi, P., Zio, E. (2010) *A comparison between probabilistic and Dempster-Shafer theory approaches to model uncertainty analysis in the performance assessment of radioactive waste repositories*, Risk Analysis, 30, 1139-1156.

Bauer, P., Attinger S., Kinzelbach, W. (2001) *Transport of a decay chain in homogenous porous media: analytical solutions*, J Contam Hydrol, 49, 217-239.

Bea, S.A., Mayer, K.U., MacQuarrie, K.T.B. (2011) *Modelling reactive transport in sedimentary rock environments - Phase II MIN3P-THCm code enhancements and illustrative simulations for a glaciation scenario*, Technical report: NWMO TR-2011-13.

Bear, J. (1972) *Dynamics of Fluids in Porous Media*, Dover Publications Inc., New York.

Bellman, R., Casti, J. (1971) *Differential quadrature and long-term integration*, Journal of Mathematical Analysis and Applications, 34, 235-238.

Bellman, R., Kashef, B.G., Casti, J. (1972) *Differential quadrature: a technique for the rapid solution of nonlinear partial differential equations*, J Comput Phys, 10, 40-52.

Berner, U. (1992) *Evolution of pore water chemistry during degradation of cement in a radioactive waste repository environment*, Waste Management and the Nuclear Fuel Cycle, 12, 201-219.

Bert, C.W., Malik, M. (1996) *Differential quadrature method in computational mechanics: a review*, Applied Mechanics Reviews, 49, 1-28.

Bethke, C.M. (1996) *Geochemical Reaction Modeling*, Oxford Univ. Press, New York.

Bethke, C.M. (2000) *How the K-d approach undermines ground water cleanup*, Ground Water, 38, 435-443.

Bhatnagar, P., Gross, E.P., Krook, M.K. (1954) *A model for collision processes in gases: I. Small amplitude processes in charged and neutral one-component system*, Phys. Rev., 94. 511-525.

Brady, P.V., Bethke, C.M. (2000) *Beyond the K-d approach*, Ground Water, 38, 321-322.

Bultreys, T., De Boever, W., Cnudde, V. (2016) *Imaging and image-based fluid transport modeling at the pore scale in geological materials: a practical introduction to the current state-of-the-art*, Earth-Sci. Rev., 155, 93-128.

Burkholder, H.C., Rosinger, E.L.J. (1980) *A model for the transport of radionuclides and their decay products through geologic media*, Nucl. Technol., 49, 150-158.

Carrayrou, J., Mos, R., Behra, P. (2004) *Operator-splitting procedures for reactive transport and comparison of mass balance errors*, Journal of Contaminant Hydrology, 68, 239-268.

Chapmann N.A., McKinley I.G. (1987) *The Geological Disposal of Nuclear Waste*, John Wiley and Sons.

Chapman, S., Cowling, T.G. (1991) *The mathematical theory of non-uniform gases: an account of the kinetic theory of viscosity, thermal conduction and diffusion in gases.* Cambridge university press.

Chapmann N., Hooper A. (2012) *The disposal of radioactive wastes underground*,Proc. Geol. Assoc., 123, 46-63.

Charlton, S.R., Parkhurst, D.L. (2011) *Modules based on the geochemical model PHREEQC for use in scripting and programming languages*, Comput. Geosci., 37, 1653-1663.

Chen, H., Chen, S., Matthaeus, W.H. (1992) *Recovery of the NavierStokes equations using a lattice-gas Boltzmann method*, Phys. Rev. A, 45 (8), R5339-R5342

Chen, S., Dawson, S.P., Doolen, G., Jenecky, D., Lawiczak, A.T. (1995) *Lattice methods for chemically reacting systems*, Comput. Chem. Eng., 19, 617-646

Chen, S., Doolen, G.D. (1998) *Lattice Boltzmann method for fluid flows*, Annu. Rev. Fluids Mech., 30, 329-364.

Cheng, J., Wang, B., Du, S. (2005) *A theoretical analysis of piezoelectric/composite laminate with largeramplitude deflection effect, Part II: hermite differential quadrature method and application*, International Journal of Solids and Structures, 42 (24-25), 6166-6180.

Chen, L., Luan, H., Feng, Y., Song, C., He, Y. L., Tao, W. Q. (2012) *Coupling between finite volume method and lattice Boltzmann method and its application to fluid flow and mass transport in proton exchange membrane fuel cell*, Int. J. Heat Mass Tran., 55(13-14), 3834-3848.

Chen, L., He, Y. L., Kang, Q., Tao, W. Q. (2013) *Coupled numerical approach combining finite volume and lattice Boltzmann methods for multi-scale multi-physicochemical processes*, J. Comp. Phys., 255, 83-105.

Chen, L., Kang, Q., Carey, B., Tao, W.-Q. (2014) *Pore-scale study of diffusion-reaction processes involving dissolution and precipitation using the lattice Boltzmann method*, Int. J. Heat Mass Tran., 75, 483-496

Chen, L., Kang, Q., Tang, Q., Robinson, B. A., He, Y. L., Tao, W. Q. (2015) *Pore-scale simulation of multicomponent multiphase reactive transport with dissolution and precipitation*, Int. J. Heat Mass Tran., 85, 935-949.

Chen, L., Zhang, R., Min, T., Kang, Q., Tao, W. (2018a)*Pore-scale study of effects of macroscopic pores and their distributions on reactive transport in hierarchical porous media*, Chemical Engineering Journal, 349, 428-437.

Chen, L., Wang, M., Kang, Q., Tao, W. (2018b) *Pore scale study of multiphase multicomponent reactive transport during CO2 dissolution trapping*, Advances in Water Resources, 116, 208-218.

Chopard, B., Droz, M. (1998) *Cellular automata modeling of physical systems*, Cambridge University Press, Cambridge, UK.

Civan, F., Sliepcevich, C.M. (1983) *Application of differential quadrature to transport process*, J. Math. Anal. Appl., 93, 206-221.

COCHEPIN, B. (2014) *Benchmark example 1: kinetic dissolution/precipitation coupled with 1D diffusive transport*, Draft report received from ANDRA, France.

Datta, D. (2011) *Non-Probabilistic Uncertainty Analysis of Analytical and Numerical Solution* *of Heat Conduction*, International Journal of Energy, Information and Communications, 2 (4), 143-156.

Datta, D. (2014) *Mathematics of Probabilistic Uncertainty Modeling*, in Chakraverty, S. (ed.) Mathematics of Uncertainty Modeling in the Analysis of Engineering and Science Problems, IGI Global, Hershey PA, vol. IV, 173-204.

Datta, D., Pal, T.K. (2016a) *Address of Geo-hydrological Problem using Lattice Boltzmann and Differential Quadrature Methods*, International Journal of Life Cycle Reliability and Safety Engineering, 5(2), 16-20.

Datta, D., Pal, T.K. (2016b) *Numerical Solution of Solute Transport Model Using Cellular Automata*, Global Journal of Pure and Applied Mathematics, 12(1), 131-135.

Datta, D., Pal, T.K. (2017) *Development of Fuzzy Differential Quadrature Numerical Method and its Application for Uncertainty Quantification of Solute Transport Model*, International Journal of Energy, Information and Communications, 8(5), 1-12.

Datta, D., Pal, T.K. (2018a) *Modeling Advection and Anisotropic Dispersion of Radionuclides through Geological Media Using Diffusion Velocity Lattice Boltzmann Scheme*, SciFed Journal of Nuclear Science, 2, 1-9.

Datta, D., Pal, T.K. (2018b) *A Lattice Boltzmann Scheme for Diffusion Equation in Spherical Coordinate*, International Journal of Mathematics and Systems Science, 2018, Accepted.

Dawson, S.P., Chen, S., Doolen, G.D. (1993) *Lattice Boltzmann computations for reaction diffusion equations*, J. Chem. Phys., 98, 1514-1523

de Dieuleveult, C., Erhel, J., Kern, M. (2009a) *A global strategy for solving reactive transport equations*, J. Comput. Phys., 228(17), 6395-6410.

de Dieuleveult, C., Erhel, J. (2009b) *A global approach to reactive transport: application to the MoMaS benchmark*, Comput. Geosci., 14(3), 451-464.

De Simoni, M., Carrera, J., Sanchez-Vila, X., Guadagnini, A. (2005) *A procedure for the solution of multicomponent reactive transport problems*, Water Resour. Res., 41(11), W11410.

Dong W., Shah H. (1987) *Vertex method for computing functions of fuzzy variables*, Fuzzy Sets Syst., 24 (1), 65-78.

Dou, C., Woldt, W., Bogardi, I., Dahab, M. (1995) *Steady-state groundwater flow simulation with imprecise parameters*, Water Resource Res., 31 (11), 2709-2719.

Dou, C., Woldt, W., Bogardi, I., Dahab, M. (1997) *Numerical solute transport simulation using fuzzy sets approach*, Journal of contaminant hydrology, 27, 107-126.

Du, H., Lim, M.K., Lin, R.M (1995) *Application of generalized differential quadrature method to vibration analysis*, J. Sound Vib., 181(2), 279-293.

Du, H., Liew, K.M., Lim, M.K. (1996) *Generalized differential quadrature method for buckling analysis*, J. Eng. Mech. ASCE, 22(2), 95-100

Fazeli, H., Patel, R., Hellevang, H. (2018) *Effect of Pore-Scale Mineral Spatial Heterogeneity on Chemically Induced Alterations of Fractured Rock: A Lattice Boltzmann Study*, Geofluids, Article ID 6046182. . .

Ferson S., Ginzburg L.R. (1996) *Different methods are needed to propagate ignorance and variability*, Reliability Eng System Saf, 54, 133-144.

Flekky, E.G. (1993) *Lattice Bhatnagar-Gross-Krook models for miscible fluids*, Phys. Rev. E, 47, 4247-4257

Frisch, U., Hasslacher, B., Pomeau, Y. (1986) *Lattice-gas automata for the NavierStokes equation*,Phys. Rev. Lett., 56 (14), 1505-1508.

Gao, J., Xing, H., Rudolph, V., Li, Q., Golding, S.D. (2015) *Parallel lattice Boltzmann computing and applications in core sample feature evaluation*, Transp. Porous Media, 107(1), 65-77.

Gao, J., Xing, H., Tian, Z., Pearce, J.K., Sedek, M., Golding, S.D., Rudolph, V. (2017) *Reactive transport in porous media for CO2 sequestration: pore scale modeling using the lattice Boltzmann method*, Comput. Geosci., 98, 9-20.

Gaucher, E.C., Blanc, P., Matray, J.M., Michau, N. (2004) *Modeling diffusion of an alkaline plume in a clay barrier*. Appl. Geochem. 19(10), 1505-1515.

Gaucher, E.C., Blanc, P. (2006) *Cement/clay interactions - a review: experiments, natural analogues, and modeling*, Waste Manag. 26 (7), 776-788.

Ginzburg, I. (2005) *Equilibrium-type and link-type lattice Boltzmann models for generic advection and anisotropic-dispersion equation*, Adv. Water Resour., 28, 1171-1195.

Glynn, P.D. (2003) *Modeling Np and Pu transport with a surface complexation model and spatially variant sorption capacities: implications for reactive transport modeling and performance assessments of nuclear waste disposal sites*, Comput. Geosci., (29), 331-349.

Goel, R.K., Prasad, V.V.R., Swarup, A., Dwivedi, R.D., Mohnot, J.K., Soni, A.K., Misra, D.D. (2003) *Testing of Rock Samples and Site-Specific Design of Underground Research Laboratory*, Technical Report, Central Mining Research Institute, Roorkee, India, GC/MT/R/1/2000-2001.

Grindrod, P., Takase, H. (1996) *Reactive chemical transport within engineered barriers*, J. Contam. Hydrol., 21, 283-296.

Guerrero, J.S.P., Skaggs, T.H., van Genuchten, M.Th. (2009) *Analytical solution for multi-*

species contaminant transport subject to sequential first-order decay reactions in finite media, Trans. Porous Med., 80, 373-387.

Guo, Z., Zhao, T.S., Shi, Y. (2006) *Physical symmetry, spatial accuracy, and relaxation time of the lattice Boltzmann equation for microgas flows*, J. Appl. Phys., 99, 074903.

Guo, L., Huang, H., Gaston, D., Permann, C., Andrs, D., Redden, G., Lu, C., Fox, D., Fujita, Y. (2013) *A parallel, fully coupled, fully implicit solution to reactive transport in porous media using the preconditioned Jacobian Free Newton-Krylov method*, Adv. Water Resour., 53, 101-108..

Hammond, G.E., Lichtner, P.C., Lu, C., Mills, R.T. (2010) *PFLOTRAN: reactive flow and transport code for use on laptops to leadership-class supercomputers*, In: Zhang, F., Yeh, G.T., Parker, J.C. (eds.) Ebook: Groundwater Reactive Transport Models. Bentham Science Publishers. ISBN 978-1-60805-029-1.

Hardy, J., Pomeau, Y., de Pazzi, O. (1973) *Time evolution of a two-dimensional classical lattice system*, Phys. Rev. Lett., 31, 276-279.

He, X., Luo, L.-S. (1997) *A priori derivation of the lattice Boltzmann equation*, Phys. Rev. E., 55 (6), 6333-6336.

He, X., Li, N. (2000) *Lattice Boltzmann simulation of electrochemical systems*, Comput. Phys. Commun., 129, 158-166.

Helgeson, H.C. (1968) *Evaluation of irreversible reactions in geochemical processes involving minerals and aqueous solutions: I. Thermodynamic relations*, Geochim. Cosmochim. Acta, 32, 853-877.

Helgeson, H.C. (1971) *Kinetics of mass transfer among silicates and aqueous solutions*, Geochim. Cosmochim. Acta, 35, 421-469.

Helton, J.C. (1994) *Treatment of uncertainty in performance assessments for complex systems*Risk Anal, 14, 483-511.

Henrik, C.M., Andersson-stling, Sandstrm R. (2009) *Survey of creep properties of copper intended for nuclear waste disposal*, SKB, TR-09-32.

Hernelind, J. (2010) *Modelling and analysis of canister and buffer for earthquake induced rock shear and glacial load*, SKB, TR-10-34.

Higashi, K., Pigford, T.H. (1980) *Analytical models for migration of radionuclides in geologic sorbing media*, J Nucl Sci Technol, 17(9), 700-709.

Higuera, F.J., Jimenez, J. (1989a) *Boltzmann Approach to Lattice Gas Simulations*, Europhysics Letters (EPL), 9, 663.

Higuera, F.J., Succi, S., Benzi, R. (1989b) *Lattice gas dynamics with enhanced collisions*, Europhysics Letters (EPL) 9, 345.

Hiorth, A., Jettestuen, E., Cathles, L.M., Madland, M.V. (2013) *Precipitation, dissolution, and ion exchange processes coupled with a lattice Boltzmann advection diffusion solver*, Geochim. Cosmochim. Acta, 104, 99-110.

Hoefner, M.L., Fogler, H.S. (1998) *Pore evolution and channel formation during flow and reaction in porous media*, AIChE J., 34 (1) , 45-53.

Hoffman F.O., Hammonds J.S. (1994) *Propagation of uncertainty in risk assessments: the need to distinguish between uncertainty due to lack of knowledge and uncertainty due to variability*Risk Anal, 14, 707-712.

Holdych, D. J., Noble, D. R., Georgiadis, J. G., Buckius, R. O. (2004) *Truncation error analysis of lattice Boltzmann methods*, Journal of Computational Physics, 193(2), 595-619.

Hora, S.C. (1996) *Aleatory and epistemic uncertainty in probability elicitation with an example from hazardous waste management*Reliab Eng Sys Saf, 54, 217-223.

Jacques, D., imunek, J. (2005) *User Manual of the Multicomponent Variably-Saturated Flow and Transport Model HP1, Description, Verification and Examples*, Version 1.0, SCKCEN-BLG-998, Waste and Disposal, SCKCEN, Mol, Belgium, 79.

Jang, S.K., Bert, C.W., Striz, A.G. (1989) *Application of differential quadrature to static analysis of structural components*, Int. J. Numer. Methods Eng., 28 (3), 561-577.

Jawerth, B., Lin, P., Sinzinger, E. (1999) *Lattice Boltzmann models for anisotropic diffusion of images*, J. Math. Imaging Vis., 11(13), 231-237.

Kang, Q., Zhang, D., Chen, S., He, X. (2002) *Lattice Boltzmann simulation of chemical dissolution in porous media*, Phys. Rev. E, 65, 036318.

Kang, Q., Zhang, D., Chen, S. (2003) *Simulation of dissolution and precipitation in porous media*, J. Geophys. Res., 108, 2505.

Kang, Q., Lichtner, P.C., Zhang, D. (2006) *Lattice Boltzmann pore-scale model for multicomponent reactive transport in porous media*, J. Geophys. Res. Solid Earth, 111, B05203.

Kang, Q., Lichtner, P.C., Zhang, D. (2007) *An improved lattice Boltzmann model for multicomponent reactive transport in porous media at the pore scale*, Water Resour. Res., 43, W12S14.

Kang, Q., Wang, M., Mukherjee, P.P., Lichtner, P.C. (2010a) *Mesoscopic modeling of multiphysicochemical transport phenomena in porous media*, Adv. Mech. Eng., 2, 1-11.

Kang, Q., Lichtner, P.C., Viswanathan, H.S., Abdel-Fattah, A.I. (2010b) *Pore scale modeling of reactive transport involved in geologic CO2 sequestration*, Transport Porous Med., 82(1), 197-213.

Kang, Q., Chen, L., Valocchi, A.J., Viswanathan, H.S. (2014) *Pore-scale study of dissolution-induced changes in permeability and porosity of porous media*, J. Hydrol., 517, 1049-1055.

Kaya, B. (2010) *Solution of the advection-diffusion equation using the Differential Quadrature Method*, KSCE Journal of Civil Engineering, 14, 69-75.

King, F. (2017) *Nuclear waste canister materials, corrosion behaviour and long-term performance in geological repository systems*, in Ahn, J., Apted, M.J. (Eds.), Geological Repository Systems for Safe Disposal of Spent Nuclear Fuels and Radioactive Waste (Second Edition), Elsevier, 365-408.

Kolditz, O., Bauer, S., Bilke, L., Bttcher, N., Delfs, J.O., Fischer, T., Grke, U.J., Kalbacher, T., Kosakowski, G., McDermott, C.I., Park, C.H., Radu, F., Rink, K., Shao, H., Shao, HB, Sun, F., Sun, Y.Y., Singh, A.K., Taron, J., Walther, M., Wang, W., Watanabe, N., Wu, N., Xie, M.,

Kirkner, D.J., Reeves, H. (1988) *Multicomponent mass transport with homogeneous and heterogeneous chemical reactions: Effect of chemistry on the choice of numerical algorithm I. Theory*, Water Resour. Res., 24, 1719-1729.

Krger, T., Kusumaatmaja, H., Kuzmin, A., Shardt, O., Silva, G., Viggen, E.M. (2017) *The Lattice Boltzmann Method: Principles and Practice*, Springer, Switzerland.

Kushwaha, H.S. (2009) *Uncertainty Modeling and Analysis*, Bhabha Atomic Research Centre, India.

Lasaga, A.C. (1984) *Chemical kinetics of water-rock interactions*, J. Geophys. Res. Solid Earth, 89, 4009-4025.

Lasaga, A.C., Soler J., Burch T. E., Nagy K. L. (1994) *Chemical weathering rate laws and global geochemical cycles*, Geochimica et Cosmochimica Acta, 58, 2361-2386.

Laura, P.A.A., Rossi, R.E. (1994) *The method of differential quadrature and its application to the approximate solution of ocean engineering problems*, Ocean Engng., 21, 57-66.

Ledieu, A., Devreux, F., Barboux, P., Sicard, L., Spalla, O. (2004) *Leaching of borosilicate glasses. I. Experiments*, J. Non-Cryst. Solids, 343, 3-12.

Lester, D.H., Jansen, G., Burkholder, H.C. (1974) *Migration of radionuclide chains through adsorbing media*, Battelle, Pacific Northwest Laboratories, Richland, Wasihington.

Levy, M., Berkowitz, B. (2003) *Measurement and analysis of non-Fickian dispersion in heterogeneous porous media*, J. Contam. Hydrol., 64 (34), 203-226.

Li, L., Steefel, C. I., Yang, L. (2008) *Scale dependence of mineral dissolution rates within single pores and fractures*, Geochim. Cosmochim. Acta, 72, 360-377.

Lichtner, P.C. (1985) *Continuum model for simultaneous chemical reactions and mass transport in hydrothermal systems*, Geochim. Cosmochim. Acta, 49, 779-800.

Lichtner, P. C. (1988) *The quasi-stationary state approximation to coupled mass transport and fluidrock interaction in a porous medium*, Geochim. Cosmochim. Acta, 52, 143-165.

Lichtner P. C. (1992) *Timespace continuum description of the fluid/rock interaction in permeable media*, Water Resources Research, 28, 3135-3155.

Lichtner, P. C. (1996) *Continuum formulation of multicomponent-multiphase reactive transport*, in Lichtner P.C., Steefel C.I., Oelkers E.H., (Eds.), Reactive Transport in Porous Media, Reviews in Mineralogy, 34, 1-81.

Lunn, M., Lunn, R.J., Mackay R. (1996) *Determining analytic solutions of multiple species contaminant transport, with sorption and decay*, J Hydrol, 180, 195-210.

MacQuarrie, K.T.B., Mayer, K.U. (2005) *Reactive transport modeling in fractured rock: A state-of-the-science review*, Earth-Science Reviews, 72(3-4), 189-227.

Malik, M., Civan, F. (1995) *A comparative study of differential quadrature and cubature methods vis--vis some conventional techniques in context of convection-diffusion-reaction problems*, Chemical Engineering Science, 50 (3), 531-547.

Marty, N.M., Munier, I., Gaucher, E., Tournassat, C., Gaboreau, S., Vong, C., Giffaut, E., Cochepin, B., Claret, F. (2014) *Simulation of Cement/clay interactions: feedback on the increasing complexity of modelling strategies*, Transp. Porous Med., 104, 385-405.

Marty, N.C.M., Bildstein, O., Blanc, P., Claret, F., Cochepin, B., Gaucher, E.C., Jacques, D., Lartigue, J.E., Liu, S.H., Mayer, K.U., Meeussen, J.C.L., Munier, I., Pointeau, I., Su D.Y., Steefel, C.I. (2015) *Benchmarks for multicomponent reactive transport across a cement/clay interface*, Comput. Geosci. 19, 635-653.

Mathur, R.K., Narayan, P.K. and Prasad, A.N. (1996) *Status of sitting and host rock characterization programme for a geological repository in India*, Isolation, Second,Worldwide Review, P.A. Witherspoon, ed., LBNL.

Mathur, R.K., Narayan, P.K., Joshi, M.R. (1998) *In situ multi heater thermomechanical experiments in Mysore Mines, Kolar gold fields*, Bhabha Atomic Research Centre, Mumbai, India, BARC/1998/I/015.

Mattila, K., Hyvluoma, J., Rossi, T., Aspns, M., Westerholm, J. (2007) *An efficient swap algorithm for the lattice Boltzmann method*, Comput. Phys. Commun., 176(3), 200-210.

Mattila, K., Hyvluoma, J., Timonen, J., Rossi, T. (2008) *Comparison of implementations of the lattice-Boltzmann method*, Comput. Math. Appl., 55(7), 1514-1524.

McNamara, G., Zanetti, G. (1988) *Use of the Boltzmann-equation to simulate lattice-gas automata*, Phys. Rev. Lett., 61 (20), 2332-2335.

Meeussen, J.C. (2003) *ORCHESTRA: An object-oriented framework for implementing chemical equilibrium models*. Environ. Sci. Technol., 37, 1175-1182.

Mohamad, A. (2011) *Lattice Boltzmann Method Fundamentals and Engineering Applications with Computer Codes*, Springer, London.

Molins, S., Carrera J., Ayora C., Saaltink M. W. (2004) *A formulation for decoupling components in reactive transport problems*, Water Resour. Res., 40, W10301

Molins, S., Trebotich, D., Steefel, C.I., Shen, C. (2012) *An investigation of the effect of pore scale flow on average geochemical reaction rates using direct numerical simulation*, Water Resour. Res., 48, W03527.

Mgler, C., Montarnal, P., Dimier, A., Trotignon, L. (2004) Reactive transport modelling in the Alliances software platform, Developments in Water Science, 55 (2), 1103-1115.

Pal, T.K., Datta, D. (2017) *Parametric uncertainty analysis of solute transport process using fuzzy lattice Boltzmann scheme*, International Journal of Life Cycle Reliability and Safety Engineering, 6(4), 239-249.

Pal, T.K., Datta, D., Bajpai, R.K. (2016a) *Numerical Simulation of Reaction-Diffusion Process in Geological Media using Lattice Boltzmann Based Diffusion Model Coupled with Geochemical Reaction Solver*, Global Journal of Pure and Applied Mathematics, 12(1), 429-433.

Pal, T.K., Datta, D., Bajpai, R.K. (2016b) *Development of Differential Quadrature based Computational Scheme in Cylindrical Geometry and Its application to Simulate Radionuclide Leaching from Radioactive Waste Form*, International Journal of Life Cycle Reliability and Safety Engineering, 5(2), 1-7.

Pal, T.K., Arumugam, V., Datta, D. (2015) *Uncertainty Analysis of Retardation Factor Using*

Monte Carlo, Fuzzy Set and Hybrid Approach, Springer Proceedings in Mathematics Statistics, 125, 153-163.

Parkhurst, D.L., Appelo, C.A.J. (1999) *User's Guide to PHREEQC (version 2) a Computer Program for Speciation, Batch-reaction, One-dimensional Transport, and Inverse Geochemical Calculations*, Water-Resources Investigation Report 99-4259; Denver, Colorado.

Parkhurst, D.L., Appelo, C.A.J. (2013) *Description of input and examples for PHREEQC version 3a computer program for speciation, batch-reaction, one-dimensional transport, and inverse geochemical calculations*, U.S. Geological Survey Techniques and Methods, book 6, chap. A43, 497.

Parkhurst, D.L., Wissmeier, L. (2015) *PhreeqcRM: A reaction module for transport simulators based on the geochemical model PHREEQC*, Adv. Water Resour., 83, 176-189.

Patel, R.A., Perko, J., Jacques, D., Schutter, G.D., Ye, G., Breugel, K.V. (2013) *Lattice Boltzmann based multicomponent reactive transport model coupled with geochemical solver for pore scale simulations*, in S. Idelsohn, M. Papadrakakis, B. Schrefler (Eds.), V International Conference on Computational Methods for Coupled Problems in Science and Engineering, Coupled problems 2013, CIMNE, Barcelona, Ibiza, Spain.

Patel, R.A., Perko, J., Jacques, D., Schutter, G.D., Breugel, K.V., Ye, G. (2014) *A versatile pore-scale multi-component reactive transport approach based on lattice Boltzmann method: Application to portlandite dissolution*, Physics and Chemistry of the Earth, Parts A/B/C, 70-71, 127-137.

Patel, R.A., Perko, J., Jacques, D., Schutter, G.D., Ye, G., Breugel, K.V. (2018) *A three-dimensional lattice Boltzmann method based reactive transport model to simulate changes in cement paste microstructure due to calcium leaching*, Constr. Build. Mater., 166 (2018), pp. 158-170.

Perko, J., Patel, R. A. (2014) *Single-relaxation-time lattice Boltzmann scheme for advection-diffusion problems with large diffusion-coefficient heterogentities and high-advection transport*, Phys. Rev. E, 89, 053309

Peterson, P. (2009) *F2PY: a tool for connecting Fortran and Python programs*, Int. J. Comput. Sci. Eng., 4(4), 296-305.

Prommer, H., Barry, D.A., Zheng C. (2003) *MODFLOW/MT3DMS-based reactive multicomponent transport modeling*, Ground Water, 41, 247-257.

Prommer, H., Post, V.E.A. (2010) *PHT3D, A Reactive Multicomponent Transport Model for Saturated Porous Media*, Users Manual v2.10. http://www.pht3d.org

Qian, Y.H., d'Humieres, D., Lallemand, P. (1992) *Lattice BGK models for Navier-Stokes equation*, Europhys. Lett., 17 (6), 479-484.

Qian, Y.H., Orszag, S.A. (1995) *Scaling in diffusion-driven reaction A+BC: numerical simulations by lattice BGK models*, J. Stat. Phys., 81(12), 237-253.

Quan, J. R., Chang, C.T. (1989a) *New insights in solving distributed system equations by the quadrature methods-I. Analysis*, Comput. Chem. Eng., 13, 778-788.

Quan, J. R., Chang, C.T. (1989b) *New insights in solving distributed system equations by the quadrature methods-II. Numerical experiments*, Comput. Chem. Eng., 13, 1017-1024.

Raj K., Prasad K.K., Bansal N.K. (2006) *Radioactive waste management practices in India*, Nuclear Engineering and Design 236, 914-930.

Reed, M.H. (1982) *Calculation of multicomponent chemical equilibria and reaction processes in systems involving minerals, gases, and an aqueous phase*, Geochim. Cosmochim. Acta., 46, 513-528.

Saaltink, M.W., Ayora, C., Carrera, J. (1998) *A mathematical formulation for reactive transport that eliminates mineral concentrations*, Water Resour. Res., 34 (7), 1649-1656.

Saaltink, M.W., Carrera, J., Ayora, C. (2001) *On the behavior of approaches to simulate reactive transport*, Journal of Contaminant Hydrology, 48, 213-235.

Salvatores, M., Palmiotti, G. (2011) *Radioactive waste partitioning and transmutation within advanced fuel cycles: achievements and challenges*, Prog. Part. Nucl. Phys., 66, 144-166.

Savage, D., Noyb, D., Miharac, M. (2002) *Modelling the interaction of bentonite with hyperalkaline fluids*, Appl. Geochem., 17, 207-223.

Sayre, W.W. (1973) *Natural mixing processes in rivers*, in Shen, H.W. (ed) Environmental impact on rivers. University of Colorado, Fort Collins.

Schwartz, M.O. (2009) *Modelling groundwater contamination above the Asse 2 medium-level nuclear waste repository, Germany*, Environ. Earth Sci., 59, 277-286.

Shan, X., Yuan, X., Chen, H. (2006) *Kinetic theory representation of hydrodynamics: a way beyond the Navier-Stokes equation*, J Fluid Mech, 550, 413-441.

Sherbourne, A.N., Pandy, M.D. (1991) *Differential quadrature method in the bucking analysis of beams and composite plates*, Comput. Struct., 40, 903-913.

Shu, C. (1991) *Generalized differential-integral quadrature and application to the simulation of incompressible viscous flows including parallel computation*, PhD thesis, Univ of Glasgow, UK.

Shu, C., Richards, B.E. (1992) *Application of generalized differential quadrature to solve two-dimensional incompressible Navier Stokes equations*, Int. J. Numer. Meth. Fluids., 15, 791-798.

Shu, C. (2000) *Differential Quadrature and Its Application in Engineering*, Springer, Berlin.

Silveira, C.S.D., Alvim, A.C.M., and Rivero Oliva, J.D.J. (2013) *Radionuclide transport in fractured rock: Numerical assessment for high level waste repository*. Science and Technology of Nuclear Installations, 1-17.

Šimůnek, J., Jacques, D., Šejna, M., van Genuchten, M.T. (2012) *The HP2 Program for HYDRUS (2D/3D): A coupled code for simulating two-dimensional variably-saturated water flow, heat transport, and biogeochemistry in porous media*, Version 1.0, PC Progress, Prague, Czech Republic, 76.

Šimůnek. J., Jacques, D., Langergraber, G., Bradford, S.A., Šejna, M., van Genuchten, M.T. (2013) *Numerical modeling of contaminant transport using HYDRUS and its specialized modules*, 93, 265-284 , ISSN: 0970-4140 Coden-JIISAD.

Spycher, N.F., Sonnenthal, E.L., Apps, J.A. (2003) *Fluid flow and reactive transport around potential nuclear waste emplacement tunnels at Yucca Mountain, Nevada*, J. Contam. Hydrol., (62), 653-673.

Srinivasan, V., Clement, T.P. (2008a) *Analytical solutions for sequentially coupled one-dimensional reactive transport problems Part I: Mathematical derivations*, Adv. Water Resour., 31, 203-218.

Srinivasan, V., Clement, T.P. (2008b) *Analytical solutions for sequentially coupled one-dimensional reactive transport problems Part II: Special cases, implementation and testing*, Adv. Water Resour. 31, 219-232.

Steefel, C. I., Lasaga, A. C. (1994a), *A coupled model for transport of multiple chemical species and kinetic precipitation/dissolution reactions with applications to reactive flow in single phase hydrothermal system* Am. J. Sci., 294, 529-592.

Steefel, C. I., Lichtner, P. C. (1994b) *Diffusion and reaction in rock matrix bordering a hyperalkaline fluid-filled fracture*, Geochimica et Cosmochimica Acta 58, 3595-3612.

Steefel, C.I., MacQuarrie, K.T.B. (1996) *Approaches to modeling reactive transport in porous media*, in Lichtner P.C., Steefel C.I., Oelkers E.H.,(Eds.), Reactive Transport in Porous Media, Reviews in Mineralogy, 34, 83-125.

Steefel, C.I., Lichtner, P.C. (1998a) *Multicomponent reactive transport in discrete fractures: I. Controls on reaction front geometry*, J. Hydrol., 209, 186-199.

Steefel, C.I., Lichtner, P.C. (1998b) *Multicomponent reactive transport in discrete fractures: II. Infiltration of hyperalkaline groundwater at Maqarin, Jordan, a natural analogue site*, J. Hydrol., 209, 200-224.

Steefel C. I., DePaolo D. J., Lichtner P. C. (2005) *Reactive transport modeling: An essential tool and a new research approach for the Earth sciences*, Earth Planet. Sci. Lett., 240, 539-558.

Steefel, C.I., Molins, S., Trebotich, D. (2013) *Pore scale processes associated with subsurface CO 2 injection and sequestration*, Rev. Mineral. Geochem. 77, 259-303.

Steefel C. I., Appelo C. A. J., Arora B., Jacques D. (2015) *Reactive transport codes for subsurface environmental simulation*, Computational Geosciences, 19, 445-478.

Stiebler, M., Tlke, J., Krafczyk, M. (2008) *Advection-diffusion lattice Boltzmann scheme for hierarchical grids*, Comput. Math. Appl., 55, 1576-1584.

Succi, S., Benzi, R., Higuera, F. (1991) *The lattice Boltzmann equation: a new tool for computational fluid dynamics*, Physica D, 47(1-2), 219-230.

Succi, S. (2001) *The Lattice Boltzmann Equation for Fluid Dynamics and Beyond*, Oxford University Press, New York.

Sukop, M.C., Thorne, Jr D.T. (2006) *Lattice Boltzmann Modelling: An Introduction for Geoscientists and Engineers*, Springer: New York.

Sunder Rajan, N.S., Ozarde, P.D. (1980) *Natural air cooling for interim storage for solidified highly radioactive wastes*, Proc. Indo-Soviet Seminar on Radioactive Waste Management, March, Moscow.

Tartakovsky, A.M., Redden, G., Lichtner, P.C., Scheibe, T.D., Meakin, P. (2008) *Mixing-induced precipitation: experimental study and multiscale numerical analysis*, Water Resour. Res., 44(6), W06S04.

Thorat, V., Pente, A.S., Mishra, R.K., Ramchandran, M., Kaushik, C.P., Raj, K. (2008) *Studies on long term leaching behaviour of vitrified waste product containing sulphate bearing high level radioactive waste*, Journal of Applied Geochemistry, 10(2A), 463-474.

Tian, Z.W.,Xing, H.L., Tan, Y.L., Gao, J.F. (2014) *A coupled lattice Boltzmann model for simulating geochemical reaction transport in CO2 injection*, Physica A, 403, 155-164.

Tian, Z., Wang, J. (2018) *Lattice Boltzmann simulation of dissolution-induced changes in permeability and porosity in 3D CO2 reactive transport*, J. Hydrol., 557, 276-290.

Van der Sman, R.G.M., Ernst, M.H. (2000) *Convection-diffusion lattice Boltzmann scheme for irregular lattices*, J. Comput. Phys., 160(92), 766-782.

Van der Lee, J., De Windt, L., Lagneau, V., Goblet, P. (2003) *Module-oriented modeling of reactive transport with HYTEC*, Comput. Geosci., 29, 265-275.

Van Leemput, P., Vandekerckhove, C., Vanroose, W., Roose, D. (2007) *Accuracy of hybrid lattice Boltzmann/finite difference schemes for reaction-diffusion systems*, Multiscale Modeling Simulation, 6(3), 838-857.

Verma, A.K., Bajpai, R.K., Singh, T.N. et al. Arab J Geosci (2011) *3D instability analysis of an underground geological repositoryan Indian case study*, Arabian Journal of Geosciences, 4 (78), 1173-1188.

Verma A.K., Gautam P., Singh T.N., Bajpai R.K. (2015) *Numerical Simulation of High Level Radioactive Waste for Disposal in Deep Underground Tunnel*, In: Lollino G., Manconi A., Clague J., Shan W., Chiarle M. (eds) Engineering Geology for Society and Territory - Volume 1. Springer, Cham.

G. A. Walter, E. Frind, D. Blowes, C. Ptacek, J. Molson*Modeling of multicomponent reactive transport in groundwater. 1. Model development and evaluation*, Water Resour. Res. 30 (11) (1994) 3137-3148.

Wang, J., Zhang X.X., Bengough. A.G., Crawford. J.W. (2005)*Domain-decomposition method for parallel lattice Boltzmann simulation of incompressible flow in porous media*, Phys Rev E, 72:016706-1-016706-11.

Wang, M., Kang, Q. (2010) *Modeling electrokinetic flows in microchannels using coupled lattice Boltzmann methods*, J. Comput. Phys., 229, 728-744.

Wang, X. (2015) *Differential quadrature and differential quadrature based element method. Theory and applications*, Butterworth-Heinemann, Oxford, UK.

Wattal, P.K. (2017) *Back end of Indian nuclear fuel cycle-A road to sustainability*, Prog. Nucl. Energy 101 (2017) 133-145.

Wellein, G., Zeiser, T., Hager, G., Donath, S. (2006) *On the single processor performance of simple lattice Boltzmann kernels*, Comput. Fluids, 35(89), 910-919.

Wexler, J. (1992) *Analytical solutions for one, two, and three-dimensional solute transport in* *ground-water systems with uniform flow*, Techniques of Water-Resources Investigations of the United States Geological Survey, United States government printing office.

Wolf-Gladrow, D.A. (2000) *Lattice-Gas Cellular Automata and Lattice Boltzmann Models: An Introduction*, Lecture Notes in Mathematics, vol. 1725, Springer, Berlin.

Xi, H., Peng, S., Chou, S.H. (1999) *Finite-volume lattice Boltzmann method*, Phys. Rev. E., 59 (5), 6202-6205

Xiao, Y., Whitaker, F., Xu, T., Steefel, C.I. (2018) *Reactive Transport Modeling: Applications in Subsurface Energy and Environmental Problems*, Wiley Online Library, ISBN:9781119060000, DOI:10.1002/978111906003.

Xu, T., Sonnenthal, E., Spycher, N., Pruess, K. (2006) *TOUGHREACT - a simulation program for non-isothermal multiphase reactive geochemical transport in variably saturated geologic media: applications to geothermal injectivity and CO2 geological sequestration*, Comput. Geosci., 32 (2006), 145-165.

Xu, T., Spycher, N., Sonnenthal, E., Zhang G., Zheng, L., Pruess, K. (2011) *TOUGHREACT Version 2.0: A simulator for subsurface reactive transport under non-isothermal multiphase flow conditions*, Comput. Geosci., 37, 763-774.

Yan, G.W., Hu, S.X. (2000a) *Simple lattice Boltzmann model for traffic flows*, ACTA Mech. Sinica, 16(1), 70-74.

Yan, G.W. (2000b) *A lattice Boltzmann equation for waves*, J. Comput. Phys., 161(9), 61-69.

Yeh, G.T., Tripathi, V.S. (1989) *A critical evaluation of recent developments in hydrogeochemical transport models of reactive multichemical components*, Water Resources Res., 25, 93-108.

Yeh, G.T., Tripathi, V.S. (1990) *HYDROGEOCHEM: A Coupled Model HYDROlogical Transport and GEOCHEMical Equilibrium of Multi Component Systems*, ORNL 6371.

Yeh, G.T., Tripathi, V.S. (1991) *A model for simulating transport of reactive multi-species components: model development and demonstration, Water Resour. Res. 27, 3075-3094.*

Yoon, H., Kang, Q., Valocchi, A. (2015) Lattice Boltzmann-based approaches for pore-scale reactive transport, Rev. Mineral. Geochem., 80, 393-431.

Zadeh, L.A. (1965) Fuzzy Sets, Inf. Control., 8, 338-353.

Zeigler, D.P. (1993) Boundary conditions for the lattice Boltzmann simulations, J. Stat. Phys., 71, 1171-1177.

Zhang D., Zhang R., Chen S., Soll W. E. (2000) Pore scale study of flow in porous media: scale dependency, REV, and statistical REV, Geophys. Res. Lett., 27, 1195-1198.

Zhang, X., Bengough, A.G., Crawford, J.W., Young, I.M. (2002) A lattice BGK model for advection and anisotropic dispersion equation, Adv. Water Resour., 25, 1-8.

Zhang, J. (2011) Lattice Boltzmann method for microfluidics: models and applications, Microfluid Nanofluid, 10 (1), 1-28.

Zhang, F., Parker, J. (2012) Groundwater reactive transport models, Bentham Science Publishers, Oak Park.

Zhang, M., Ye, G., van Breugel, K. (2014a) Multiscale lattice Boltzmann-finite element modelling of chloride diffusivity in cementitious materials. Part I: Algorithms and implementation, Mechanics Research Communications, 58, 53-63.

Zhang, M., Ye, G., van Breugel, K. (2014b) Multiscale lattice Boltzmann-finite element modelling of chloride diffusivity in cementitious materials. Part II: Simulation results and validation, Mechanics Research Communications, 58, 64-72.

Zhou, J. G. (2009) A lattice Boltzmann method for solute transport, Int. J. Numer. Meth. Fluids, 61, 848-863.

Zio, E., Apostolakis, G. E. (1996) Two methods for the structures assessment of model uncertainty by experts in performance assessments of radioactive waste repositories, Reliability Engineering and System Safety, 54, 225-241.

Zong Z., Zhang Y., (2009) Advanced differential quadrature methods, CRC Press, New York.